Thermal Integrity Profiling for Detecting Flaws in Drilled Shafts

Andrew Boeckmann, P.E. and J. Erik Loehr, Ph.D., P.E.

University of Missouri

WisDOT ID no. 0092-16-07

December 2018

RESEARCH & LIBRARY UNIT

WISCONSIN HIGHWAY RESEARCH PROGRAM

WISCONSIN DOT

PUTTING RESEARCH TO WORK

TECHNICAL REPORT DOCUMENTATION PAGE

1. Report No. 0092-16-07	**2. Government Accession No.**	**3. Recipient's Catalog No.**
4. Title and Subtitle Thermal Integrity Profiling for Detecting Flaws in Drilled Shafts		**5. Report Date** December 2018 **6. Performing Organization Code**
7. Author(s) Andrew Boeckmann, J. Erik Loehr		**8. Performing Organization Report No.**
9. Performing Organization Name and Address University of Missouri Civil and Environmental Engineering E2509 Lafferre Hall Columbia, MO 65211-2200		**10. Work Unit No.** **11. Contract or Grant No.** **Project 0092-16-07**
12. Sponsoring Agency Name and Address Wisconsin Department of Transportation Research & Library Unit 4822 Madison Yards Way, Madison, WI 53705		**13. Type of Report and Period Covered** Final Report November 2016 - December 2018 **14. Sponsoring Agency Code**

15. Supplementary Notes

16. Abstract

Thermal Integrity Profiling (TIP) methods for evaluating drilled shaft concrete integrity have emerged in recent years as a viable alternative to Crosshole Sonic Logging (CSL) methods. TIP methods use measurements of concrete temperatures along the length of the drilled shaft reinforcing cage to identify potential defect locations from zones of low temperature. TIP methods are appealing because they should be sensitive to defects outside the reinforcing cage, an area not evaluated with CSL. To evaluate the ability to detect defects with TIP methods compared with CSL methods, three 4 ft diameter by 30 ft long drilled shafts with ten intentional defects were installed in Waukesha, Wisconsin. The defects varied in location, size, and material. TIP and CSL tests were performed on all three shafts. The results revealed TIP and CSL to be complementary. Each test is particularly well-suited to identifying certain types of defects but limited or incapable of identifying other types of defects. The alignment of detection abilities attributed to each method is such that virtually any significant defect should be detectible by one or both tests. The results indicated TIP is effective for identifying defects due to weak concrete and defects outside the reinforcing cage. Smaller temperature decreases were observed for tremie breach defects and inclusions within the reinforcing cage, and no TIP effect could be discerned for soft bottom defects. CSL results were sensitive to defects within the reinforcing cage, including inclusions, tremie breach effects, and soft bottom conditions but not weak concrete. CSL results were also not affected by defects outside the reinforcing cage. TIP measurements indicated significantly greater sensitivity to defects at times corresponding to roughly half the time to peak temperature. Improvements to TIP interpretation methods would likely improve defect detection.

17. Key Words Drilled shaft, deep foundation, concrete, concrete integrity, thermal integrity profiling, crosshole sonic logging	**18. Distribution Statement** No restrictions. This document is available through the National Technical Information Service. 5285 Port Royal Road Springfield, VA 22161

19. Security Classif. (of this report) Unclassified	**20. Security Classif. (of this page)** Unclassified	**21. No. of Pages** 113	**22. Price**

Form DOT F 1700.7 (8-72) Reproduction of completed page authorized

Disclaimer

This research was funded through the Wisconsin Highway Research Program by the Wisconsin Department of Transportation and the Federal Highway Administration under Project 0092-16-07. The contents of this report reflect the views of the authors who are responsible for the facts and accuracy of the data presented herein. The contents do not necessarily reflect the official views of the Wisconsin Department of Transportation or the Federal Highway Administration at the time of publication.

Executive Summary

Thermal Integrity Profiling (TIP) methods have emerged as a viable alternative to the Crosshole Sonic Logging (CSL) method used by many agencies for concrete integrity testing. Whereas CSL uses geophysical measurements to identify zones of defective concrete, TIP methods identify defective zones using temperature measurements. Hydration of cement generates significant heat, so depths with defective concrete are expected register temperature dips in the TIP temperature records. Experience has revealed several concerns commonly held regarding CSL method, in particular concerns regarding the frequency of false positives and concerns regarding the lack of integrity information outside the reinforcing cage. However, there are also concerns regarding TIP methods. The chief concerns regard the ability of TIP to detect defects, especially defects near the center of the shaft cross-section, and how to interpret TIP records.

This research project has three specific objectives:

1. Demonstrate the effectiveness of TIP testing methods, specifically by evaluating the ability of TIP to identify defects of various locations and size.
2. Evaluate TIP's viability as an alternative to CSL by comparing the effectiveness of each method.
3. If supported by data, modify WisDOT Standard Specifications to allow TIP testing and include recommended TIP procedures.

The research objectives were achieved through evaluation of existing TIP experience from WisDOT and previous research, as well as through collection of new data from full-scale field research. The field research involved performing TIP and CSL testing on three drilled shafts with planned concrete defects.

Previous Work

Mullins et al. (2007) outlined four levels of TIP analysis. Level 1 is the simplest type of analysis that involves a primarily qualitative review of the TIP temperature measurements. The other levels involve inferring the "effective radius" of the shaft from the TIP results using models relating temperature and radius. For Level 2, the model is based on concrete volume measurements during construction. Analytical thermal models are used to develop the temperature-radius models for Level 3, and the same thermal models are calibrated using the TIP measurements in Level 4. TIP reports that present effective radius interpretations are generally derived from the Level 2 approach.

A review of previous research revealed three studies involving drilled shafts with intentional defects. Test shafts for each study had diameters of 4 or 5 ft. Two studies (Mullins et al., 2007; Ashlock and Fotouhi, 2014) observed relatively modest TIP temperature effects (about 5° F or less) for defects representing about 10% of the cross section. Another study (Schoen et al., 2018) observed greater TIP effects (about 13° F) for defects representing about 15% of the cross-section. Schoen et al. also observed that the greatest effect occurred at about half the time to peak, with the effect diminishing by about half by the time peak temperatures developed.

TIP records were reviewed for more than 50 shafts from the WisDOT Zoo Interchange project in Milwaukee. Tremie breaches were documented for two shafts, and the effect of the breaches was evident in CSL records. CSL records also indicated three shafts had soft bottom conditions. All five defects were confirmed with coring. Most of the defects were not identified from TIP results because of wire breakage, but a drop in temperature was observed for one of the tremie breaches. The TIP report for that shaft recommended "provisionally accepting" the shaft, contingent on a review of CSL results and noting adequate cover based on the effective radius interpretation of the TIP results. Improved wire design has significantly reduced the incidence of wire failures, according to users who routinely use TIP wires.

Experimental Methods and Results

To further evaluate the ability to detect defects with TIP methods compared with CSL methods, three 4 ft diameter by 30 ft long drilled shafts with ten intentional defects were installed in Waukesha, Wisconsin. The defects varied in location, size, and material. Four defects were included to evaluate the effect of defect location within the cross-section, particularly how the sensitivity of TIP compares for defects

outsides the reinforcing cage and defects inside the reinforcing cage. Two defects were included to evaluate soft bottom conditions, two defects were included to evaluate zones of weak concrete, and one was included to evaluate a tremie breach. The last defect involved lubrication of the access tubes to promote debonding to evaluate potential false positives in CSL records.

Of the nine intentional defects (neglecting the tube debonding defect), TIP measurements produced temperature decreases greater than 5° F for four defects, decreases between 3 and 5° F for two defects, and no discernable temperature decrease for the other three defects. The greatest decreases were observed for weak concrete defects and defects outside the reinforcing cage, while limited temperature decreases were observed for inclusions within the reinforcing cage and the tremie breach defect. No temperature decrease was observed for the soft bottom defects or the smaller inside-cage inclusion.

The magnitude of defect effects on TIP temperatures was greatest at about the time temperatures were rising most quickly. This generally occurred at roughly half the peak time. For three of four types of defects evaluated, temperature differences attributed to the defects diminished significantly after peaking at the time of maximum rate of temperature increase. For two defect types, the temperature differences had decreased to zero within 30 hours of concrete placement.

The defects were more difficult to detect using effective radius interpretations than from simply evaluating the measured temperatures. Effective radius profiles combine observations from concrete placement with temperature observations from TIP. This can have the effect of obscuring effects that might be evident from separate consideration of concrete volume and temperature measurements. For one test shaft, the significant temperature effect of weak concrete at the top of the shaft was offset by the volume effect of over excavation, resulting in effective radius values that were generally greater than the nominal radius despite the presence of significantly “watered down” concrete.

CSL measurements indicated at least 10% increases in arrival times and at least 5 dB decreases in relative energy for five of the intentional defects, with no discernable increase in arrival time or decrease in relative energy for the other four defects. However, results for one of the five “successful” defects, Defect 3, are suspect as the anomaly was only apparent in one of the tube pairings. The remaining successfully identified defects were defects within the reinforcing cage, including a soft bottom defect, and the tremie breach defect. CSL measurements did not produce significant indications for defects outside the reinforcing cage (except the suspect result) or for weak concrete. The tendency for false positive CSL results due to tube debonding was demonstrated with significantly delayed arrival times and decreased relative energy for CSL measurements at Defect 4.

Conclusions

Assessments of the sensitivity of TIP and CSL test methods to drilled shaft concrete defects are presented the table below. The assessments are based on the results summarized above from previous studies, this study, and project applications. The assessments in the table are based on experimental studies, including this one, that attempt to identify a lower bound for the severity of defect that can be detected. Accordingly, the defects evaluated represent relatively small portions of the drilled shaft cross-section, typically 10 to 15%. Defects of similar size were studied by Sarhan et al. (2000) and shown to have a relatively modest effect on structural resistance, although the effects of defects depend on the specific details of a given project and shaft.

Defect Type	Ability to Detect Relatively Modest Defects	
	TIP	CSL
Inclusions in cage interior	Difficult to detect	Readily detectible
Defects outside reinforcing cage	Readily detectible	Not detectible
Soft bottom	Not detectible	Readily detectible
Weak concrete	Readily detectible	Difficult to detect
Tremie breach	Potentially detectible	Readily detectible

Comparison of the evaluations in the table reveals TIP and CSL are complementary in terms of the types of defects they can detect. Each test is particularly well suited for some types of defects and rather poorly suited for other types of defects, but together the tests can identify virtually any type of defect.

Other significant findings from this study include:

- Defects are significantly more detectable with TIP methods when the evaluation temperatures are from about half the time to peak temperature development.

- Interpretation of TIP results using the effective radius method can make identification of defects more difficult than by simply evaluating the temperature data directly and with consideration of field information, including concrete yield plots.

- Reinforcing cage misalignment makes identification of concrete defects via TIP methods significantly more difficult.

- Evaluation of relative energy for CSL test results can be used to identify defects that are not apparent in CSL arrival time results for the same shaft.

- Improvements to current methods for interpreting TIP measurements may improve the ability to detect drilled shaft defects with TIP methods. Two potential improvements involve closer examination of how TIP measurements for a shaft change with time and processing TIP data within the context of analytical or numerical thermal models that account for effects from concrete mix, ground conditions, and other significant factors.

Recommendations

TIP methods should be an allowable concrete integrity test method that could be used as a replacement for CSL, an allowable alternative to CSL, or in conjunction with CSL. A logical approach would be to allow both test methods, with the specific method for any given project selected on the basis of project considerations, e.g. predominant loading type. Both test methods should be used for technique shafts.

Additional significant recommendations implemented in the specification language (Appendix E) include:

- TIP testing should be performed using sacrificial wires, not the probe method. Many points of discussion could be included in a debate of the merits of each method, but this is the only one that matters: the continuous time record of concrete temperatures provided by the wire method greatly improves the likelihood of detecting defects.

- TIP interpretation should include evaluation of temperature versus time plots for suspected defects.

- Evaluation of TIP data should be based on raw temperature measurements only, not analyses of effective radius. The evaluation of TIP data should be accompanied by evaluation of available records of drilled shaft installation, including concrete yield plots.

- Evaluations of TIP results should be based on relatively open-ended language that defers to the professional judgment of the TIP engineer. Any significant temperature deviations should be identified in a TIP report and trigger evaluation by the design engineer of the shaft. The design engineer would deem the deviations as either permissible or requiring further investigation or remediation.

Acknowledgements

Financial Support
Wisconsin Department of Transportation

WisDOT and WHRP Personnel
Jeff Horsfall
Heidi Noble
Laura Shadewald
Andrew Zimmer

Pile Dynamics, Inc.
Jim Zammataro

Drilled Shaft Construction
Riley Padron and Gene Sheedy of Midwest Drilled Foundations and Engineering, Inc.
Taylor Ridge Drilled Foundations, Inc.

Jacobs (formerly CH2M)
Kevin Brusso

University of Wisconsin
Sabrina Bradshaw
Dante Fratta

University of Missouri
Zakaria El-tayash
Martin Wallace

Table of Contents

Executive Summary iii

Acknowledgements vi

1. Introduction 1

2. Concrete Integrity Test Methods and the Significance of Defects 3

2.1 Terminology 3

2.2 Crosshole Sonic Logging (CSL) 3

2.3 Thermal Integrity Profiling 4

2.3.1 Example TIP Records 5

2.3.2 Time to Peak Temperature 6

2.3.3 Probe versus Wire 7

2.3.4 Interpretation of TIP Results 8

2.3.5 TIP Costs 13

2.4 Gamma Gamma Logging (GGL) 14

2.5 Acceptance Criteria for CSL and TIP 14

2.6 Significance of Drilled Shaft Concrete Defects 16

2.6.1 Sarhan et al. (2000) 16

2.6.2 Piscalko et al. (2016) 17

3. Sensitivity of TIP Results to Defects 18

3.1 Previous Research regarding TIP Sensitivity to Defects 18

3.1.1 Florida DOT Study by Mullins et al. (2007) 18

3.1.2 Iowa DOT Study by Ashlock and Fotouhi (2014) 19

3.1.3 Schoen et al. (2018) 22

3.2 Agency Experiences with TIP 23

3.2.1 WisDOT: Zoo Interchange 23

3.2.2 South Carolina DOT 25

3.2.3 Other Agencies 25

4. Field Testing Program 26

4.1 Experimental Design and Construction Plans 26

4.2 Test Site 27

4.3 Drilled Shaft Construction 28

4.3.1 Shaft Excavation and Temporary Casing 28

4.3.2 Reinforcing Cages and Defects 29

4.3.3 Concrete: Mix Design, Placement and Defects, and Compressive Strength 33

4.4 Concrete Integrity Testing 38
4.4.1 TIP Via Wires 38
4.4.2 TIP Via Probe 40
4.4.3 CSL 42
5. Experimental Results 44
5.1 Summary Plots 44
5.2 Qualitative Evaluation of Results 52
5.2.1 Qualitative Evaluation of TIP Results: Temperature 52
5.2.2 Qualitative Evaluation of TIP Results: Effective Radius 53
5.2.3 Qualitative Evaluation of CSL Results 55
5.3 Quantitative Evaluation of Results 56
5.3.1 Quantitative Evaluation of TIP Results 56
5.3.2 Quantitative Evaluation of CSL Results 57
5.4 Effect of Time on TIP Temperatures and TIP Sensitivity to Defects 59
5.5 TIP Probe Results 64
6. Summary and Discussion 67
6.1 Summary of Results from Previous Work and Field Tests 67
6.2 Sensitivity of TIP and CSL to Concrete Defects 69
6.3 Summary of Advantages and Limitations of TIP and CSL 69
7. Conclusions & Recommendations 71
7.1 Conclusions 71
7.2 Recommendations: Implementation of TIP 72
7.2.1 Potential Approaches to Implementing TIP 72
7.2.2 TIP Test Procedures and Use of Probe 73
7.2.3 TIP Test Interpretation 73
7.2.4 Acceptance Criteria 73
7.3 Recommendations: CSL 74
7.4 Recommendations: Future Research 74
References 76
Appendix A – Final Construction Plans for Field Research Drilled Shafts A-1
Appendix B – As-Built Construction Plans for Field Research Drilled Shafts B-1
Appendix C – Boring Logs C-1
Appendix D – Concrete Placement Logs D-1
Appendix E – Proposed TIP Specification E-1

Table of Figures

Figure 1: Drilled shaft cross-sections showing access tubes and ray paths for (a) small-diameter shaft with four access tubes and (b) large-diameter shaft with eight access tubes. 3

Figure 2: (a) Example time record for a single depth and single access tube pairing; (b) example plots of FAT (red line, left) and relative energy (blue line, right) versus depth. Modified from ASTM (2016). 4

Figure 3: Example TIP result from Mullins (2010). 5

Figure 4: Example TIP result from Piscalko et al. (2016): (a) TIP record and (b) core photograph from a depth of 90 ft. 6

Figure 5: Drilled shaft temperatures as a function of radial position and shaft radius. From Johnson (2016) and Mullins (2013). 9

Figure 6: Example concrete volume record from FHWA's Drilled Shaft manual (Brown et al., 2010). 10

Figure 7: TIP data used for example temperature-radius model by Mullins and Winters (2011). 10

Figure 8: Example Level 2 temperature-radius model from Mullins and Winters (2011). Model is based on the data from Figure 6. 11

Figure 9: Example effective radius analysis from Mullins and Winters (2011) using TIP data from the example of Figure 6 and the temperature-radius model shown in Figure 8. 11

Figure 10: Single-point method for temperature-radius models from Johnson (2016). 12

Figure 11: Curve fitting at roll-off zones at top of shaft (TOS) and bottom of shaft (BOS) from Johnson (2014). 13

Figure 12: Results of FDOT TIP study by Mullins et al. (2007), as presented by Mullins and Winters (2011). 18

Figure 13: TIP results for Test Shaft 1 from Ashlock and Fotouhi (2014): (a) temperature and (b) effective radius 20

Figure 14: TIP results for Test Shaft 2 from Ashlock and Fotouhi (2014): (a) temperature and (b) effective radius 20

Figure 15: CSL results for Test Shaft 2 from Ashlock and Fotouhi (2014). 21

Figure 16: CSL results for Test Shaft 2 from Ashlock and Fotouhi (2014). 21

Figure 17: Example TIP result showing decreases in temperature at two known defect locations: (a) 14 hours and (b) 34 hours, the peak time. From Schoen et al. (2018). 22

Figure 18: Location of Waukesha test site (Google Earth, 2018). 27

Figure 19: Overview of test site with crane, loader, and drill rig in operation. 28

Figure 20: Excavation of shaft with 48 in. auger through telescoping casing. 29

Figure 21: Reinforcing cages prior to installation of most defects. 29

Figure 22: Defect 1 consisted of three 70 lb sandbags tied inside the reinforcing cage for the Control Shaft. 30

Figure 23: Defect 2 consisted of six 70 lb sandbags tied around the bottom of the reinforcing cage for Test Shaft 1. 30

Figure 24: Defect 3 consisted of six 24 lb sandbags tied concentrically around the edge of the reinforcing cage for Test Shaft 1 at a depth of 21 ft. 31

Figure 25: Defect 4 consisted of wheel bearing grease applied around the outside of the access tubes for a length of 1 ft. Defect 4 was installed in two locations: at a depth of 16.5 ft in Test Shaft 1 and a depth of 4.5 ft in Test Shaft 2. 31

Figure 26: Defect 5 consisted of two 70 lb sandbags outside one side of the reinforcing cage for Test Shaft 1 at a depth of 12 ft. 32

Figure 27: Defect 9 consisted of five 70 lb sandbags placed inside the reinforcing cage for Test Shaft 2 at a depth of 12 ft. *Defects 6, 7, and 8 are presented in the next section.* 32

Figure 28: Reinforcing cage is lowered into the hole for Test Shaft 2. Sandbags for Defect 9 are visible near the cage mid-height. 33

Figure 29: Placement of concrete from the concrete truck to the tremie pipe. 34

Figure 30: Concrete slump test. 34

Figure 31: Concrete volume yield plots for all test shafts. Theoretical lines are all equivalent below a depth of 19 ft. 35

Figure 32: After placing the reinforcing cage but prior to placing concrete for Test Shaft 2, 420 lbs of sand was poured into the bottom of the excavated shaft to simulate a soft bottom for Defect 7. 36

Figure 33: To simulate a tremie breach for Defect 8: (a) the tremie was removed from the shaft prior to (b) placing 30 gallons of water and 70 lbs of sand into the shaft (to simulate a tremie breach in a wet shaft). 36

Figure 34: Concrete placement near the top of shaft: (a) normal concrete in Control Shaft and (b) weak concrete for Defect 6 in Test Shaft 1. 37

Figure 35: Completed Test Shaft 1 shortly after completion of concrete placement. Bleed water from the weak concrete of Defect 6 is evident at the top of the shaft. 37

Figure 36: Close view of a TIP wire with sensor. 39

Figure 37: TIP wires exiting the top of the reinforcing cages. Two sensors were above the top of the shaft to measure ambient temperature. 39

Figure 38: One TAP box was connected to each TIP wire to collect and store temperature data. 40

Figure 39: The Thermal Integrity Profiler tablet by PDI reads and displays temperature data from the TAPs 40

Figure 40: The access tubes were dewatered prior to performing TIP test via probe method. 41

Figure 41: TIP testing via the probe method utilizes a depth encoder pulley that logs the probe depth as it is raised from the bottom of the access tube. 41

Figure 42: TIP testing by probe method for Test Shaft 2 was completed with ambient temperatures near 30° F. 42

Figure 43: CSL testing included all pairs of access tubes. 42

Figure 44: CSL testing utilized equipment by Olson Instruments, Inc., including a dual depth encoder pulley used to lower the source and receiver probes down two access tubes simultaneously. 43

Figure 45: CSL access tube pairings. 44

Figure 46: Results of TIP testing of the Control Shaft, with effective radius from PDI software. 46

Figure 47: Results of TIP testing of Test Shaft 1, with effective radius from PDI software. 47

Figure 48: Results of TIP testing of Test Shaft 2, with effective radius from PDI software. 48

Figure 49: Results of CSL testing of the Control Shaft. 49

Figure 50: Results of CSL testing of Test Shaft 1. 50

Figure 51: Results of CSL testing of Test Shaft 2. 51

Figure 52: Effective radius interpretation for Test Shaft 1 at time of maximum rate of temperature rise. Results are very similar to the interpretation at peak temperature, as shown in Figure 44. 54

Figure 53: Temperature versus time for peak depths of each shaft. 61

Figure 54: Temperature versus time for peak depths of each shaft during first 48 hours after concrete placement. 61

Figure 55: Temperature versus time for analysis of Defect 3, six 24 lb sandbags around entire circumference of reinforcing cage. 62

Figure 56: Temperature versus time for analysis of Defect 5, two 70 lb sandbags outside one side of reinforcing cage. 62

Figure 57: Temperature versus time for analysis of Defect 9, five 70 lb sandbags inside reinforcing cage. 63

Figure 58: Temperature versus time for analysis of Defect 10, weak concrete near top of shaft. 63

Figure 59: Temperature versus time for analysis of bottom of shaft conditions. 64

Figure 60: TIP results for Control Shaft 42 hours after concrete placement: (a) probe and (b) wire. 65

Figure 61: TIP results for Test Shaft 1 24 hours after concrete placement: (a) probe and (b) wire. 65

Figure 62: TIP results for Test Shaft 2 22 hours after concrete placement: (a) probe and (b) wire. 66

Table of Tables

Table 1: Comparison of TIP probe and wire methods. 7

Table 2: Acceptance criteria for CSL and TIP from various sources. 14

Table 3: Summary of structural resistance factors for drilled shafts with various defects from the results of Sarhan et al. (2000). 17

Table 4: Summary of defect characteristics from Ashlock and Fotouhi (2014) study 19

Table 5: Summary of concrete integrity testing results for the six shafts at Zoo Interchange that were cored. Defects were confirmed in five of the six shafts; all five were remediated via grouting 23

Table 6: Information from other transportation agencies with relevant TIP experience. 25

Table 7: Summary of intentional defects 27

Table 8: Concrete mix design specifications 33

Table 9: Results of concrete compressive strength testing. 38

Table 10: Results of quantitative analysis of TIP data. 57

Table 11: Results of quantitative analysis of CSL data. 59

Table 12: Summary of the ability to detect various types of defects for TIP and CSL 69

Table 13: Significant advantages and limitations of TIP and CSL for evaluation of drilled shaft concrete integrity. 70

1. Introduction

Recent years have witnessed a significant increase in the diameters and depths commonly specified for drilled shafts, driven by demands for greater load capacity and facilitated by advances in drilling technology. The larger shafts result in challenging concrete pours requiring large volumes of concrete to maintain workability throughout long duration pours and along long flow paths through congested reinforcing cages. Concrete integrity test methods can provide post-installation assurance that drilled shaft concrete is sound, making the methods a useful complement to appropriate agency concrete mix design and construction practices.

Thermal Integrity Profiling (TIP) methods have emerged as a viable alternative to the Crosshole Sonic Logging (CSL) method used by many agencies for concrete integrity testing. Whereas CSL uses geophysical measurements to identify zones of defective concrete, TIP methods identify defective zones using temperature measurements. Hydration of cement generates significant heat, so depths with defective concrete are expected result in temperature dips in TIP temperature records. A 2015 FHWA report on deep foundation concrete practices (Boeckmann and Loehr, 2015) investigated the procedures of 13 agencies, including WisDOT, that were identified by FHWA as leaders in drilled shaft construction. The report found that six of the agencies had performed TIP testing on a limited number of projects and anticipated further implementation.

The FHWA report identified two widespread agency concerns regarding CSL: (1) frequent “false positives” – anomalies that, upon coring, do not reveal any significant defect – and (2) the lack of integrity information outside the reinforcing cage. The first concern, often triggered by debonding of the CSL access tubes, leads to coring of sound shafts, which unnecessarily consumes agency time and resources. The second concern acknowledges a significant limitation of CSL testing. Concrete outside the reinforcing cage is critical for side resistance and shaft durability. In addition, the area outside the reinforcement is often at greater risk for defects than the center of the shaft, especially when the reinforcing cage is congested.

However, there are also concerns regarding TIP methods. The concerns primarily relate to interpretation of TIP measurements:

- What is the detection ability of TIP?
- How sensitive is it to defects?
- How should TIP records be evaluated?
- What magnitude of temperature dip should be considered problematic?

These questions are closely related to one another, and also to the relatively complicated thermodynamics of drilled shaft concrete. Importantly, these concerns primarily relate to interpretation of the test rather than limitations of the test itself. Interpretation improvements could therefore reduce concerns about TIP methods.

The goal of this research project was to support potential implementation of TIP methods for WisDOT drilled shaft projects. Results of this research provide information to help answer the questions surrounding interpretation of TIP methods, although the overall focus of the project was to produce practical recommendations regarding TIP implementation. The project had three specific objectives:

1. Demonstrate the effectiveness of TIP testing methods, specifically by evaluating the ability of TIP to identify defects of various locations and size.
2. Evaluate TIP’s viability as an alternative to CSL by comparing the effectiveness of each method.
3. If supported by data, modify WisDOT Standard Specifications to allow TIP testing and include recommended TIP procedures.

The research objectives were achieved through evaluation of previous TIP experience from WisDOT and other agencies as well as through collection of new data from full-scale field research. The field research involved performing TIP and CSL testing on three drilled shafts with planned concrete defects.

Background regarding CSL and TIP testing is provided in Chapter 2 of this report, which also summarizes the advantages and limitations of each test method and acceptance criteria for both. Chapter 3 summarizes previous research. Chapter 4 describes the field testing program, the results of which are presented in Chapter 5. Results of the field research and previous research are summarized and discussed in Chapter 6, and conclusions and recommendations are presented in Chapter 7.

2. Concrete Integrity Test Methods and the Significance of Defects

Information about methodology, advantages, and limitations of CSL and TIP test methods are presented in this chapter. Various acceptance criteria for both tests are also presented. Also included in the chapter is a summary of published results regarding the impact of drilled shaft defects on structural integrity.

2.1 Terminology

In this report, “defect” is used to refer to concrete within a drilled shaft that is compromised, e.g. weak concrete, segregated concrete, missing concrete (necking or otherwise), an inclusion of soil or slurry, etc. “Anomaly” is used to refer to concrete integrity test results that indicate a portion of a drilled shaft has an increased likelihood of being defective. Anomalies that are revealed to not be associated with defective concrete are false positives. If a concrete integrity test does not result in an anomaly where a defect is known, a false negative has occurred.

Some of the concrete integrity test literature and acceptance criteria use the terms “flaw” and “defect” to describe different levels of severity of an anomalous result. Such usage is confusing and can be misleading. In this report, the term “flaw” is avoided and “defect” is used only to refer to an actual deficiency in the concrete.

2.2 Crosshole Sonic Logging (CSL)

CSL (ASTM D6760, 2016) is the most common concrete integrity test performed for drilled shafts. The test involves measuring the passage of ultrasonic waves through access tubes attached to opposite sides of the shaft reinforcing cage as depicted in Figure 1. Incongruities in the resulting signal indicate potential anomalies of the concrete within the shaft reinforcing cage; concrete between reinforcing bars and outside the reinforcing cage is not evaluated. In the 2015 FHWA study of drilled shaft concrete practices (Boeckmann and Loehr), all 13 of the study agencies reported using CSL for concrete integrity testing for at least some drilled shafts, and eight of the 13 agencies reported using CSL in all shafts.

The area of the shaft investigated using CSL depends on the number of access tubes, as shown in Figure 1. The figure depicts CSL access tubes positioned inside the reinforcing cage for two shafts, one small-diameter shaft with four tubes and one large-diameter shaft with eight tubes. Assuming all access tube pairings are tested, the proportion of the shaft that is investigated is significantly greater for eight tubes than for four tubes. The greater number of tubes is associated with better coverage in the zone just inside of the reinforcing cage, as well as smaller zones of uninspected concrete between the ray paths. Importantly, the area outside the reinforcing cage is not inspected by CSL, regardless of the number of access tubes. In addition, the required personnel time to perform the test increases with the number of tube pairings.

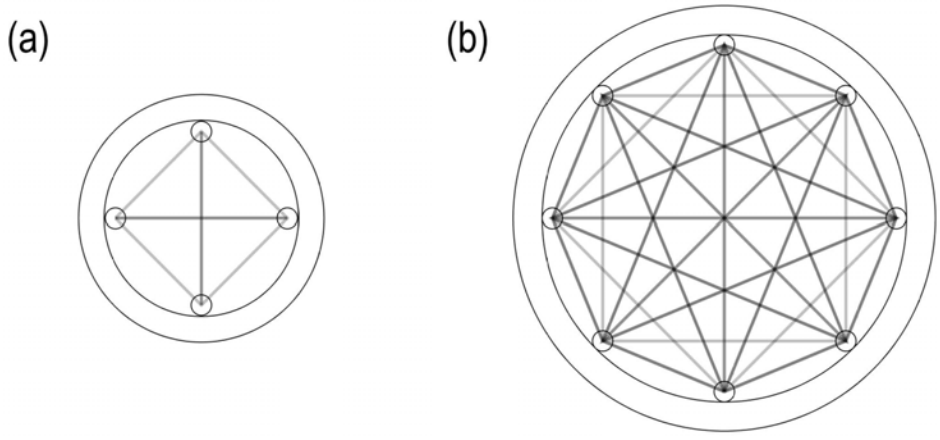

Figure 1: Drilled shaft cross-sections showing access tubes and ray paths for (a) small-diameter shaft with four access tubes and (b) large-diameter shaft with eight access tubes.

Access tubes for CSL testing are typically 2 in. diameter, Schedule 40 steel pipe. PVC pipe is also sometimes used, but PVC pipe is more susceptible to concrete debonding and pipe deformation, both of which produce false positive results. The number of access tubes included on reinforcing cages generally increases with shaft diameter, with many agencies requiring one tube per foot of shaft diameter and a minimum of four tubes for small shafts. The tubes should be water-filled to prevent debonding, and for operation of the test probes during the test procedure.

During the test, a source probe and receiver probe (geophones) are simultaneously raised from the bottom of separate access tubes. Per ASTM D6760, a common pulley equipped with a depth-encoding device is used to raise the probes. Ultrasonic pulses are sent from the source to the receiver as the probes are raised, and the ultrasonic response from the receiver is recorded for many depths. An example time record is shown in Figure 2(a) (ASTM, 2016). From each time record, the first arrival time (FAT) is interpreted, typically automatically by proprietary test software (rather than by test personnel). From the FAT, wave velocity can be interpreted by dividing the distance between tubes by the FAT. The relative energy is also commonly calculated for each time record from the amplitude of the pulses. The test is repeated for each combination of access tubes. The most common method for reporting results is to plot profiles with depth of FAT or wave velocity and relative energy for each combination of access tubes. An example profile set (FAT and relative energy) is shown in Figure 2(b) (ASTM, 2016). Spikes in arrival time and/or relative energy can be used to identify defective concrete, as discussed at the end of this chapter. For the record of Figure 2(b), spikes near 2, 8, and 14 m might indicate defects.

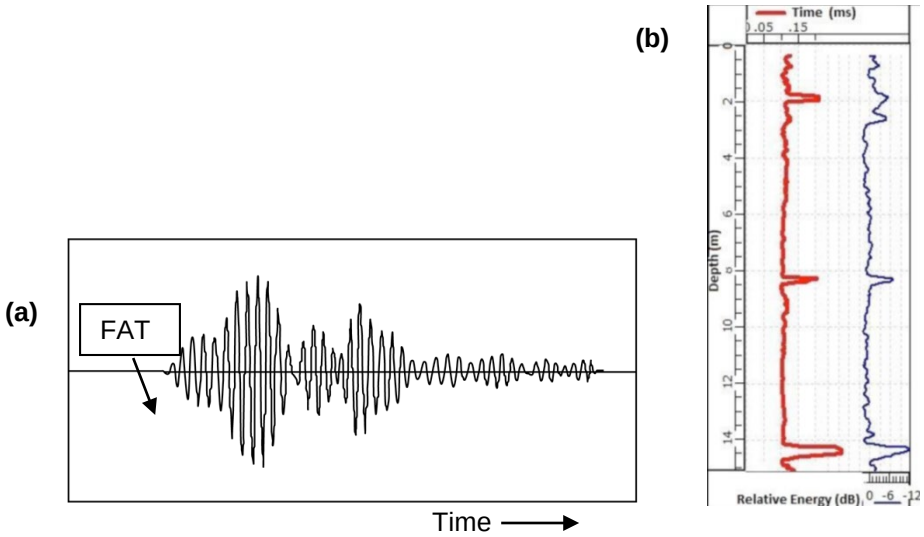

Figure 2: (a) Example time record for a single depth and single access tube pairing; (b) example plots of FAT (red line, left) and relative energy (blue line, right) versus depth. Modified from ASTM (2016).

2.3 Thermal Integrity Profiling

TIP methods (ASTM D7949, 2014) originated at the University of South Florida from work for the Florida DOT (Mullins et al., 2007). TIP test methods involve measuring drilled shaft temperature versus depth during concrete curing. Hydration of cement generates heat that increases shaft temperatures during curing. Defective or absent concrete results in less heat generation and therefore lower temperatures whereas bulges in the shaft produce greater temperatures. TIP results have also been used to infer the diameter of a drilled shaft and centrality of the reinforcing cage, but these inferences are based on interpretations rather than direct measurements.

Temperatures are measured along the length of the reinforcing cage using either a probe lowered down access tubes on the cage or using temperature sensors along sacrificial wires tied to the cage. Similar to CSL, the number of access tubes or wires generally increases with shaft diameter, one tube or wire per foot of shaft diameter is often specified, and a minimum of four tubes or wires is often required.

The 2015 FHWA study of drilled shaft concrete practices found that TIP methods were not as common as CSL, with six of 13 agencies indicating experience with TIP methods. The agencies generally expressed an interest in further implementation of TIP methods. One of the agencies, Washington State DOT (WSDOT), has incorporated TIP methods into its standard specifications.

2.3.1 Example TIP Records

Example TIP results for a drilled shaft with sound concrete are shown in Figure 3. The example case was documented by Mullins (2010). The data are from a 10 ft diameter shaft with 10 access tubes, with data collected by the probe method. The top 15 ft of the access tubes were in the stick-up length of the casing, which did not contain concrete but was likely heated by heat radiating from the top of the concrete. Below the top of concrete, the temperatures are relatively consistent, with a few noteworthy exceptions. First, a slight increase in average temperature is evident at 32 ft. Mullins explains that this blip corresponds to the groundwater depth at the time of drilling, when some minor sloughing occurred prior to slurry introduction. Second, the temperature variation from one tube to the next indicates eccentricity of the reinforcing cage, which causes some tubes to be closer to the center of the shaft while tubes on the opposite side of the shaft are further from the center. Third, temperatures decrease near the top and bottom of the concrete in the so-called “roll-off” zones. Roll-off occurs because heat flow at the ends of the shaft is dominated by longitudinal flow of heat out of the shaft, whereas along the rest of the shaft, heat flow is primarily radial out the sides of the shaft, which is insulated by soil and/or rock.

Example TIP results with a zone of defective concrete are shown in Figure 4. The example case was documented by Piscalko et al. (2016). The TIP data were recorded for a 10 ft diameter by 125 ft long drilled shaft with 10 TIP wires. A significant decrease in temperatures was observed in the TIP data at a depth of 90 ft (Figure 4(a)). The shaft was cored to investigate the potential defect. As shown in the photograph of Figure 4(b), the core results confirmed segregated concrete at 90 ft. The shaft was subsequently repaired by grouting.

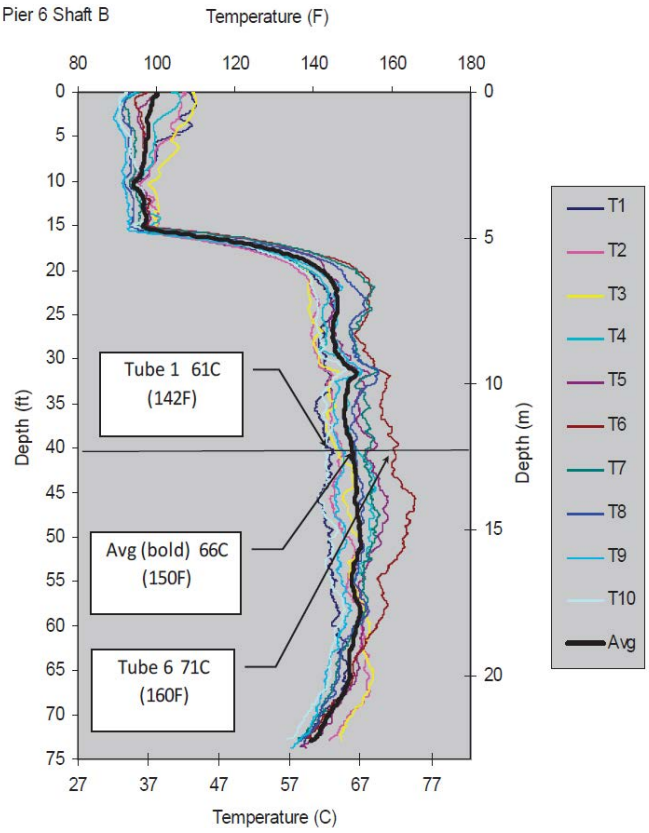

Figure 3: Example TIP result from Mullins (2010).

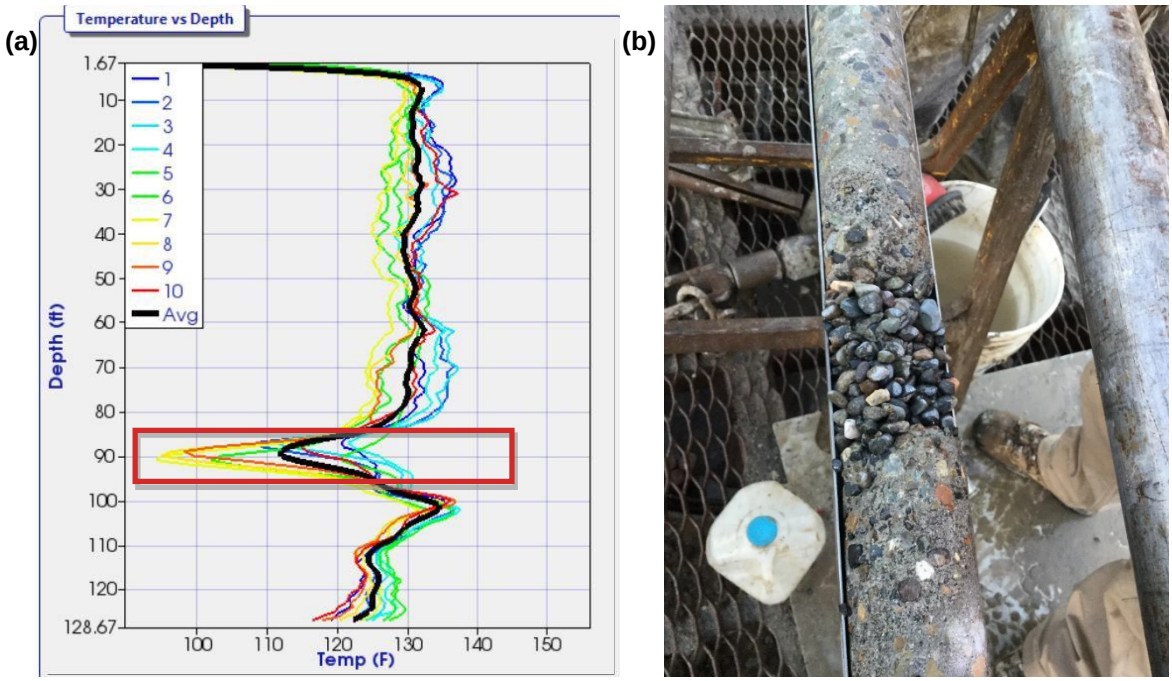

Figure 4: Example TIP result from Piscalko et al. (2016): (a) TIP record and (b) core photograph from a depth of 90 ft.

2.3.2 Time to Peak Temperature

The testing window for TIP methods is limited to the period of elevated temperatures in the drilled shaft concrete. The time to peak drilled shaft concrete temperature is variable. Drilled shaft concrete temperatures often peak in less than one day, but it is also common for peak temperatures to develop within one to three days, or even longer for some shafts. The time to peak temperature is greater for larger shafts, and it also varies considerably with concrete mix parameters. The ASTM standard recommends testing "near the time of peak temperature in the concrete." Since the time to peak cannot be known ahead of time (although it can be predicted), the ASTM standard recommends a testing window extending from 12 hours to D days, where D is the shaft diameter in feet.

Although references to "peak temperature" are included in virtually every TIP report and throughout published literature regarding TIP methods, no definition of peak temperature has been formally defined in any of the publications. It is important to note that during concrete curing, temperatures within a drilled shaft vary spatially—with depth and with distance from the center of the shaft cross-section—and with time. In addition, there is interaction between these effects. In other words, different locations within the shaft experience maximum temperatures at different times. Therefore, any given point in time may represent pre-peak, peak, or post-peak conditions, depending on location. These complications present challenges for defining peak temperature.

Several potential definitions of peak temperature are possible:

1. The maximum temperature observed in any of the TIP wires (or probes) at any depth (i.e. the single greatest measurement of all temperatures recorded).
2. The maximum temperature at any depth for the average temperature profile (i.e. the profile defined by averaging results from each of the wires).
3. The maximum temperature, averaged for all depths and all wires.

The second definition above was used for this project. For the purpose of interpreting TIP data, the peak temperature is primarily of interest as a means of normalizing the test interpretation time (e.g. evaluating

records at the time of peak temperature, at half peak, after peak, etc.). As discussed in the Section 2.3.4 below, the interpretation of TIP data is typically based on shaft temperatures at a single point in time.

It is possible that for many projects, the time to peak temperature would be similar for all three definitions above, but significant differences are also conceivable. The middle definition is likely to produce the most consistent definitions of time to peak temperature. The first definition is likely susceptible to cage misalignment, or simply to measurement outliers. In contrast, the last definition "averages out" significant effects like changes in diameter, casing, groundwater, and geology. Averaging these effects may be inappropriate when it could be more effective to define multiple peak temperatures (e.g. one time for a narrower portion near the bottom of a shaft and a later time for the top part of the shaft).

2.3.3 Probe versus Wire

Typically, TIP measurements are taken along the reinforcing cage either with a probe lowered down access tubes (Method A in ASTM D7949) or with sacrificial wires with temperature gages, typically spaced at 1 ft increments (Method B). Access tubes for the probe method can be the same as those used for CSL testing, but the tubes must be dewatered before inserting the temperature probe. PVC pipes can also be used as access tubes. A summary of advantages and disadvantages of the probe and wire methods are summarized in Table 1. Because TIP methods are premised on temperature development during curing, the window for testing is limited to the period of elevated temperatures as described previously. The test window limitation is significant for the probe method, which requires testing personnel to actively collect data whereas the wires are equipped with loggers that record data from the time of logger installation. Because of the testing window limitation, decreases in wire costs, and improvements in wire construction (i.e. reduced wire breakage as reported in Chapter 3), wire method implementations of TIP have greatly surpassed probe methods (J. Zammataro, personal communication, Nov. 14, 2017).

Some consultants have taken to performing TIP testing by suspending TIP wires in CSL access tubes, attempting to simultaneously realize (1) the advantages of maintaining the ability to perform subsequent CSL testing with (2) the time record from the wires (and without the expense of the probe). However, Schoen et al. (2018) showed convincingly that the effect of defects on measured temperatures is greatly diminished when wires are suspended in access tubes. In addition, the ASTM standard does not include the suspended wire approach. The suspended wire approach is therefore not recommended and was not evaluated in the field research.

Table 1: Comparison of TIP probe and wire methods.

	Advantages	Limitations
Thermal Probe (Method A)	• Access ducts support TIP as well as CSL. • Probe can be reused or rented.	• Difficult or impossible to detect defects if collection occurs too far before or after peak shaft temperatures develop. • Time-consuming data collection. • Difficulties interpreting data for large shafts due to temperature changes during data collection time. • Initial equipment cost.
Wire (Method B)	• Nearly continuous record of temperatures: o Improves interpretation. o Eliminates risk of missing peak temperatures. o Additional data may be useful for thermal modeling. • Data collection is simple.	• Cannot perform CSL unless access tubes are installed separately. • Wires are sacrificial. • Data collected at relatively larger intervals (typically 1 ft).

2.3.4 Interpretation of TIP Results

The fundamental concept that is the basis for TIP – drilled shaft concrete temperatures can be used to identify defective concrete – is fairly simple, but interpreting the results of TIP tests can be less so, particularly if a quantitative interpretation is required. In a report for WSDOT regarding TIP testing, Mullins and Winters (2011) established four levels of TIP interpretation:

- Level 1 – Direct observation of the temperature profiles
- Level 2 – Superimposed construction logs and concrete yield data
- Level 3 – Three dimensional thermal modeling
- Level 4 – Signal matching numerical models to field data

The vast majority of TIP applications use Level 1 and/or Level 2 interpretation, both of which are detailed below. Level 3 and Level 4 interpretations are less common: none of the many published project applications of TIP included Level 3 or 4 analysis. Mullins and Winters did not outline Level 3 and Level 4 analysis procedures in the WSDOT report, but they did apply Level 3 analyses to the test cases they interpreted. In addition, details of a thermal modeling approach for drilled shafts are provided in the original TIP development report by Mullins et al. (2007).

Level 1 analysis is a qualitative assessment of TIP data. The discussion of the examples in the previous section could be considered Level 1-type analyses. In short, TIP results for the example from Figure 3 indicated sound concrete with no major concerns, but the results for the example of Figure 4 indicated a potential defect at a depth of 90 ft. Importantly, Level 1 analysis of the second example would be sufficient to trigger action (the coring that was performed). Mullins and Winters describe effects that can be considered during a Level 1 assessment. The list below includes items from their report as well as some supplementary considerations:

- Changes in shaft diameter, as indicated by the average temperature. Diameter changes could be part of the shaft design (e.g. telescoping casing), incidental to construction (e.g. temporarily cased segments of the shaft typically have a slightly greater diameter than uncased sections of the same nominal diameter), or indicate defects (e.g. bulging or necking).
- Proper cage alignment, as indicated by relative uniformity among wire (or tube) temperatures.
- Roll-off zones at the top and bottom of the shaft. Mullins and Winters note the length of each roll-off zone is typically within one shaft diameter.
- Groundwater table
    - Greater temperatures at the location of the groundwater table can be produced by bulging, especially in granular materials (e.g. Figure 3)
    - Saturated materials have greater thermal conductivity; all else equal, greater temperatures would generally be anticipated above the groundwater table.

The engineer's responsibility during a Level 1-type assessment is to evaluate how trends in the observed TIP data can be explained by effects like those explained above. The responsibility further includes evaluating how significant any deviations are, and whether they warrant further action, but this responsibility is common to all levels of TIP interpretation, and to other integrity tests. Information regarding the potential significance of defects is included at the end of Chapter 3.

Level 2 (and Level 3 and 4) assessments are based on interpretations of "effective radius," which Mullins and Winters defined as the predicted radius that would produce the observed temperature in the TIP data. The concept behind the effective radius approach is to "convert" the observed temperatures to shaft radius at each wire and for every depth. The effective radius values can then be used to assess average shaft diameter, cage eccentricity, and concrete cover, all of which are generally more meaningful parameters for evaluating concrete integrity than raw concrete temperature. Pile Dynamics, Inc. (PDI), which manufacturers the most commonly used TIP equipment, has adopted the effective radius approach within its TIP software, so it is common to see plots of effective radius presented with temperature plots in TIP reports. Details of the effective radius approach are presented in this section.

The premise of the effective radius approach is that concrete temperatures near the edge of a drilled shaft are strongly influenced by two factors: shaft radius and radial position, defined as the distance from the center of the shaft. This concept can be observed in Figure 5. The graph in Figure 5 is from Johnson (2016), who based the graph on results of analytical thermal models by Mullins (2013). The sloping surfaces shown in the figure represent significant increases in temperature with (1) increasing shaft radius and (2) decreasing distance from the shaft center. Applied to TIP, this means that depths of greater-than-average measured temperatures could be explained by either (1) the shaft being larger or (2) the measurement points being closer to the center of the shaft. These explanations correspond to the yellow circle points in Figure 5 being (1) further right along the black dashed line or (2) being closer to the center along the solid red line. By incorporating multiple TIP wires (or access tubes), it is possible to distinguish between the two effects at a given depth: (1) increases in temperature due to larger shaft radius would be indicated by increases in the average wire temperature whereas (2) increases in temperature due to wire location would be indicated by differences in the temperatures among the various wires.

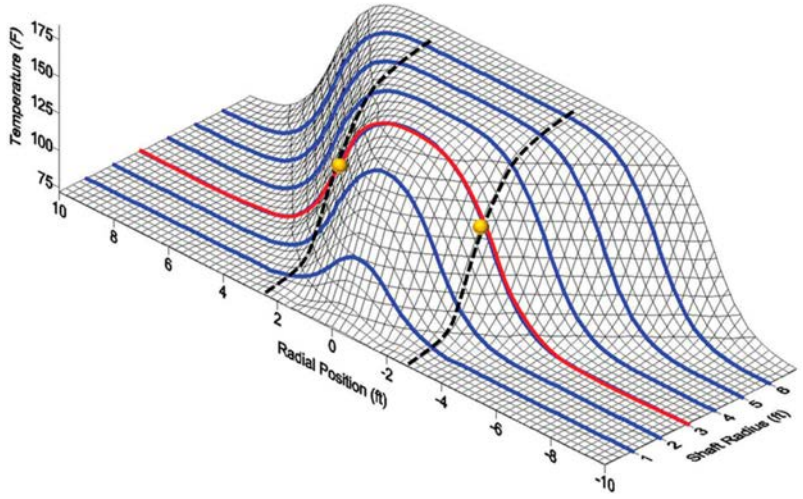

Figure 5: Drilled shaft temperatures as a function of radial position and shaft radius. From Johnson (2016) and Mullins (2013).

Practically, the effective radius premise for TIP interpretations is implemented through temperature-radius models, which are relationships used to infer radius from temperature measurements. There are several methods for creating temperature-radius models. Level 2 assessments create the models empirically using TIP results and concrete volume records from the drilled shaft installation. Concrete volume information is a recommended component of drilled shaft construction QA/QC procedures (e.g. FHWA's Drilled Shaft manual; Brown et al., 2010). A useful means for conveying concrete volume information is to plot the cumulative volume of concrete placed versus depth. An example concrete volume plot is shown in Figure 6. The plot includes points for each volume measurement, which typically represents the volume placed from one concrete truck. The plot also shows the theoretical volume for the design shaft, which is generally less than the actual volume. The slope of the actual volume versus depth line corresponds to the cross-sectional area of the shaft, from which the shaft radius can be calculated. Thus, for each line segment on the concrete volume plot, one shaft radius value can be interpreted.

Level 3 analyses are similar to Level 2, but the temperature-radius model is developed using a thermal model rather than using the concrete volume measurements. Level 4 analyses contain all of the components of a Level 3 analysis. In addition, the thermal model for a Level 4 analysis is calibrated so that predicted temperatures are consistent with TIP measurements. The temperature versus radius model used to interpret the effective radius values is based on the calibrated thermal model. No examples of Level 4 analyses were found in the literature.

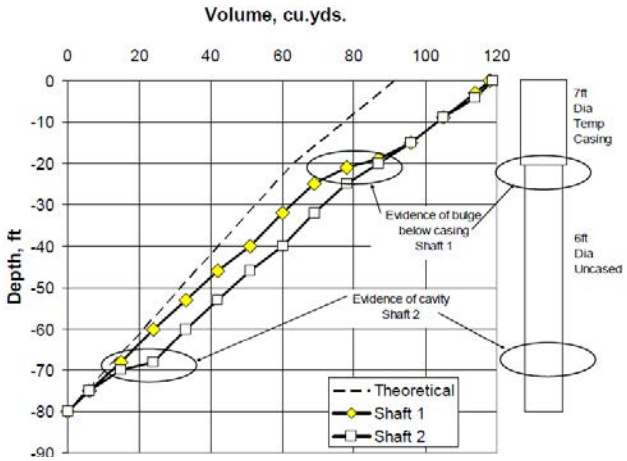

Figure 6: Example concrete volume record from FHWA's Drilled Shaft manual (Brown et al., 2010).

Example temperature-radius data for a Level 2 assessment by Mullins and Winters (2011) are shown in Figure 7, which is a profile of TIP and shaft diameter values with depth for a 7 ft diameter shaft. The heavy black line in the figure is the average temperature from the TIP data, and the pink line with square dots is the shaft diameter as interpreted from the concrete volume log. There appears to be significant correlation between the average temperature and the shaft diameter, as the shape of both plots is similar. The correlation is confirmed by the temperature-radius model shown in Figure 8. The temperature-radius relationship used for the data is from linear regression.

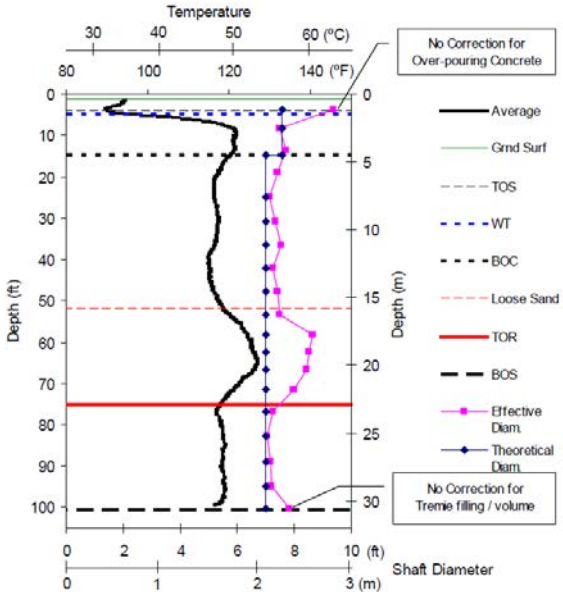

Figure 7: TIP data used for example temperature-radius model by Mullins and Winters (2011).

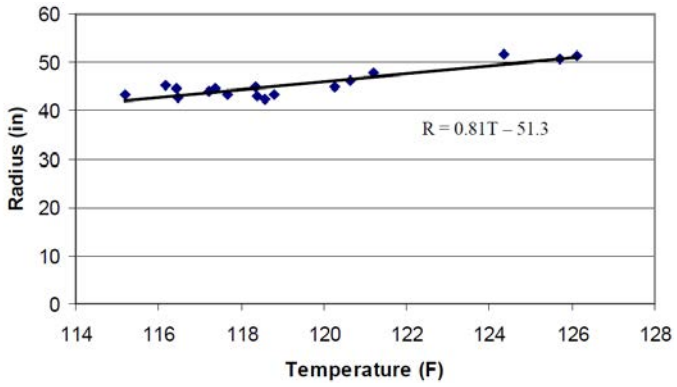

Figure 8: Example Level 2 temperature-radius model from Mullins and Winters (2011). Model is based on the data from Figure 7.

Figure 9 shows the results of applying the temperature-radius model from Figure 8 to all of the TIP data collected for the shaft in order to produce effective radius values. Specifically, each TIP temperature measurement is used in the regression equation to infer the effective radius with depth for each TIP access tube. Also shown in Figure 9 is the design radius of 3.5 ft, represented by a vertical blue line. The effective radius interpretation implies the overall average shaft radius is greater than design, since most points are to the right of the blue line. This implication follows directly from the observation that the total volume of concrete placed was greater than the theoretical volume. The vertical dashed black line in Figure 9 represents the design cage location; the distance between the dashed black line and the solid blue line, 6 in., is the design concrete cover distance. Accordingly, the effective radius results near a depth of 50 ft imply a complete loss of cover at TIP access tubes t3 and t4.

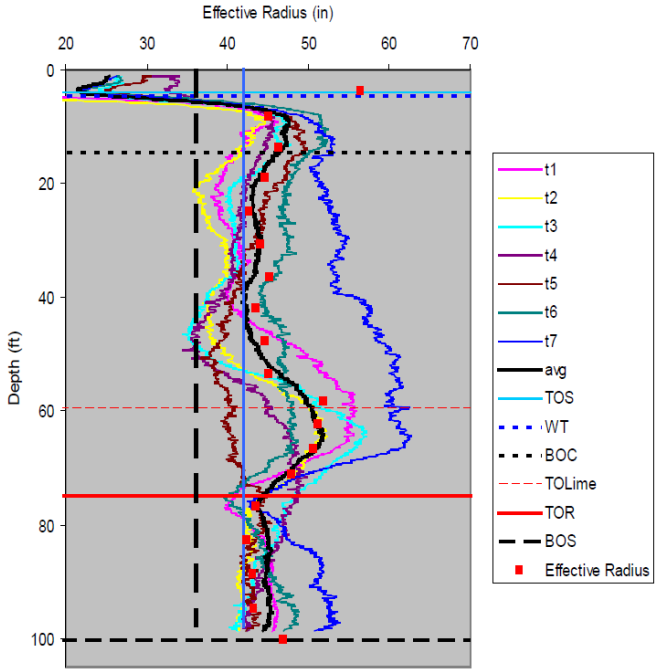

Figure 9: Example effective radius analysis from Mullins and Winters (2011) using TIP data from the example of Figure 7 and the temperature-radius model shown in Figure 9.

For some shafts, there may not be sufficient volume data to generate a temperature-radius model like the one shown in Figure 8. This is especially likely for small-volume shafts requiring only a small number of trucks and/or with partial truck volumes. For such shafts, Johnson (2014, 2016) outlines a “single-point”

method for developing temperature-radius models. The single-point concept is presented in Figure 10. The yellow diamond represents the "single-point" consisting of one average radius value based on the total volume of concrete placed in the shaft and the average overall shaft temperature. Rather than regressing through multiple points as in Figure 8, the temperature-radius model extends from the origin through the single, averaged point. Johnson (2014) explains the single-point method leads to "conservative" interpretations of TIP data (i.e. over-prediction of necking or bulging) compared to interpretations using the "true" theoretical model represented by the blue line in Figure 10. Incidentally, the theoretical model represented by the blue line is an example of the type of temperature-radius models used for Level 3 analysis.

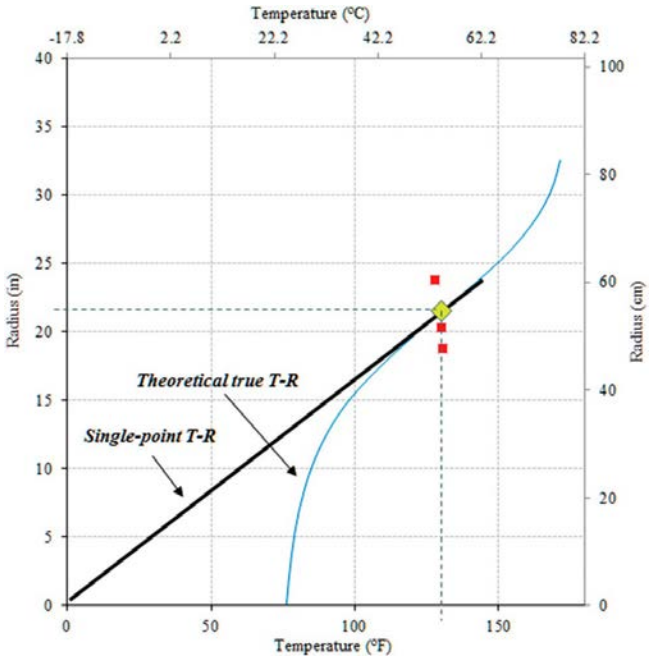

Figure 10: Single-point method for temperature-radius models from Johnson (2016).

Johnson also notes that the empirical temperature-radius models (e.g. the model shown in Figure 8 and the single-point model in Figure 10) only apply to zones where heat flow is predominantly out the sides of the shaft with negligible longitudinal (vertical) heat flow. The roll-off zones at the top and bottom of every shaft violate this assumption, as do several other potential shaft "transition" scenarios: changes in diameter, changes in geology, presence of groundwater, and likely others. To account for the roll-off and transition zones, Johnson (2014) describes a curve-fitting approach depicted in Figure 11. The approach involves fitting a hyperbolic tangent function to the TIP measurements and then calculating "corrected" temperatures from the difference between measurements and the fitted curve. The corrected temperatures are essentially normalized to the temperatures just below the top roll-off zone or just above the bottom roll-off zone. The corrected temperatures were conceived to represent the temperatures that would be expected without the longitudinal heat flow, and therefore to be useful both for developing temperature-radius models (e.g. as in Figure 8) and for interpreting TIP measurements.

In Figure 11, the black points represent TIP measurements, the solid red line is the fitted hyperbolic tangent function, and the dashed blue line is the corrected temperatures. Because the hyperbolic curves fit the measured data at the top and bottom of the shaft well, the corrected temperatures in the roll-off zones are similar to the temperatures just outside the roll-off zones. If the agreement between measured temperatures and the fitted hyperbolic tangent curve were weaker, corrected temperatures would deviate from the temperatures outside the roll-off zones. The TIP software implemented by PDI applies the corrected temperature adjustments at the top and bottom of each shaft by default. It also includes an option to include adjustments at user-specified depths for transitions between the ends of the shaft.

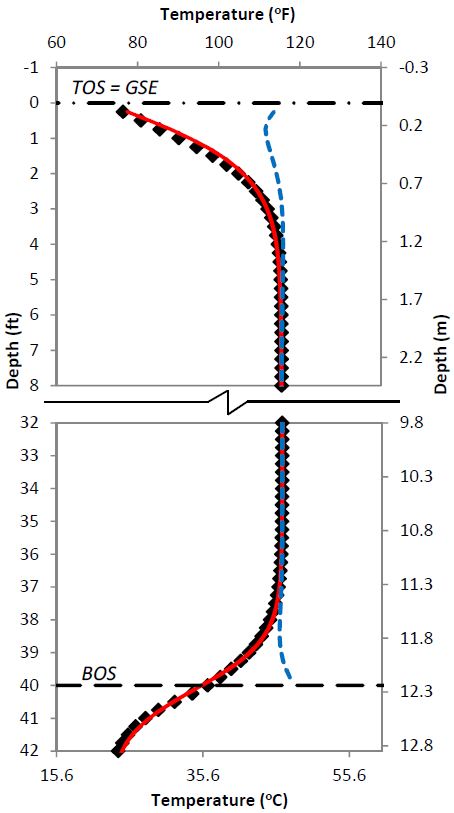

Figure 11: Curve fitting at roll-off zones at top of shaft (TOS) and bottom of shaft (BOS) from Johnson (2014).

2.3.5 TIP Costs

The cost of TIP testing depends on drilled shaft diameter, project size, the number (percentage) of shafts to be instrumented, and likely other factors. The cost also depends on whether the probe or wire method is used. If the probe method is used, material costs are associated with the access tubes and related hardware and the electronics equipment, which can be rented or purchased. Labor costs for the probe method result from installing the access tubes on the reinforcing cage, performing the test, and analyzing the data. If the wire method is used, material costs are associated with the sacrificial thermal wires and the equipment used to collect and analyze data from the wires. The equipment can be rented or purchased. In 2018, a general unit price for estimating the delivered (not installed) cost of thermal wires is $5 per foot, plus $25 for each individual wire and any freight expenses. Labor costs for the wire method result from three tasks: installing the wires on the reinforcing cage, collecting the data, and analyzing the data. In addition to material and labor costs, there may also be mobilization and travel expenses for each test method.

The cost of TIP compared with CSL also depends on which method is used. For the probe method, costs are generally similar to CSL since the tests use the same access tubes and have similar time requirements on site. For the wire method, cost comparison depends on the scale of the project. Material and labor costs for installation of TIP wires and associated test equipment are generally comparable to material and labor costs for installation of CSL access tubes and CSL test equipment. Accordingly, the total cost of TIP wires and CSL is likely similar for small projects. For projects with many drilled shafts to be tested, the cost of TIP may be less than the cost of CSL because TIP wire data can often be downloaded by the contractor whereas CSL requires a testing crew to perform CSL tests several days after each shaft is completed. For any given project, the cost of analysis and interpretation of the results should be comparable for TIP by probe, TIP by wire, and CSL.

2.4 Gamma Gamma Logging (GGL)

A third concrete integrity test method, Gamma Gamma Logging (GGL), is also available but commonly used only in California. The GGL test measures gamma rays to interpret concrete integrity in a zone approximately 3 in. around PVC access tubes attached to the reinforcing cage. The test is useful for evaluating concrete in the cover zone, but it does not identify defects in the center of the cage. In addition, there are practical drawbacks: it requires a nuclear source and it requires PVC access tubes that cannot be bundled with vertical reinforcement on the reinforcing cage, so it complicates cage design and congestion.

2.5 Acceptance Criteria for CSL and TIP

A critical aspect of concrete integrity tests is acceptance criteria: the methodology for evaluating the interpreted test results to reach a conclusion of either accepting the concrete placement or requiring further action (e.g. engineering analysis, coring, etc.). State transportation agency specifications, research reports, project reports, and TIP literature were reviewed to identify both suggested and adopted acceptance criteria for CSL and TIP. Results of the review are summarized in Table 2.

Table 2: Acceptance criteria for CSL and TIP from various sources.

Source	Acceptance Criteria	
	CSL	**TIP**
ASTM	No specific criteria. “How one applies the results obtained using this standard is beyond its scope.”	No specific criteria. “Interpretation …should contain proper engineering judgment and experience.”
Washington State DOT Standard Specifications (2018)	Good: No signal distortion and decrease in signal velocity of 10% or less. Questionable: Minor signal distortion and lower signal amplitude with a decrease in velocity between 10 and 20%. Poor: Severe signal distortion and much lower signal amplitude with a decrease in signal velocity of 20% or more.	Satisfactory: 0 to 6% reduction in effective shaft radius and cover criteria met. Questionable: effective local radius reduction > 6%, effective local average diameter reduction > 4%, or cover criteria not met.
Florida DOT Standard Specifications (2018)	Velocity reduction greater than 30% is not acceptable without 3D tomography and subsequent engineering analysis.	No specific criteria, but requires reports to indicate “unusual temperatures, including cooler local deviations from the average at any depth [or] from the overall average over the entire length.” Reports must also include “a conclusion stating whether the tested shaft is free from integrity defects and meets the minimum concrete cover and diameter requirements by the specifications.” Thermal modeling (i.e. Level 3 interpretation) is required to satisfy report requirements.

Source	Acceptance Criteria	
	CSL	**TIP**
Mullins et al. (2009) Draft Specifications for FDOT *Note: Not implemented (per above row)*	N/A	Included two potential criteria, both of which require thermal modeling: (1) "Test results with deviations greater than 5 degrees over a 1 ft length shall be further evaluated using Signal Matching Analyses to determine the possible shaft cross-section loss." (2) "Drilled shafts with either insufficient cover or 5 degree Fahrenheit reduction from the model norm over a length of shaft at least 2 ft in length will not be accepted without an engineering analysis."
Likins and Mullins (2011)	Good: Velocity reduction less than or equal to 10%. Questionable: Velocity reduction between 11 and 29%. Poor: Velocity reduction 30% or greater.	Good: No reduction in effective radius. Questionable: Radius reduction less than or equal to 1 in. Poor: Radius reduction greater than 1 in.
Piscalko et al. (2016) (See also Section 2.6.2)	N/A	Satisfactory: 0 to 6% reduction in effective radius ***and*** local cover criteria satisfied. Anomaly: Greater than 6% reduction in effective radius ***or*** local cover criteria not satisfied.
GRL Engineers Documentation (2015)	Good: First Arrival Time (FAT) increase less than 10%; energy reduction less than 6 dB Questionable: FAT increase between 10 and 20%; energy reduction between 6 and 9 dB Flaw: FAT increase between 20 and 30%; energy reduction between 9 and 12 dB Defect: FAT increase greater than 30%; energy reduction greater than 12 dB	N/A
PDI Documentation (2017)	N/A	No specific criteria, but requires potential local anomalies be reported. Local anomalies are indicated by "locally low temperatures relative to the average temperature at that depth, or average temperatures significantly lower than the average temperatures at other depths."
Deep Foundations Institute (2018)	Defines three rating classes graphically based on combinations of FAT increase (%) and energy reduction (dB). Class A ratings are acceptable, Class B ratings are conditionally acceptable, and Class C ratings are highly abnormal.	N/A

Table 2 reveals significant differences in the states of practice for interpretation of CSL and TIP:

- Acceptance criteria for CSL are relatively consistent. The criteria are generally based on quantitative interpretation of measured values (arrival times) and values calculated directly from the measurements (velocity and energy). There are some ambiguities in the interpretation:
    - How is the "baseline" arrival time or energy measurement for calculation of percent change determined?
    - Should the Engineer consider anomalies based on either arrival time (velocity) or energy, or must both quantities be anomalous to trigger the various action levels?

- Compared to CSL, acceptance criteria for TIP are less explicit, with many TIP specifications either not establishing acceptance criteria or recommending acceptance based on the Engineer's judgment. The quantitative acceptance criteria that have been implemented are primarily based on inferred values of effective radius rather than direct measurements of temperature. The effective radius is calculated from the techniques described in the previous section.

That the state of practice for interpretation of TIP is less quantitative and perhaps less consistent than CSL is not surprising considering TIP methods are newer. The lack of consistent criteria for TIP also presents an opportunity to develop interpretation approaches that are best suited for identifying defects.

2.6 Significance of Drilled Shaft Concrete Defects

Many concrete integrity test acceptance criteria call for an engineering assessment in the case of anomalies. A fundamental consideration in such assessments is the impact of the potential defect on drilled shaft capacity. Two published studies examining this topic were reviewed. The first, a major research study by Sarhan et al. (2000) for ADSC, FHWA, and a pool of DOTs, considered multiple types of defects under various loading configurations, with results based on finite element models calibrated to the results of lab and full-scale field tests. The second (Piscalko et al., 2016) was a narrower study hypothesizing on potential effects of drilled shaft radius reduction on various capacities.

2.6.1 Sarhan et al. (2000)

A comprehensive study of the effect of drilled shaft defects on structural resistance was performed by Sarhan et al. (2000) for ADSC (The International Association of Foundation Drilling), FHWA, and a pool of state DOTs. The study included five phases:

1. A geotechnical field study consisting of one control shaft and five 30 in. diameter drilled shafts with intentional defects installed at the National Geotechnical Experimentation Site in Houston. Lateral load tests were performed to determine the effect of the defects on lateral resistance.
2. Shaft excavation and calibration of the test results using a finite-difference code capable of analyzing the defective shaft cross-sections.
3. Scaled structural lab tests of model drilled shafts under various combinations of axial and flexural loading.
4. Structural load tests of full-scale (30 in. diameter) drilled shafts at FHWA's Turner-Fairbank Research Laboratory to validate the scaled model lab test results from Phase 3.
5. Calibration of the results from Phases 3 and 4 with finite element models and subsequent analysis of various combinations of axial and bending loading with various types of drilled shaft defects.

For Phases 3 and 5, multiple types of defects were considered:

- Necking voids on the compression side of the shaft with areas equivalent to 15% of the shaft cross-sectional area
- Reinforcing cage offsets of 4%
- Reinforcing bar corrosion for bars on voided side of shaft, with a cumulative loss of 15% of the total steel in the cross-section
- Reduction in concrete compressive strength (f'_c) of 15%

The Phase 5 analyses of full-scale drilled shafts considered axial and flexural loading of shafts with one defect as well as shafts with combinations of two and three defects. For all analyses, the defects were assumed to occur at the critical drilled shaft depth, i.e. the depth with the greatest impact on capacity. Deterministic resistance factors were calculated for all load-defect combinations as the ratio of the capacity of the defective section to the capacity of the non-defective section. The results are summarized in Table 3. For a single defect, the effects are relatively modest, representing at most an 18% loss of axial capacity and a 27% loss of flexural capacity. Necking voids produced the most significant reductions in capacity for both axial and flexural loading. The reduction in capacity is significantly worse when combinations of two and three defects are considered. However, Sarhan et al. note that the possibility of multiple critical defects occurring simultaneously at the critical positions along the shaft is "believed to be extremely remote."

Table 3: Summary of structural resistance factors for drilled shafts with various defects from the results of Sarhan et al. (2000).

Type of Defect	Axial Resistance Factor	Flexural Resistance Factor
Necking Void	0.82-0.89	0.73-0.87
Cage Offset	1.00	0.95
Corrosion	0.94	0.81
Reduction in f'_c	0.90	0.97
Combination of Two Defects	0.76-0.94	0.57-0.93
Combination of Three Defects	0.63-0.67	0.53-0.57

2.6.2 Piscalko et al. (2016)

Piscalko et al. (2016) used the results of a simple geometric analysis to justify acceptance criteria for TIP testing based on effective radius interpretations. The acceptance criteria are presented in Table 2. The premise of the approach is that various types of structural and geotechnical drilled shaft capacities are directly related to radius:

- Side resistance is related to the circumference of the shaft and therefore the radius.
- Compression capacity is related to the shaft area and therefore the square of the radius.
- Bending capacity is related to the shaft moment of inertia and therefore the radius raised to the fourth power.

The resulting criteria developed by Piscalko et al. are based on simple calculations of circumference, area, and moment of inertia. They assume a concentric loss of radius and do not include any structural analysis. The results by Sarhan et al. (2000) are therefore a more realistic assessment of the impact of defects on structural resistance.

3. Sensitivity of TIP Results to Defects

One of the primary objectives of this research is to evaluate the ability of TIP to detect concrete defects. In addition to performing field research to investigate TIP sensitivity, a review of literature and engineering practice was performed to identify previous related works. The review was conducted prior to the field research in order to improve the experimental design of this project (Chapter 4). Results of the review are presented in this chapter.

3.1 Previous Research regarding TIP Sensitivity to Defects

Several previous studies have been conducted to investigate the ability of TIP measurements to identify drilled shaft defects. Three such studies are presented in this section.

3.1.1 Florida DOT Study by Mullins et al. (2007)

The original study of TIP by Mullins et al. (2007) included construction of a test shaft with planned defects to evaluate TIP sensitivity. The 4 ft diameter, 25 ft deep test shaft was installed in relatively uniform, saturated sandy soil. Two defects were installed, both consisting of bagged native soil tied to the outside of the reinforcing cage. The cross-sectional area of each defect represented approximately 10% of the shaft. The shallower defect, at a depth of 8 ft, had bags tied to two opposite sides of the reinforcing cage as shown at the bottom of Figure 12. The deeper defect, at a depth of 17 ft, had all bags tied on one side of the reinforcing cage, centered around Tube 1 as shown in Figure 12.

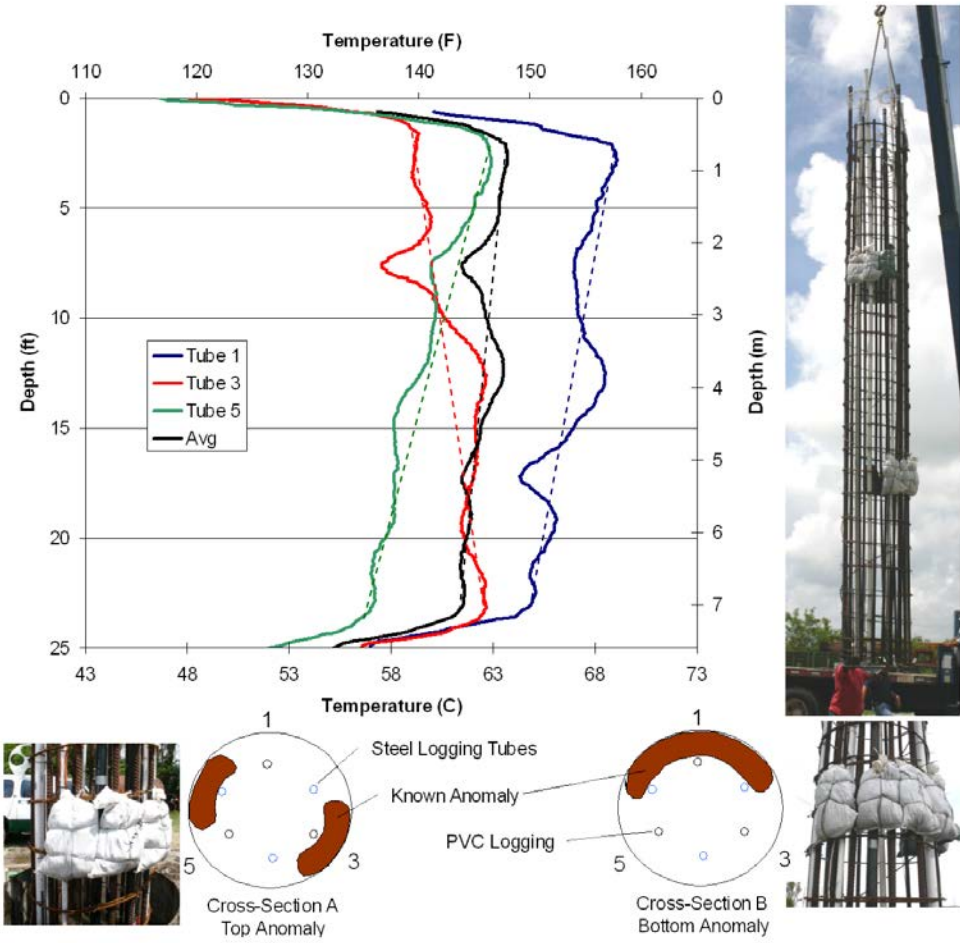

Figure 12: Results of FDOT TIP study by Mullins et al. (2007), as presented by Mullins and Winters (2011).

Mullins et al. performed TIP testing by probe every 3 hours. Results of the TIP testing 15 hours after concrete placement are shown in Figure 12. The exact peak time is not clear from the original reporting, but it is likely around the time shown in Figure 12 (15 hours). Before examining the influence of the defects on TIP temperatures, it is worth noting the wide variation in temperatures among the three access tubes. Mullins and Winters (2011) attributed the variation to poor cage alignment, which could also explain the tendency for tube temperatures to increase or decrease with depth.

It is helpful to consider the effect of cage alignment when evaluating the effect of the defects, which is why Mullins and Winters included the dashed lines in Figure 12. Temperature decreases were observed in all three tubes at the top defect, but the decrease was most significant in Tube 3. The temperature in Tube 3 decreased to 137° F at the defect depth, but it is uncertain what the temperature might have been without the defect. If the dashed line of Figure 12 is correct, the decrease was only 4° F, but the temperature without the defect could likely have been greater than implied by the dashed line considering the curvature of the Tube 3 temperature profile. It is similarly difficult to evaluate the effect of the bottom defect. There is a clear decrease in temperature in Tube 1 near the bottom defect to about 149° F. If the dashed line is correct, this represents approximately a 3° F decrease, but it is likely the temperature that would have been observed without the defect would have been greater than implied by the dashed line based on the curvature of the profile. If the presence of the defects were not known, it is not certain the bottom defect would be detected, especially considering temperatures in Tube 3 were above average.

3.1.2 Iowa DOT Study by Ashlock and Fotouhi (2014)

Ashlock and Fotouhi (2014) conducted research for the Iowa DOT that investigated the sensitivity of TIP and CSL to defects. The research included two 5 ft diameter, 80 ft long shafts installed at a site near Des Moines with approximately 45 ft of sand over interbedded shale, limestone, and sandstone. The top 11 ft of the test shafts were temporarily cased with a 6 ft diameter casing. Each test shaft included two defects, which are summarized in Table 4. All defects were installed on the inside of the reinforcing cage and concentrated on one side of the cage (rather than concentrically around the cage). The defects were small, at 3 to 8% of shaft cross-sectional area. For comparison, the defects by Mullins et al. (2007) represented 10% of cross-sectional area. For Test Shaft 1, the defects consisted of hardened concrete cylinders with low cement content to achieve compressive strength around 600 psi. The defects for Test Shaft 2 were cylinders filled with sand, gravel, and water in similar proportion to the first test shaft concrete mix, but without cement.

Table 4: Summary of defect characteristics from Ashlock and Fotouhi (2014) study.

	Type of Defect	Defect Depth, ft	Size of Defect, % of cross section
Test Shaft 1	Cylinders of weak concrete	8	3
		29	4
Test Shaft 2	Cylinders of aggregate and water	15	8
		32	8

Ashlock and Fotouhi performed TIP testing via the probe method. Results of TIP testing are shown in Figure 13 for Test Shaft 1 and Figure 14 for Test Shaft 2. Results include temperatures as well as effective radius interpretations according to the Level 2 method outlined in Chapter 2. For Test Shaft 1, there was no perceptible decrease in temperature or effective radius at either defect location. For Test Shaft 2, the TIP response is dominated by cage misalignment, which resulted in temperature variations as great as 25° F among tubes near the shaft mid-height. Such variation makes interpretation of a temperature change due to the defects challenging. There is perhaps a modest decrease in temperatures near Tube 3 for both defects, but this decrease is at most 3° F for the top defect and 2° F for the bottom defect. These decreases are considerably less than the significant increase in temperatures near a depth of 45 ft. SoniCaliper results and concrete volume log results indicate a bulge at this depth corresponding to about a 4 or 5 in. radius increase. A bi-directional load testing cell (“O-cell”) was included in both test shafts. For both shafts, the temperature decreases due to the O-cell were greater than those due to the intentional defects.

CSL results from Ashlock and Fotouhi (2014) are presented in Figure 15 for Test Shaft 1 and in Figure 16 for Test Shaft 2. CSL results for Test Shaft 1 showed no significant increase in arrival time for either defect. For Test Shaft 2, an increase in arrival time of approximately 25% was observed for both defects. Such an increase straddles the line between questionable and actionable, depending on acceptance criteria (Table 2).

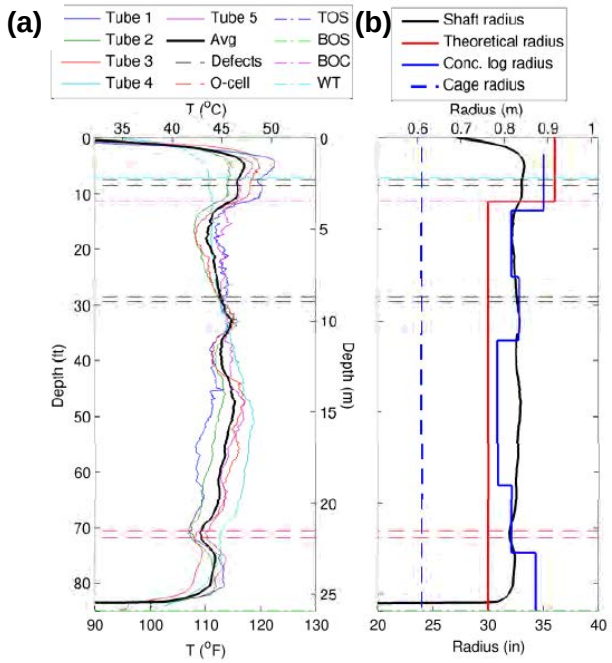

Figure 13: TIP results for Test Shaft 1 from Ashlock and Fotouhi (2014): (a) temperature and (b) effective radius.

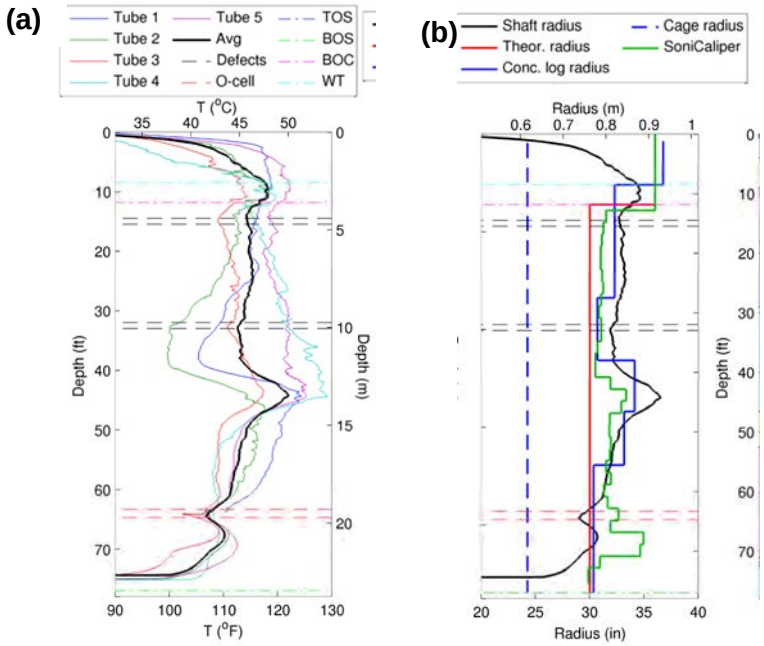

Figure 14: TIP results for Test Shaft 2 from Ashlock and Fotouhi (2014): (a) temperature and (b) effective radius.

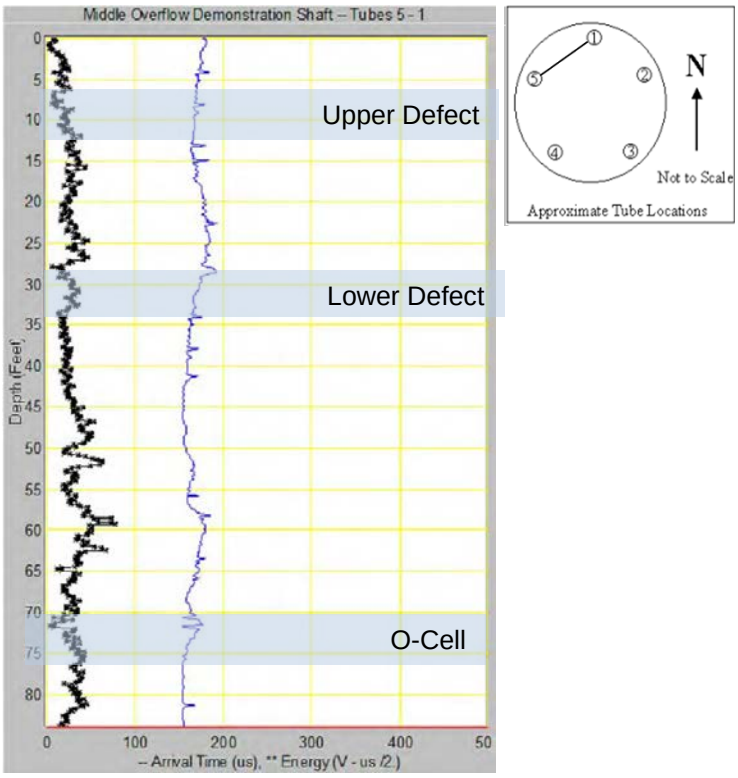

Figure 15: CSL results for Test Shaft 2 from Ashlock and Fotouhi (2014).

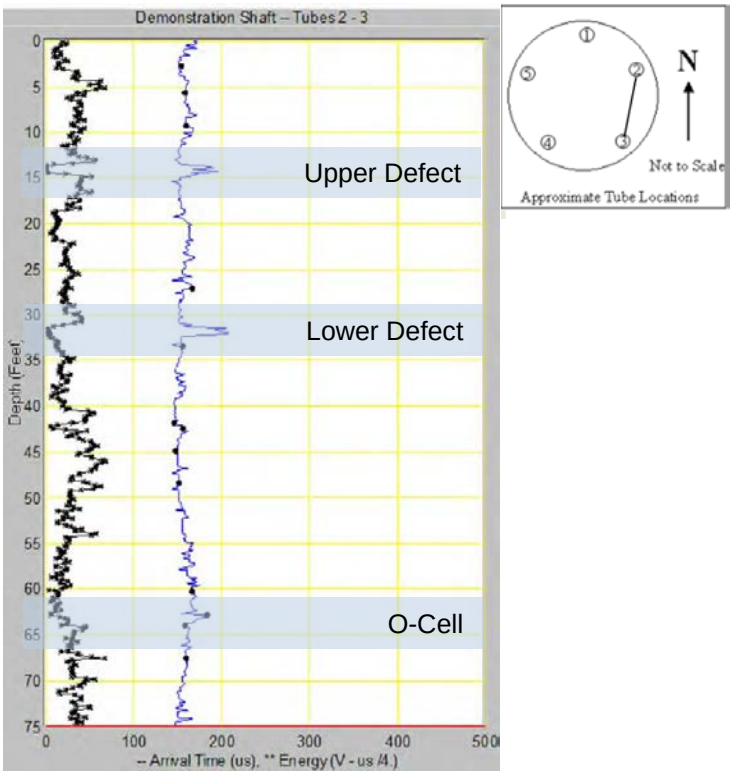

Figure 16: CSL results for Test Shaft 2 from Ashlock and Fotouhi (2014).

3.1.3 Schoen et al. (2018)

Schoen et al. (2018) documented TIP testing for a 102 ft long by 5 ft diameter drilled shaft in South Carolina. The shaft was constructed as a design-phase load test shaft. Schoen et al. installed known defects consisting of gravel-filled concrete bags attached to the inside of the reinforcing cage at depths of 3 ft and 21 ft below the top of shaft. The gravel bags represented approximately 15% of the shaft cross-sectional area and were attached to only one side of the reinforcing cage (rather than concentrically around the entire cage).

TIP records for the shaft are shown in Figure 17. Figure 17(a) shows temperatures 14 hours after concrete placement, and Figure 17(b) shows temperatures at the peak time of 34 hours. Both defects are clearly evident at 14 hours. The top defect resulted in a 12° F decrease in temperature in Wire 5, and the bottom defect resulted in a decrease of approximately 14° F, assuming the temperature without defects would have been halfway between the temperature above and the temperature below the bottom defect. At 14 hours, the reduction in the average temperature is modest at both defects. At about 5° F, the decreases in average temperature are noticeable, but not necessarily sufficient to cause concern without considering the reductions at Wire 5.

Evidence of the defects at the peak time of 34 hours (Figure 17(b)) is considerably weaker. For the top defect, there is limited evidence of a defect, with only a 2 or 3° F decrease at Wire 5. One might reasonably conclude the cage was off-center at the top of the shaft since the average temperature profile is relatively consistent and the wire temperatures are relatively evenly distributed about the average. For the bottom defect, the reduction in temperature at Wire 5 was about 8° F, a notable decrease, but only slightly more than half the decrease observed at 14 hours.

CSL was also performed on the shaft documented by Schoen et al. CSL plots were not presented in the research paper, but Schoen et al. note that CSL testing indicated both defects. Schoen et al. noted that the CSL testing firm was aware of the defects.

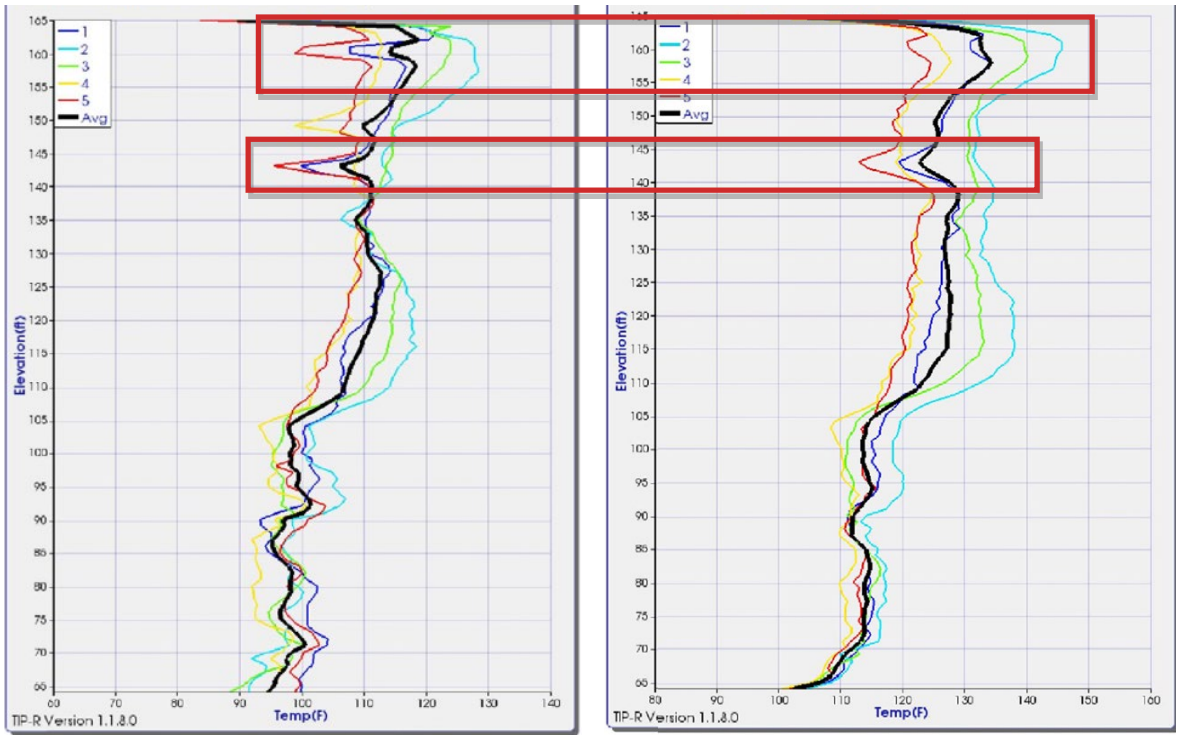

Figure 17: Example TIP result showing decreases in temperature at two known defect locations: (a) 14 hours and (b) 34 hours, the peak time. From Schoen et al. (2018).

3.2 Agency Experiences with TIP

Project applications of TIP offer another opportunity to evaluate TIP sensitivity to defects. Project applications are not controlled (or quasi-controlled) like the research projects described in the previous section, but they offer practical lessons and a quantity of data not frequently encountered in research projects. Most of the information in this section is derived from the WisDOT Zoo Interchange project, but TIP lessons from other transportation agencies are also documented.

3.2.1 WisDOT: Zoo Interchange

We have reviewed drilled shaft installation records, results of CSL and TIP tests, and, where applicable, results of coring and concrete remediation for the Zoo Interchange project drilled shafts. The shafts were 8 or 10 ft in diameter, with lengths varying from 30 to greater than 100 ft. The shafts were installed using temporary casing, and a tremie pipe was used to place concrete in the water-filled shafts. Table 5 summarizes results for the six shafts for which coring was completed in response to potential defects indicated in CSL and/or TIP test results. For five of the six shafts, coring confirmed defects, which were remediated by grouting.

Table 5: Summary of concrete integrity testing results for the six shafts at Zoo Interchange that were cored. Defects were confirmed in five of the six shafts; all five were remediated via grouting.

Shaft	Field Notes	CSL Results	TIP Results	Coring Results	Comments
WS07	Nothing unusual noted.	Spike in arrival times for many pairs on NW side of shaft in the top 5 to 10 ft. Coring recommended.	Perhaps some temperature deviations, but difficult to interpret in zone near top of shaft.	One core of top of shaft did not reveal any defects.	Core could have missed a defect? Core in SW quadrant; CSL indicated NW. Otherwise, could indicate CSL overly sensitive?
NE01	Tremie breached at a depth of 42 ft.	Spike in arrival times for 20 of 28 pairs at depth of tremie breach. Recommend further review by engineer and possibly coring.	No data below 35 ft due to “unknown failures” of five wires.	Two of three cores revealed 6 in. defect zones at the depth of the tremie breach.	
ES03	Tremie breached at a depth of 37 ft.	Spike in arrival times for all 45 pairs at depth of tremie beach. Coring recommended.	Temperature dips at depth of breach deemed “provisionally acceptable, if the minimum cover meets the design requirements and CSL test results indicate acceptable integrity.”	Three of four cores revealed 6 in. defect zones at the depth of tremie breach.	

Shaft	Field Notes	CSL Results	TIP Results	Coring Results	Comments
ES12	Evidence of soft bottom (cage sinking slowly for last 6 in.).	Spike in arrival times for all 28 pairs at base of shaft. Coring recommended.	Difficult to discern temperature decreases at base of shaft from typical "roll-off." Roll-off zone is 6 ft, less than 8 ft diameter. Interpreted radius values at base were less than design, but similar deviations were noted at other depths. Further engineering analysis recommended for shaft.	Defects in all four cores for 1.5 ft near bottom of shaft.	"Further engineering analysis" was a common recommendation in TIP reports. The recommendation was not specific to a particular depth.
WN11	Nothing unusual reported.	Spike in arrival times for 29 of 45 pairs at bottom of shaft. Recommend further review by engineer and possibly coring.	Difficult to discern temperature decreases at base of shaft from typical "roll-off." The TIP report concluded the shaft concrete integrity was acceptable.	Two of three cores revealed defect zones about 6 in. thick.	
WN06	6 in. of silt noted at bottom of shaft before pour.	Spike in arrival times for 40 of 45 pairs at the base of shaft. Recommend further review by engineer and possibly coring.	No TIP test – wires broke during shaft installation.	Two of three cores revealed defect zones about 6-in. thick.	

The only shaft in which coring did not confirm defects, WS07, is potentially a false positive CSL result. A false positive would be consistent with reports of CSL being overly sensitive, particularly near the top of drilled shafts where the effects of bleed water are most prevalent. However, it is certainly possible that the core location missed a real defect, especially considering the core location was near the edge of the zone indicated by the anomalous tube pairings (rather than being in the center of that zone). For two of the five shafts with confirmed defects, NE01 and ES03, the depth of defective concrete is consistent with the depth of a tremie breach. For both shafts, the CSL report recommended coring, although one such recommendation was conditional upon the engineer's review. For one shaft with a tremie breach, there was no TIP test because the wires failed; for the other, there was a notable dip in shaft temperatures at the depth of the breach, but the TIP report recommended "provisionally accepting" the shaft since the effective radius indicated almost 4 in. of concrete cover. For the other three shafts with defective concrete (ES12, WN11, WN06), the defects occurred at the bottom of the shaft, presumably because of an accumulation of soft material at the base of the shaft in the time between shaft excavation and concrete placement (i.e. "soft bottom"). For all three, CSL reports recommended coring, with two of the recommendations conditional upon the engineer's review. For one of the shafts, there was no TIP test because of wire failure; for the other two, TIP recommended further engineering analysis (a common conclusion among TIP reports) or acceptable integrity. It is difficult to discern lower temperatures due to soft bottom conditions because the temperature gradient is steep in this "roll-off" zone.

The Zoo Interchange concrete integrity data leads to three general observations:

- Broken wires were a recurring issue for the Zoo Interchange project. The manufacturer of the TIP wires for Zoo Interchange and all other projects encountered, has indicated a new wire design with cable strain relief has greatly reduced these issues. The improvement has been confirmed

with other users of TIP wires, who report about 1 to 2% breakage with the new wires in a recent project with a large number of TIP tests.

- It is difficult to detect defects in the top and bottom of shafts from TIP testing. Boundary conditions (loss of heat to air or soil) produce a roll-off zone with significant vertical temperature gradients. It is difficult to isolate temperature effects from a potential defect from the roll-off temperature gradients, especially since the length of the roll-off zone varies.
- Reports of CSL results were generally more informative and included clearer recommendations compared to the reports of TIP results. Testing was performed by two different firms, so it is difficult to discern whether the differences were a result of different firms having different reporting standards, the lack of standard interpretation and acceptance criteria for TIP (see Section 2.5), or both.

3.2.2 South Carolina DOT

In the 2015 FHWA study regarding drilled shaft concrete (Boeckmann and Loehr, 2015), South Carolina DOT (SCDOT) was described as having allowed TIP as an alternative to CSL for several years. SCDOT implements TIP via special provisions, but the agency is considering adding TIP to its standard specifications. The agency has observed significant bleed water in many large-diameter shafts. The bleed water has been observed through coring to produce "thumb size" bleed channels that result in significant CSL anomalies (hence coring) but generally not significant concern regarding the shaft's structural integrity. SCDOT has used TIP in large part because of the high incidence of coring based on CSL report recommendations.

3.2.3 Other Agencies

In addition to SCDOT, seven other state DOTs with TIP experience were contacted. Three agencies (Missouri DOT, Minnesota DOT, Utah DOT) did not have any data to share. Florida DOT referenced reports by Mullins (e.g. Mullins et al., 2007). Information from the three agencies that offered information is summarized in Table 6.

Table 6: Information from other transportation agencies with relevant TIP experience.

Agency	Experience with TIP Testing	Other Comments
Washington DOT	Manette Bridge: TIP data confirmed soil caving that was observed prior to concrete placement (higher temperatures due to larger shaft). No CSL testing on project. I-5 M-Street: TIP identified bulge of concrete and cage racking near tip. No CSL testing on project. Portland Ave, Pier 9: TIP showed temperature dips of 35° F at depths of 100 ft in the 120 ft long shaft. Coring indicated segregated concrete with strengths of 1800 psi adjacent to 9000 psi concrete. Not clear from field logs what caused defect. No CSL testing on project. Portland Ave, Pier 1: CSL and TIP performed side-by-side on five shafts. Neither test indicated any significant anomalies in any of the shafts; no coring was performed.	In January 2017, WSDOT updated its standard specifications to include TIP as an allowable CSL alternative (see Table 2). WSDOT intends to keep using CSL test, but likes TIP as an alternative, especially for larger, deeper shafts. Indicated cost of TIP is comparable to CSL.
Nevada DOT	US95/CC-215 Interchange: CSL and TIP performed side-by-side on Shaft 8. Neither test indicated significant defects, and no coring was performed.	
Louisiana DOTD	CSL and TIP used side-by-side for a test shaft in 2013. No defects were reported for either test. Subsequent load test did not reveal any structural deficiencies.	Agency noted TIP can be useful when cage is too congested for CSL tubes.

4. Field Testing Program

Field research was performed to further evaluate the sensitivity of TIP to drilled shaft defects and the potential agency-wide implementation of TIP for drilled shaft integrity testing. The field research involved installation and testing of three 52 to 58 in. diameter by 30 ft long drilled shafts. One shaft was primarily a control shaft, albeit with one intentional defect, and the other two were test shafts with several different intentional defects. After installation, TIP and CSL testing were performed on all shafts. This chapter describes the experimental design of the field research as well as installation and design of the drilled shafts. Results are presented in the next chapter.

4.1 Experimental Design and Construction Plans

To evaluate the ability of TIP and CSL to detect various drilled shaft defects, ten defects were installed in the test shafts. The defects are outlined in Table 7 and detailed in the construction plans included in the appendices. Appendix A is the final set of pre-construction plans, and Appendix B is the as-built construction plans. Details and photographs of the defect installation are included in Sections 4.3.2 and 4.3.3. The number of defects, ten, was selected to balance two competing interests. The first is the need to evaluate the ability of TIP and CSL to identify various concrete integrity issues commonly observed within drilled shafts. The second is the experimental requirement to avoid these effects interacting with one another.

The nature of the individual defects was selected to evaluate the most pertinent findings from Chapter 3. Four defects were included to evaluate the effect of defect location within the cross-section, particularly how the sensitivity of TIP compares for defects outside the reinforcing cage (Defects 3 and 5) and defects inside the reinforcing cage (Defects 1 and 9). Defects 2 and 7 were included to evaluate sensitivity to soft bottom conditions, particularly in light of the Zoo Interchange finding that CSL was more sensitive to soft bottom conditions than TIP. Defect 8 was included to evaluate tremie breach (based on Zoo Interchange records), and Defects 6 and 10 were included to evaluate zones of weak concrete. Lastly, Defects 4a and 4b were installed to promote debonding of the access tubes, which is commonly reported to lead to false positive CSL anomalies. The defects were created by applying wheel bearing grease around the outside of the tubes.

In general, the defects were sized to build on the work by Mullins et al. (2007), Ashlock and Fotouhi (2014), and Schoen et al. (2018). Collectively, the previous studies suggested a lower bound cross-sectional area for detection with TIP was somewhere between 8 and 15% of the total shaft area, so defect sizes (except soft bottom defects) were set at 10 and 15% of the test shaft cross-sectional area.

Table 7: Summary of intentional defects.

Defect	Modeled Defect	Shaft	Depth below Ground Surface	Cross-section Location	Size, Relative to Shaft Area
1	Inclusion in cage interior	Control	15 ft	Center of shaft	10%
2	Soft bottom	Test 1	30 ft	Shaft perimeter	50%
3	Necking	Test 1	21 ft	Entire cage perimeter	10%
4	Debonded CSL tubes	Test 1	16.5 ft	Reinforcing cage	N/A
5	Defect outside cage	Test 1	12 ft	1/3 of cage Perimeter	10%
6	5 ft zone of weak concrete	Test 1	Top of shaft to 3 ft	N/A	N/A
7	Soft bottom	Test 2	30 ft	Entire shaft bottom	100%
8	Tremie breach / cold joint	Test 2	20.5 ft	N/A	N/A
9	Inclusion in cage interior	Test 2	12 ft	Center of shaft	15%
10	5 ft zone of weak concrete	Test 2	Top of shaft to 3 ft	N/A	N/A

4.2 Test Site

The test site is located in Waukesha, Wisconsin, approximately 20 miles west of Milwaukee. As shown in Figure 18, the test site is about 1 mile south of Interstate 94, just east of the Waukesha airport and just west of the Fox River. Borings for the test site are included in Appendix C. The mud rotary borings indicate 2 to 3 ft of silty clay over silty sand and sandy silt to a depth of 40 ft, where the borings were terminated. The sandy material was generally dense to very dense, with SPT blow counts from 25 to greater than 100. Both borings encountered possible cobbles. Groundwater was not observed in either boring, but the mud rotary technique can make groundwater detection difficult.

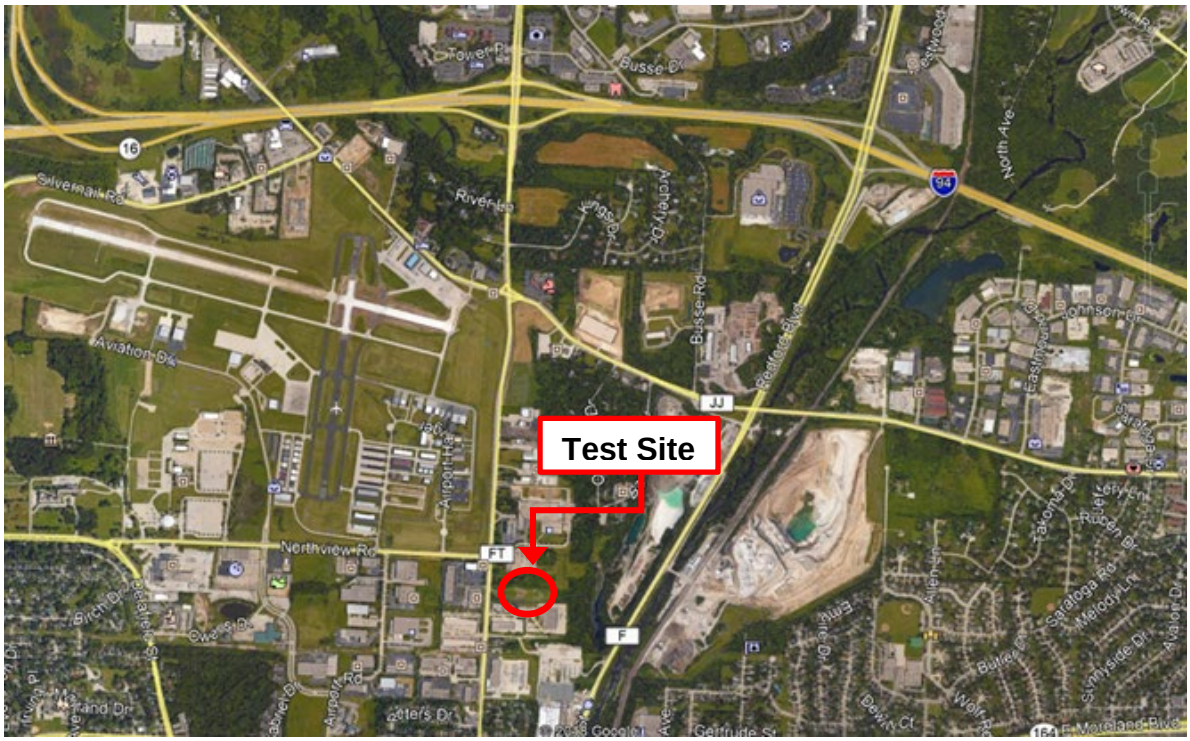

Figure 18: Location of Waukesha test site (Google Earth, 2018).

4.3 Drilled Shaft Construction

Three drilled shafts were constructed at the Waukesha test site by a joint venture of Midwest Drilled Foundations and Engineering, Inc. and Taylor Ridge Drilled Foundations, Inc. The shafts were installed between November 13 and November 17, 2017. The Control Shaft was constructed first, followed by Test Shaft 1 and then Test Shaft 2. As-built drawings documenting the constructed shafts are included in Appendix B, and logs of drilled shaft concrete placement are included in Appendix D.

4.3.1 Shaft Excavation and Temporary Casing

Photographs of the drilling process are shown in Figure 19 and Figure 20. The shafts were excavated with a 48 in. auger. Groundwater was not encountered for any of the shafts, but the sandy material was prone to raveling. Temporary casing was used to reduce raveling and improve hole stability, but the casings were not placed until after the material had been excavated (rather than driving the casing ahead of drilling), so the excavated shaft diameter is likely somewhat greater than the diameter of the casings. Below a depth of approximately 10 ft, cobbles were occasionally encountered in each of the shafts. The cobbles complicated drilling and casing placement, slowed progress, and likely increased the degree of overexcavation. The temporary casing was telescoped to reduce side friction and facilitate removal of the casing as concrete was placed. The diameter of the outer (upper) casing was 58 in., and the diameter of the inner casing was 52 in. The casings were placed in the holes after excavating to the depths shown in the as-built drawings.

Figure 19: Overview of test site with crane, loader, and drill rig in operation.

Figure 20: Excavation of shaft with 48 in. auger through telescoping casing.

4.3.2 Reinforcing Cages and Defects

Reinforcing cages for the drilled shafts are shown in Figure 21. Longitudinal reinforcement consisted of twelve No. 8 reinforcing bars; transverse steel consisted of No. 4 stirrups on 12 in. centers. The reinforcing cages also included four 2 in. diameter Sch. 40 steel pipes for CSL testing and TIP testing by the probe method. The integrity testing pipes were installed on the inside of the cages, spaced evenly at 90 deg. As shown in Figure 21, additional steel was included around the outside of the reinforcing cages to improve cage stability. Reinforcing cages were lowered into the shafts with wheel spacers to keep the cages centered within the hole and with chairs to support the cages on the bottom of the hole.

Figure 21: Reinforcing cages prior to installation of most defects.

Defects 1 through 5 and 9 were affixed to the reinforcing cages prior to lowering the cages into the excavated shafts. Photographs of the defects affixed to the cages are shown in Figure 22 through Figure 28. The figure captions list details of the defects, which are also described in Table 7 and shown in the as-built drawings of Appendix B. Defects were tied to the reinforcing cages using rebar tie wire. For the inside-cage defects (Defects 1 and 9), sandbags were tied with extra tie wire length between the cage and the sandbags. The extra length was approximately equal to the reinforcing cage radius. The intention for including the extra tie wire length was for the sandbags to float toward the center of the reinforcing cage, thus creating a center-of-shaft defect for evaluation with TIP and CSL. The reinforcing cages were observed carefully as they were lowered into the excavated shafts; no defects were compromised.

Figure 22: Defect 1 consisted of three 70 lb sandbags tied inside the reinforcing cage for the Control Shaft.

Figure 23: Defect 2 consisted of six 70 lb sandbags tied around the bottom of the reinforcing cage for Test Shaft 1.

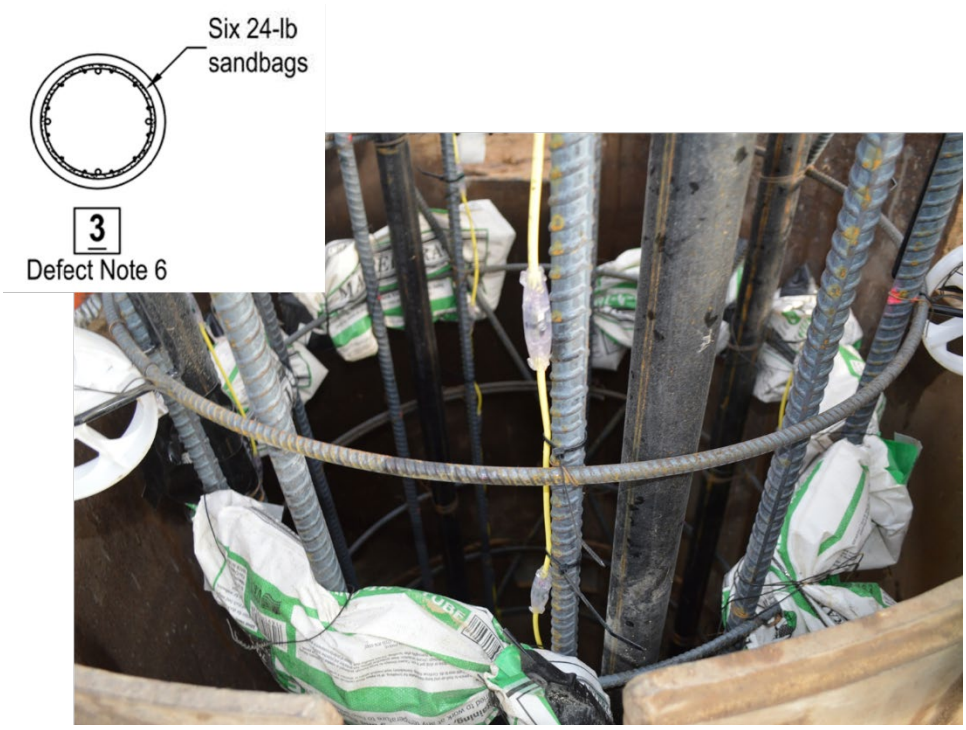

Figure 24: Defect 3 consisted of six 24 lb sandbags tied concentrically around the edge of the reinforcing cage for Test Shaft 1 at a depth of 21 ft.

Figure 25: Defect 4 consisted of wheel bearing grease applied around the outside of the access tubes for a length of 1 ft. Defect 4 was installed in two locations: at a depth of 16.5 ft in Test Shaft 1 and a depth of 4.5 ft in Test Shaft 2.

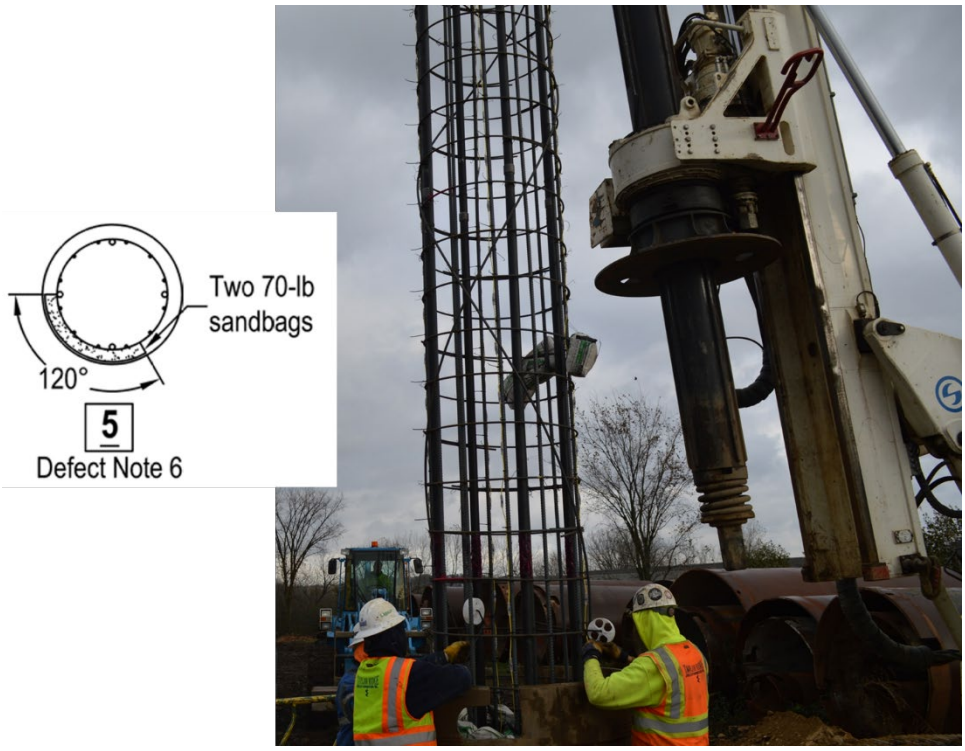

Figure 26: Defect 5 consisted of two 70 lb sandbags outside one side of the reinforcing cage for Test Shaft 1 at a depth of 12 ft.

Figure 27: Defect 9 consisted of five 70 lb sandbags placed inside the reinforcing cage for Test Shaft 2 at a depth of 12 ft. ***Defects 6, 7, and 8 are presented in the next section.***

Figure 28: Reinforcing cage is lowered into the hole for Test Shaft 2. Sandbags for Defect 9 are visible near the cage mid-height.

4.3.3 Concrete: Mix Design, Placement and Defects, and Compressive Strength

The concrete mix design specifications are shown in Table 8. The mix design is equivalent to the mix specified for the Zoo Interchange project. The mix has a water-cement ratio of 0.45. The target slump was 7 to 9.5 in. Concrete was sourced from Rivcrete Ready Mix of Milwaukee.

Table 8: Concrete mix design specifications.

Material	Quantity per Cubic Yard of	Specification
Cement	460 lb	ASTM C150, Type I
Fly Ash	200 lb	ASTM C618, Class C
Fine Aggregate	1,777 lb	WisDOT 501.2.5.3
Coarse Aggregate	1,185 lb	WisDOT 501.2.5.4 but with AASHTO No. 89 stone (ASTM D448) gradation. Rounded stone was used.
Water (potable)	35.5 gal	
Air Entrainment Admixture	1.6 oz	ASTM C260
Retarder Admixture	40 oz	ASTM C494, Type B
Water Reducing Admixture	40 oz	ASTM C494, Type D
High-Range Water Reducing Admixture	26 oz	ASTM C494, Type F

Detailed descriptions of concrete placement are included in the logs of Appendix D. As shown in Figure 29, concrete was placed in the dry holes using a tremie pipe supported by a crane. Concrete slump was tested per ASTM C143 for each truck, and cylinders were also cast for subsequent compressive strength testing per ASTM C39. A photograph of slump testing is shown in Figure 30. Except for concrete from one truck, slump values were all 10 to 11 in., which is above the target range of 7 to 9.5 in. However, the fluid concrete appeared cohesive and stable without signs of segregation or bleed. Quality assurance personnel from the concrete plant visited the test site to observe the delivered concrete during the concrete pour for Test Shaft 2. The following truck delivered concrete with a slump value of 7.5 in. (the lone value less than 10 in. referenced previously). The placement temperature of the fresh concrete ranged from 52 to 68° F.

Figure 29: Placement of concrete from the concrete truck to the tremie pipe.

Figure 30: Concrete slump test.

The volume of concrete placed in each shaft was approximated by tracking the number of truckloads and partial truckloads, with a full truck delivering about 7 cubic yards (cy) and perhaps as much as 7.5 cy. The resulting concrete yield plots for each shaft are shown in Figure 31 and included in Appendix D. The plots include lines representing the theoretical shaft volume and separate points representing placed volumes estimated by truckloads. The points are based on 7 cy per truck, with error bars reflecting the potential 0.5 cy overfill. The theoretical yield lines vary for the top half of the shafts because the outer temporary casing depth varied for each shaft. In addition, the inner temporary casing could not be removed from Test Shaft 2, so it became a permanent casing. Thus, Test Shaft 2 differed from the Control Shaft and Test Shaft 1 in three important ways: (1) it has a full-length permanent casing, (2) it likely has an annular

gap between soil and casing, and (3) its diameter is 6 in. smaller (52 in. versus 58 in.). For all shafts, the measured volumes are greater than the theoretical volumes, indicating the actual shaft diameters are greater than the design values. Oversized holes are typical in drilled shaft construction, especially in granular material. Unsurprisingly, the difference between measured and theoretical values is small for Test Shaft 2, which had a permanent casing. The first (bottom) volume measurement for the control shaft indicates significant overexcavation (approximately 40% by volume or 20% by diameter) in the bottom half of the shaft. However, the next measurement (near a depth of 10 ft) is closer to the theoretical curve, which suggests the first measurement could have been in error.

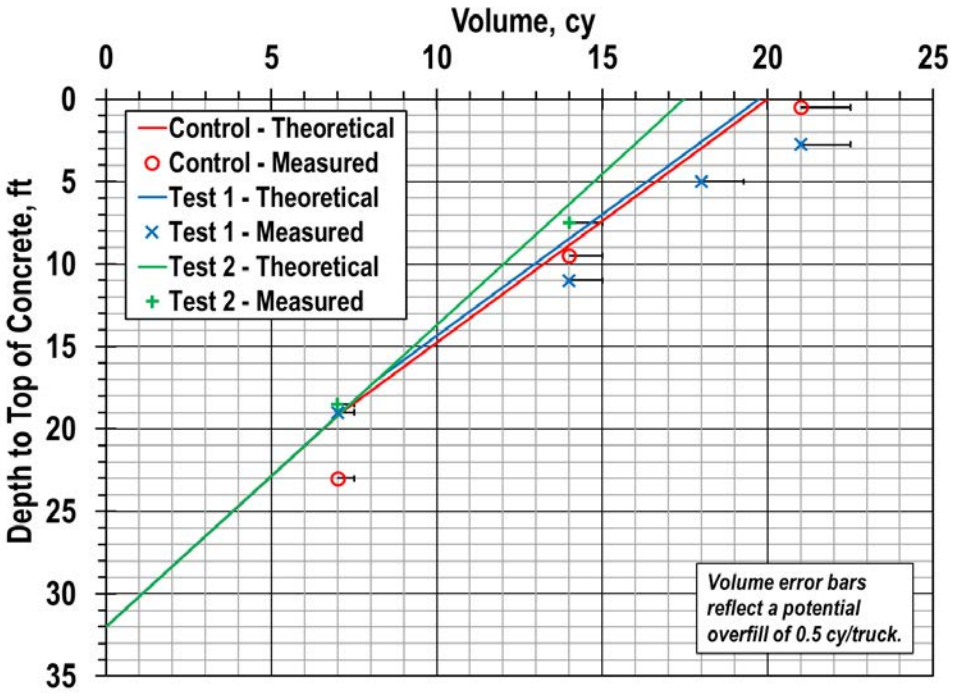

Figure 31: Concrete volume yield plots for all test shafts. Theoretical lines are all equivalent below a depth of 19 ft.

Defects 6, 7, 8, and 10 were installed during concrete placement, whereas the other defects were attached to the reinforcing cages. Photographs of the concrete placement defects are shown in Figure 32 through Figure 35. Defect 7 was intended to mimic soft bottom conditions. Similar to Defect 2, it consisted of 420 lb of sand at the bottom of the shaft, but the sand for Defect 7 was poured from the surface both inside and outside the reinforcing cage (Figure 32) whereas Defect 2 consisted of sandbags tied around the outside of the bottom of the reinforcing cage. Defect 8 was intended to mimic a tremie breach, which caused problems for the Zoo Interchange project. Since the shafts for this project were dry, the effect of a tremie breach was simulated by removing the tremie and then pouring 30 gallons of water and 70 lb of sand in the hole. After placing the water and sand for Defect 8, the remaining concrete was placed with the tremie suspended above the top of concrete surface. Defects 6 and 10 consisted of zones of weak concrete at the top of Test Shaft 1 and Test Shaft 2, respectively. To achieve weak concrete, the concrete placement by tremie was terminated when the top of concrete was 3 ft below the ground surface. The volume of concrete remaining in the truck was estimated from the yield plots (Figure 31), and water was added to the concrete in the truck to achieve a water-cement ratio of 0.6 for Defect 6 and 0.52 for Defect 10. The concrete was mixed in the truck after adding the water prior to placing the concrete by free fall. As shown in Figure 34, the weakened concrete was significantly more fluid than the normal concrete. The weakened concrete also produced significant bleed water, as shown in Figure 35.

Figure 32: After placing the reinforcing cage but prior to placing concrete for Test Shaft 2, 420 lbs of sand was poured into the bottom of the excavated shaft to simulate a soft bottom for Defect 7.

Figure 33: To simulate a tremie breach for Defect 8: (a) the tremie was removed from the shaft prior to (b) placing 30 gallons of water and 70 lbs of sand into the shaft (to simulate a tremie breach in a wet shaft).

Figure 34: Concrete placement near the top of shaft: (a) normal concrete in Control Shaft and (b) weak concrete for Defect 6 in Test Shaft 1.

Figure 35: Completed Test Shaft 1 shortly after completion of concrete placement. Bleed water from the weak concrete of Defect 6 is evident at the top of the shaft.

Compressive strength tests were conducted per ASTM C39 by PSI, Inc. in Waukesha. The diameter of the test cylinders was 6 in. Results of concrete compressive strength testing are listed in Table 9. The strength values are highly variable. For the Control Shaft, two of the three cylinders had compressive strength values around 3,000 psi, which is significantly less than the design value of 4,000 psi. The other cylinder from the Control Shaft had a compressive strength of 6,500 psi, significantly greater than design. For both Test Shaft 1 and Test Shaft 2, the compressive strength values were all substantially greater than design, except in the zones of weak concrete (Defect 6 and Defect 10). The non-defective strength values were all between 5,800 and 8,500 psi, with most values greater than 8,000 psi. Even in the defective zones, the strength values were near, and in most cases greater, than 4,000 psi. The average value for Defect 6 was 4,600 psi, and the average value for Defect 10 was 4,200 psi.

The low compressive strength values observed in the Control Shaft are questionable in light of the strength values for samples from Defect 6 and Defect 10. The fresh concrete for all three shafts appeared similar, with notably consistent slump values. After adding water to the mix for Defect 6 and Defect 10, the resulting fresh concrete appeared visibly unstable and produced significant bleed water. It is difficult to believe the strength of the Defect 6 and Defect 10 concrete could be greater than the visibly stable concrete from the Control Shaft. Most likely, improper sampling or cylinder handling resulted in the low strength results.

Table 9: Results of concrete compressive strength testing.

Shaft	Placement Date	Age at Test, days	Depth, ft	Slump, in.	Compressive Strength, psi	Comments
Control Shaft	11/14/2017	28	Unknown	10-11	2640 3010 6480	Truck number not specified on cylinder, so depth is unknown.
Test Shaft 1	11/16/2017	28	0-5	N/A	3810 4190 5800	Defect 6, $w/c = 0.60$
			5-11	10.5	8290	
			11-19	10	8320	
			20-30	10	8430	
Test Shaft 2	11/17/2017	28	0-5	N/A	3420 4920	Defect 10, $w/c = 0.52$
			7.5-18.5	7.5	8500	
			18.5-30	11	7160	

4.4 Concrete Integrity Testing

Both TIP and CSL tests were performed on all three shafts. TIP testing was performed using both wires and probes. Details of the data collection are presented in this section. Results of the tests are presented in the next chapter.

4.4.1 TIP Via Wires

Four TIP wires were included on all shafts. Photographs of the wires are shown in Figure 36 and Figure 37. The wires were manufactured by PDI, as was the data acquisition system. The wires include one temperature sensor per foot. The wires were affixed to vertical reinforcing bars using plastic cable ties, with one tie between each sensor for most of the wire length. The four wires were affixed to vertical reinforcing bars adjacent to the access tubes for probe testing and CSL, which resulted in approximately equally spaced wires.

One Thermal Acquisition Port (TAP) was attached to the top of each wire to record data. A photograph of installed TAPs is shown in Figure 38. The TAPs began reading and recording temperature data shortly after they were connected to the TIP wires. By default, the TAPs record data every 15 minutes. The Thermal Integrity Profiler tablet, shown in Figure 39, was used to collect and review temperature data in the field. The TAPs were left in place for approximately three weeks after concrete placement before the final dataset was collected.

Figure 36: Close view of a TIP wire with sensor.

Figure 37: TIP wires exiting the top of the reinforcing cages. Two sensors were above the top of the shaft to measure ambient temperature.

Figure 38: One TAP box was connected to each TIP wire to collect and store temperature data.

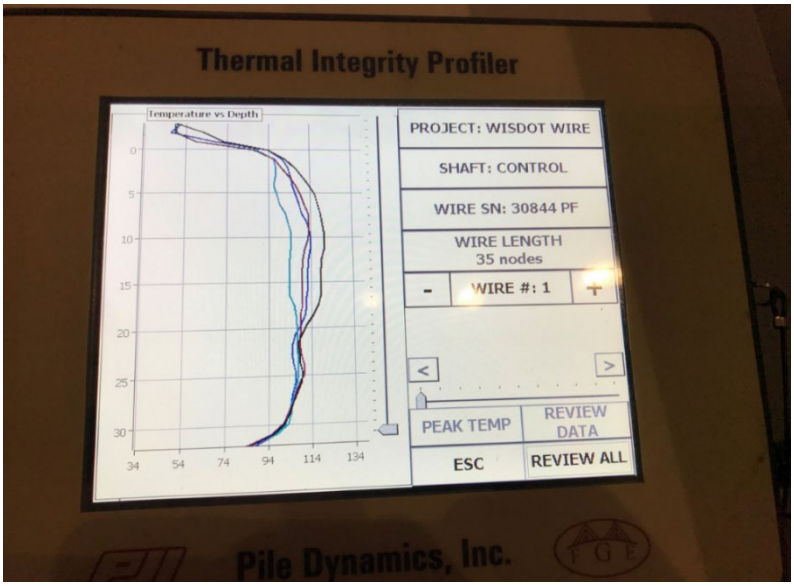

Figure 39: The Thermal Integrity Profiler tablet by PDI reads and displays temperature data from the TAPs.

4.4.2 TIP Via Probe

TIP data was also collected using the probe method. The probe tests were performed by first dewatering the access tube (Figure 40) and then lowering a temperature probe to the bottom of the access tube (Figure 41). As the probe was lowered, temperature data were read and recorded, as was the depth of the probe for each measurement. Depths were automatically recorded using a depth encoder pulley. The rate of lowering the probe was limited to 6 in. per second to produce stable measurements. The process was repeated for each access tube. The water that was removed from each access tube was stored in a large plastic container and returned to the access tube upon completion of the probe run. Storage and reuse of the access tube water is recommended in ASTM D7949 (2014). The access tube water is typically warm due to cement hydration; replacement with cool water could result in access tube debonding. The temperature probe and depth encoder pulley used for testing were manufactured by PDI.

For all shafts, the probe tests were performed one day after concrete placement. Weather during the week of concrete placement was relatively cold. Daytime temperatures were between 40 and 45° F for most of the week, including when TIP testing was performed by probe method for the Control Shaft and Test Shaft 1. The weather was particularly cold the day TIP testing was performed by the probe method for Test Shaft 2. The temperature during Test Shaft 2 testing was approximately 30° F, with snow falling as shown in Figure 42. It is likely the probe readings were impacted by the ambient temperature. The probe likely should have been allowed to acclimate to the temperature inside the access tubes for a longer period of time. The temperature inside the tubes was approximately 80° F warmer than the outside air temperature, based on wire measurements.

Figure 40: The access tubes were dewatered prior to performing TIP test via probe method.

Figure 41: TIP testing via the probe method utilizes a depth encoder pulley that logs the probe depth as it is raised from the bottom of the access tube.

Figure 42: TIP testing by probe method for Test Shaft 2 was completed with ambient temperatures near 30° F.

4.4.3 CSL

CSL tests were performed on all three shafts approximately three weeks after concrete placement. Photographs of the CSL testing are shown in Figure 43 and Figure 44. The tests were conducted by lowering the source and receiver probes to the bottom of different water-filled access tubes and then raising the probes simultaneously using a dual pulley. As the probes are raised, ultrasonic pulses are transmitted from the source to receiver and the time records are logged by the recording device. For all shafts, all possible access tube pairings were tested, resulting in six pairings per shaft. All test equipment used for the CSL tests was manufactured by Olson Instruments, Inc.

Figure 43: CSL testing included all pairs of access tubes.

Figure 44: CSL testing utilized equipment by Olson Instruments, Inc., including a dual depth encoder pulley used to lower the source and receiver probes down two access tubes simultaneously.

5. Experimental Results

Results of the field testing program described in Chapter 4 are presented in this chapter. Results are first presented on large sheets with summary plots for all TIP and CSL tests. Results are then evaluated qualitatively prior to analyzing the results quantitatively. TIP results from the probe tests are presented at the end of the chapter.

5.1 Summary Plots

Results of TIP wire and CSL tests are presented in Figure 46 through Figure 51. Each figure is an 11 x 17 in. sheet summarizing results of either TIP testing or CSL testing for a single shaft. To the left of each figure is the as-built profile of the shaft showing the defect locations; horizontal lines are included across the figures to line up defect depths with test results. Importantly, the diameters indicated in the as-built profiles are nominal values based on casing diameters, not measured values. TIP results are presented first, with the Control Shaft as Figure 46, Test Shaft 1 as Figure 47, and Test Shaft 2 as Figure 48. CSL results are presented after the TIP results, with the Control Shaft as Figure 49, Test Shaft 1 as Figure 50, and Test Shaft 2 as Figure 51.

Three plots are shown on each of the TIP figures. To the left are temperature profiles at the time of maximum rate of temperature rise (defined below), in the middle are temperature profiles at the time of peak temperature, and to the right are profiles of the effective radius, as calculated by PDI software according to the Level 2 analysis procedure explained in Section 2.3.4. Five lines are included for each plot, one for each TIP wire and one for the average of the four wires. As explained in Section 2.3.2, peak temperature was defined as the maximum temperature at any depth for the average temperature profile (i.e. the profile defined by the black lines in the middle plots of Figure 46 through Figure 48). The peak temperature was 113.6° F for the Control Shaft, 114.3° F for Test Shaft 1, and 106.2° F for Test Shaft 2. The rate of temperature rise was calculated as the first derivative of the temperature data with respect to time:

$$rate_i = \frac{temp_i - temp_{i-1}}{time_i - time_{i-1}}$$

Rate of rise was calculated for each depth. The maximum rate of rise was defined similar to peak temperature: the maximum rate of rise at any depth for the average temperature profile.

Each of the CSL figures includes six plots of first arrival time (FAT) and relative energy profiles, one for each of the access tube pairings shown in Figure 45. From the left, the first four profiles are for the pairings with ray paths closer to the edge of the reinforcing cage, while the two profiles to the right are for the pairings with ray paths through the center of the shaft. FAT values are generally greater for the rightmost profiles because the ray path distances are greater.

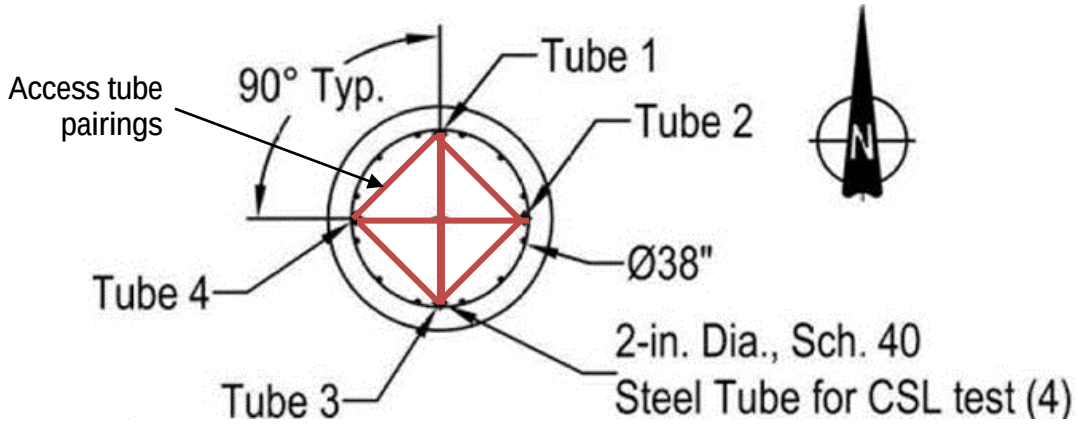

Figure 45: CSL access tube pairings.

FAT values were identified from the time records using the algorithm automatically applied by Olson Instruments, Inc.'s software. Three "threshold" values for FAT interpretation were considered by the software: 30 mV, 40 mV, and 50 mV. The threshold value is used within the algorithm to filter out noise from the response; only amplitudes exceeding the threshold value are used to define the FAT. Accordingly, the 30 mV threshold is the most sensitive criteria and is the default value applied by Olson Instruments, Inc. for interpretation. Using greater values of the threshold tends to reduce noise in the FAT profiles by eliminating interpretation of unreasonably small arrival times. However, if the threshold is set too high, the interpretation will "miss" real arrival times. For the data from this project, the threshold value has a noticeable effect on the FAT profiles for the Control Shaft, but limited effect for the two test shafts. For the Control Shaft, the 50 mV threshold profiles are relatively uniform with depth, whereas the 30 mV and 40 mV profiles show more spikes with depth. Although spikes are typically associated with anomalous results, it is important to note that the low threshold spikes in the Control Shaft CSL records are toward faster arrivals, not slower arrivals. Faster arrivals are not likely as they would indicate zones of extremely stiff material. The only concern, therefore, is that the CSL time records for the Control Shaft include some degree of noise. This is a relatively minor concern.

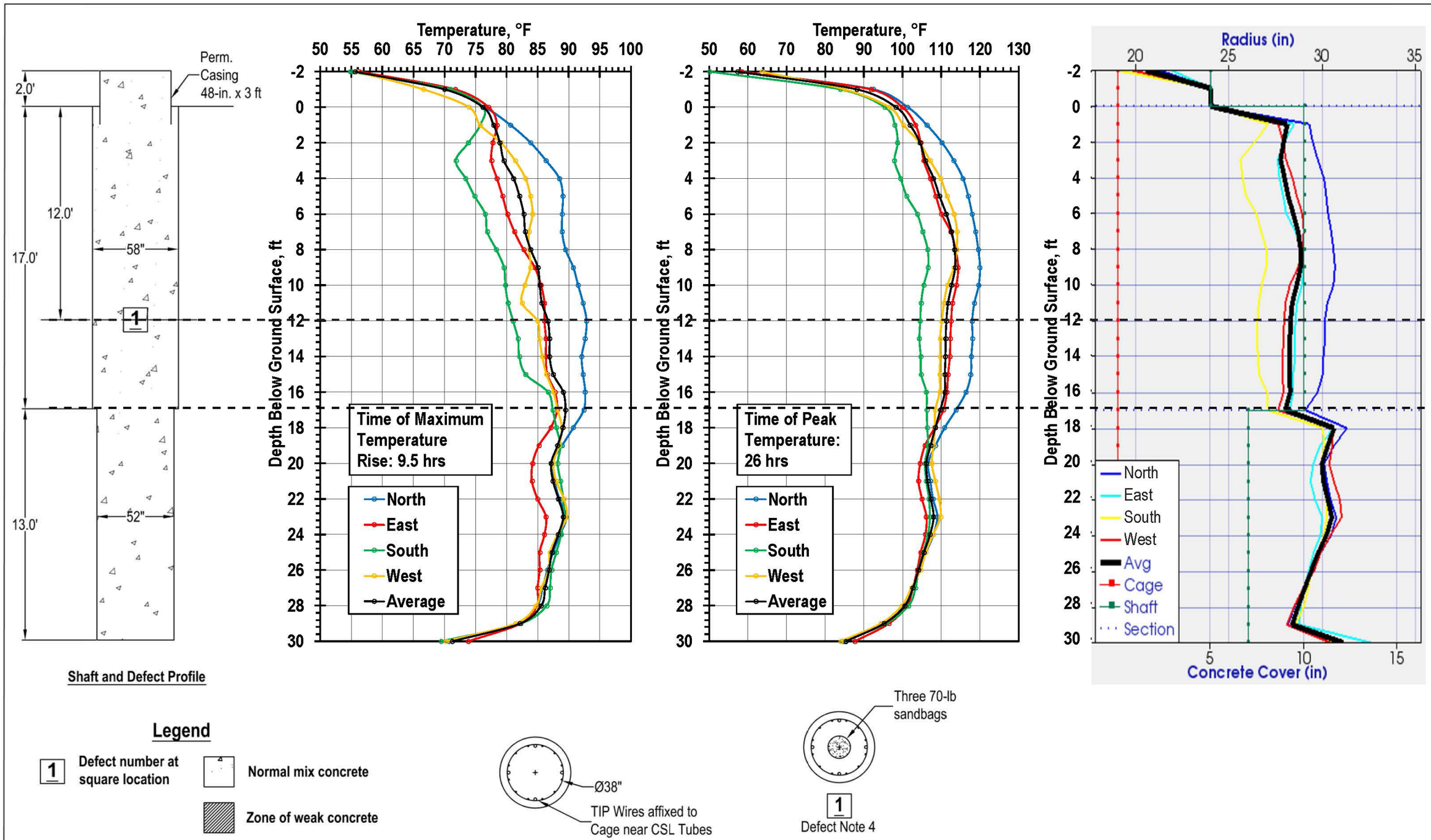

Figure 46: Results of TIP testing of the Control Shaft, with effective radius from PDI software.

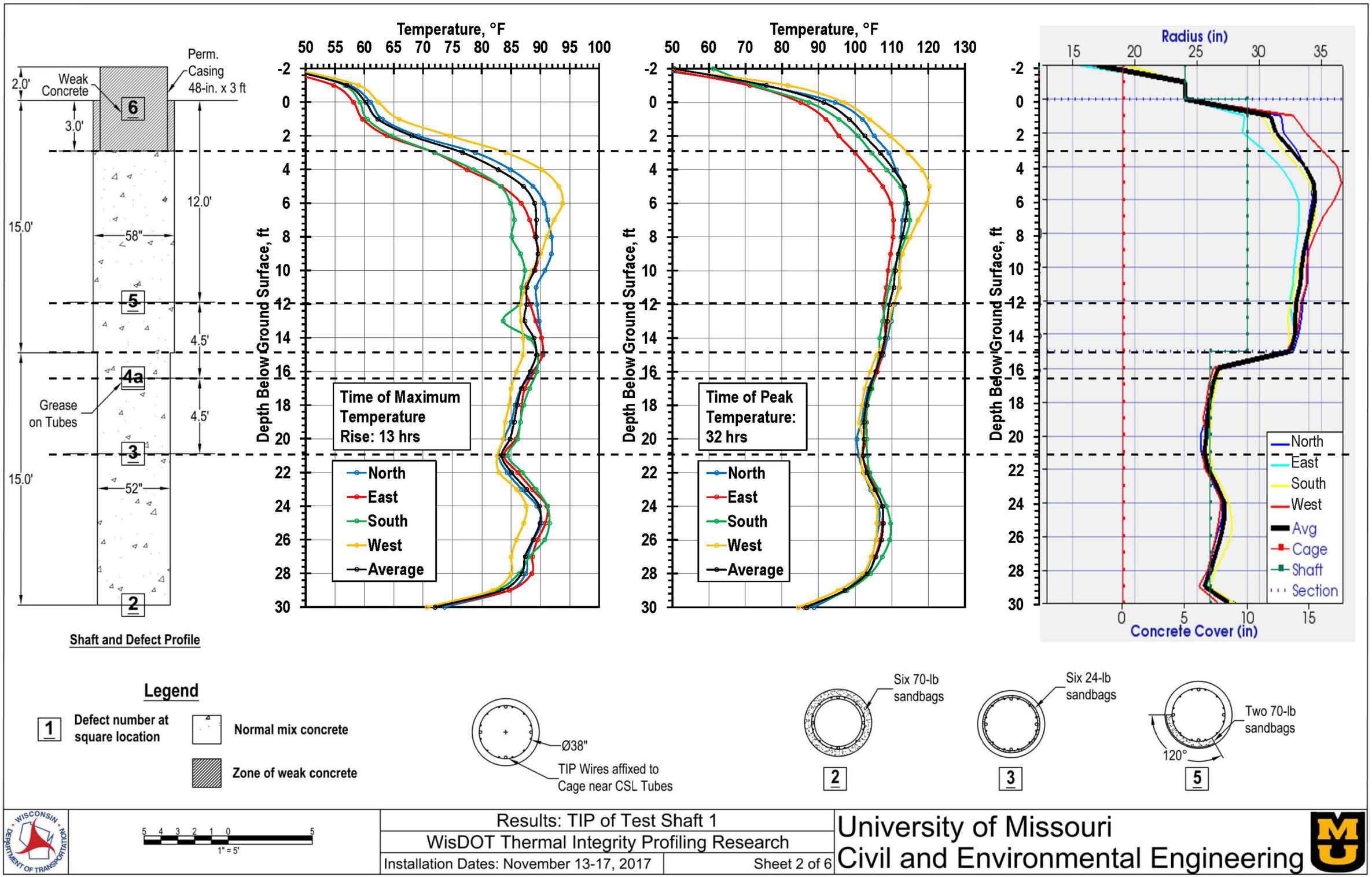

Figure 47: Results of TIP testing of Test Shaft 1, with effective radius from PDI software.

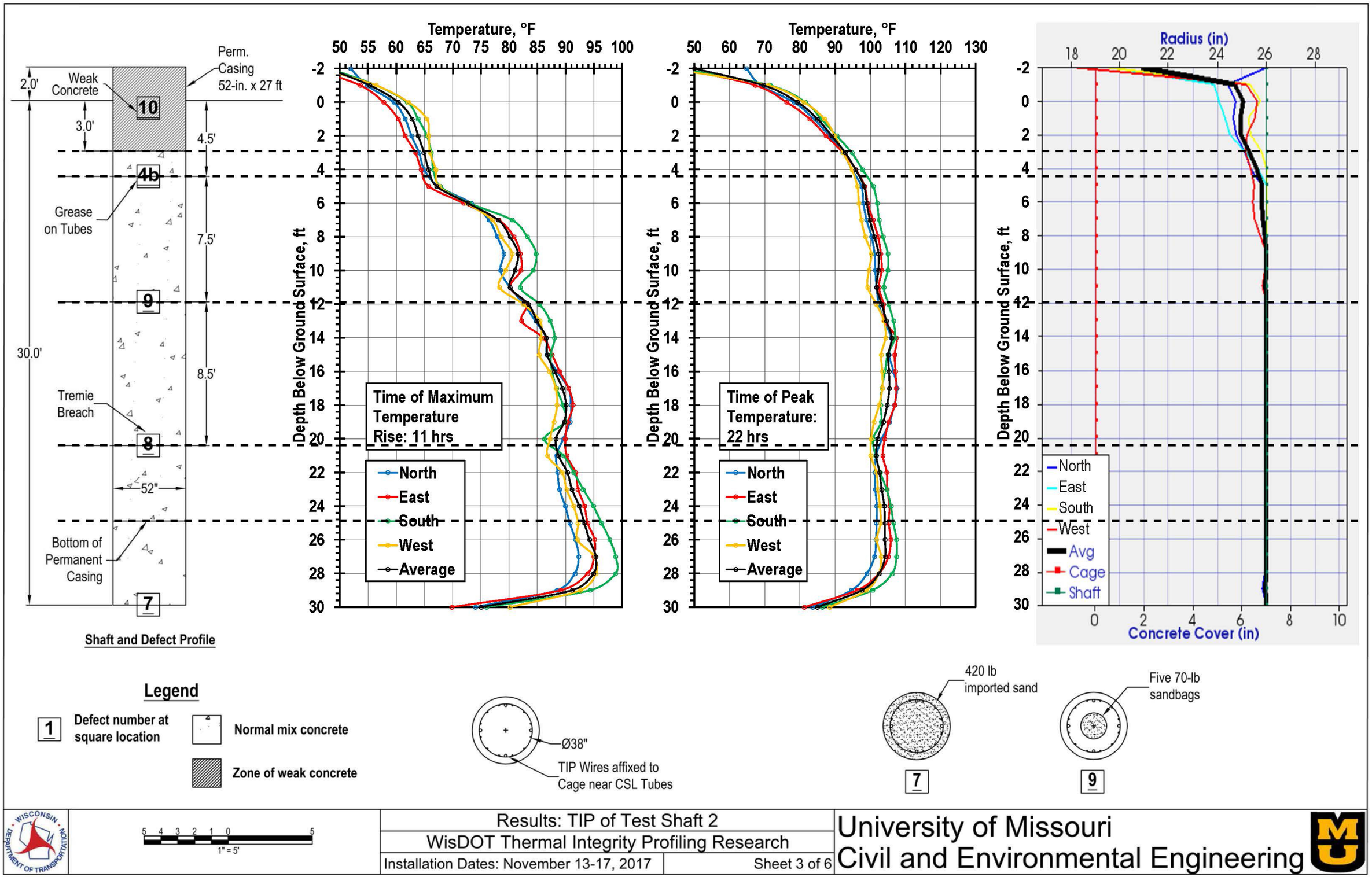

Figure 48: Results of TIP testing of Test Shaft 2, with effective radius from PDI software.

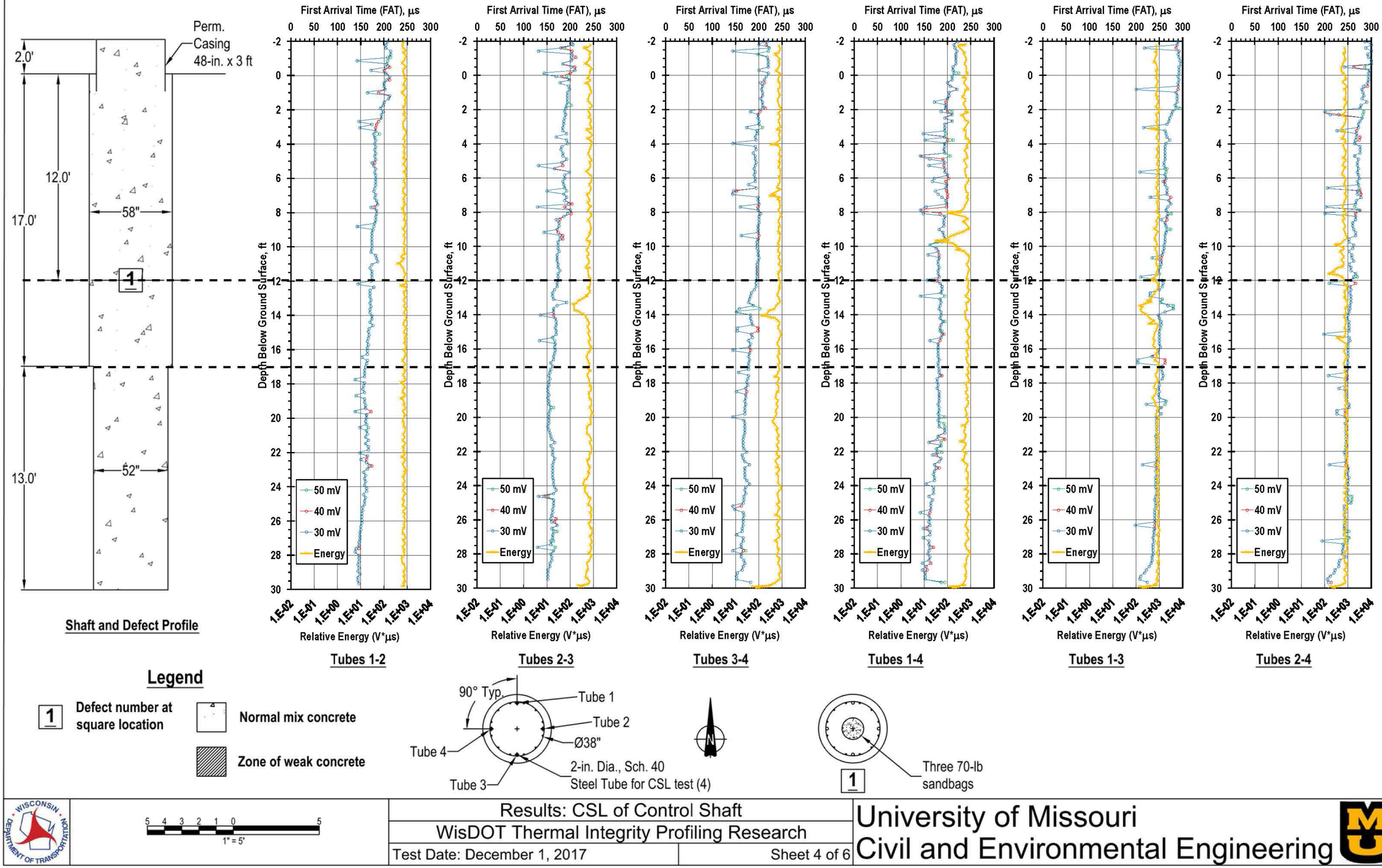

Figure 49: Results of CSL testing of the Control Shaft.

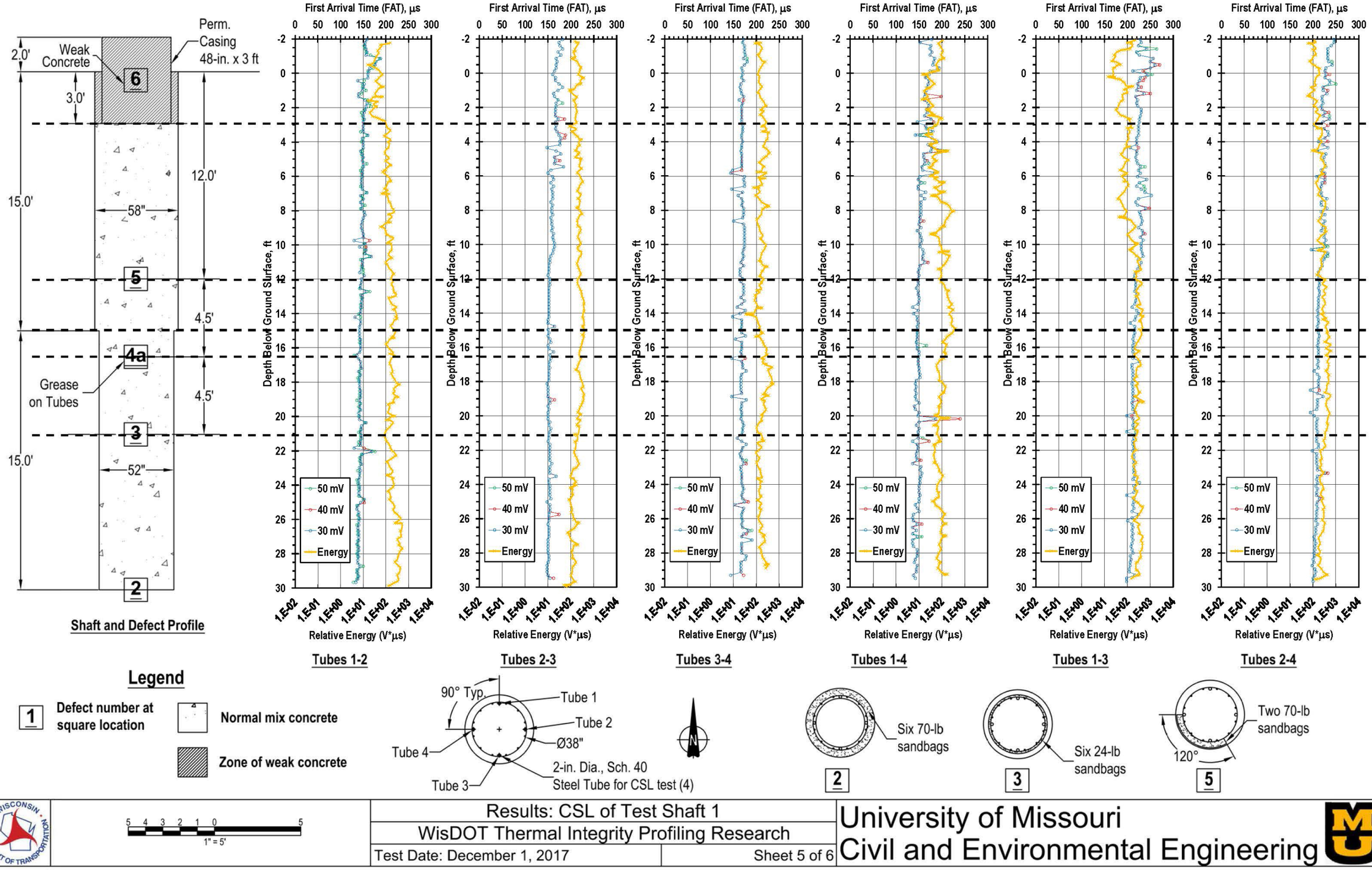

Figure 50: Results of CSL testing of Test Shaft 1.

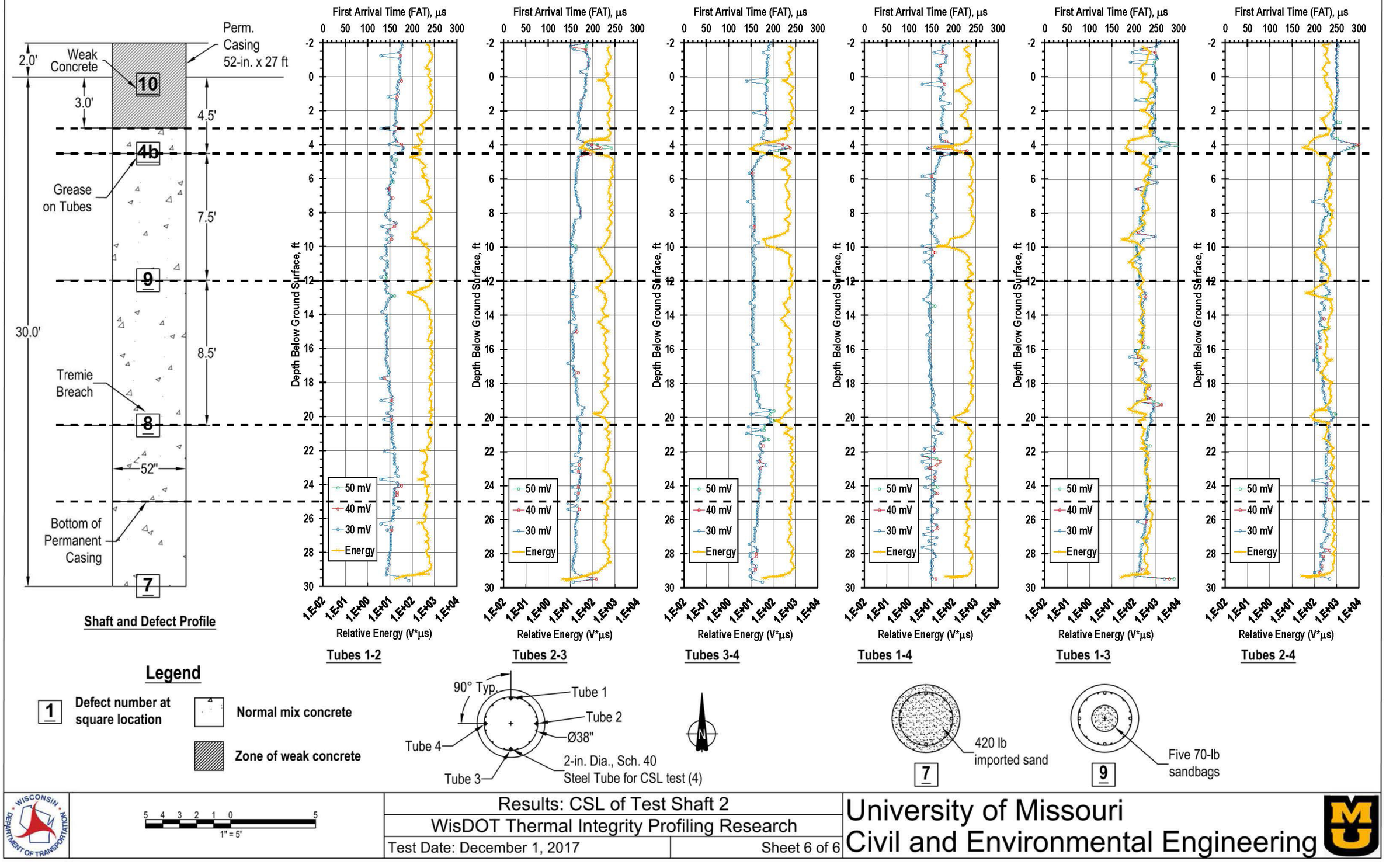

Figure 51: Results of CSL testing of Test Shaft 2.

5.2 Qualitative Evaluation of Results

Results from the concrete integrity tests are interpreted qualitatively in this section. The qualitative interpretations focus on visual observations of trends in the data, especially with respect to defects. Quantitative interpretation is included in the next section.

5.2.1 Qualitative Evaluation of TIP Results: Temperature

TIP results for the Control Shaft (Figure 46) show a fairly straightforward temperature profile. Several observations are notable regarding the profile at peak time:

- Temperature profiles are relatively consistent with depth, other than the roll-off zones at the ends of the shaft.
- Temperatures decrease slightly in the bottom half of the shaft, which is to be expected based on the diameter change. Consistent with this expectation, the approximate location of the decrease corresponds to the telescoping casing transition.
- The east and west wires were consistent with the average, but the north wire was warmer and the south wire cooler than average, particularly for the upper portion of the shaft. This suggests the reinforcing cage was off-center in the top half of the shaft, with the cage offset southward (resulting in the north wire closer to the center).
- At both ends of the shaft, most of the temperature roll-off occurs over a distance of 2 ft. At the bottom of the shaft, the vast majority of the roll-off occurs over these 2 ft for the time of maximum temperature rate of increase, but the roll-off is more gradual and occurs over a longer distance for the time of peak temperatures. Roll-off at the top of the shaft is likely influenced by the change in diameter of the ground surface, which causes the roll-off to appear to extend to greater depths than it would for a shaft of constant diameter. A similar effect could be possible at the bottom of the shaft if the radius decreases near the tip. This is likely true of many uncased shafts, particularly those in sand.

The temperature profiles in the Control Shaft at the time of maximum rate of temperature rise are similar in shape to those at the peak time, although temperatures appear to rise more slowly in the top 10 ft of the shaft than in the rest of the shaft. There is no clear evidence of Defect 1 (inside-cage inclusion) in either set of temperature measurements.

TIP results for Test Shaft 1 (Figure 47) are similar in temperature magnitudes and profile shape compared with the Control Shaft, with the important exception of the defect locations. TIP results for Test Shaft 1 show much clearer evidence of defects. Of the four defects installed in the shaft, effects from Defects 3 (necking) and 6 (weak concrete) are clearly evident, the effect of Defect 5 (inclusion outside one side of cage) is muted, and there is no clear effect from Defect 2 (outside-cage soft bottom). (Defect 4a, tube debonding, was intended to evaluate CSL testing only and is therefore not discussed here.) Each detail is discussed below:

- Defect 3, which consisted of six 24 lb sandbags wrapped around the entire outside of the reinforcing cage, produced a notable decrease in temperatures. The effect is considerably sharper at the time of maximum rate of temperature rise than at the peak time. Not only is the effect of the defect clearer at the time of maximum rate of rise, but the location is more evident as well. At peak time, the effect of Defect 3 appears to have been muted by the buildup of temperatures from the surrounding concrete.
- Defect 6, the zone of weak concrete with a water-cement ratio of 0.60, resulted in considerably lower temperatures at the top of the shaft. At the time of peak temperatures, the effect of Defect 6 is similar to a deeper roll-off zone (e.g. compared to the Control Shaft), but the Defect 6 effect is so severe it is unlikely any engineer would confuse the lower temperatures for the effect of roll-off. The effect of Defect 6 is much clearer at the time of maximum rate of temperature rise, an observation that was also noted for Defect 3. The Defect 6 concrete appears to have barely heated compared with the rest of the shaft.

- Defect 5 consisted of two 70 lb sandbags outside the south side of the reinforcing cage. The weight of sand for Defect 5 was therefore similar to Defect 3, but the effect of Defect 5 was less apparent than the effect of Defect 3. There is essentially no evidence of a temperature decrease due to Defect 5 at the time of peak temperature, and only a relatively minor decrease in the temperature in the south wire at the time of maximum rate of rise. The decrease in south wire temperature due to Defect 5 at the time of maximum rate of rise was approximately equal to the decrease that was observed in all four wires due to Defect 3 at the same time.
- Defect 2, the soft bottom concentrated around the reinforcing cage, produced no effect discernable from the roll-off effect. This observation is even true if the bottom of shaft temperatures from Test Shaft 1 are compared with those from the Control Shaft. The two responses are nearly identical, despite the considerable volume of sand surrounding the TIP sensors at the bottom of Test Shaft 1 (Figure 23).

Overall, temperatures in Test Shaft 2 (Figure 48) were lower than in either of the other shafts, presumably because of the effect of the permanent casing, which resulted in a smaller diameter and reduced volume of concrete as well as annular space around the casing. In addition, ambient temperatures were lower on the day of placement and the day following placement for Test Shaft 2. Otherwise, the TIP response in Test Shaft 2 appears to be dominated by the effect of Defect 10 (weak concrete). The effect of Defect 10 is similar to that of Defect 6 as described above for Test Shaft 1, but even more pronounced. At the time of maximum rate of temperature rise, temperatures in the Defect 10 zone were notably low with little increase with depth and a transition zone below the defect that appears similar in shape to the effect of roll-off.

The other defects in Test Shaft 2 are less evident. Defect 7 (uniform soft bottom) had no clear effect. For both Defect 8 (tremie breach) and Defect 9 (inside-cage inclusion), slight temperature decreases are apparent at the time of maximum temperature increase, but not at the time of peak temperatures. From the TIP measurements at the time of maximum temperature increase, it is also possible that both Defect 8 and Defect 9 were not installed at precisely the depth shown in the as-built records, or that they were not installed precisely in the center of the shaft. Defect 8 appears to have had the greatest effect slightly above the as-built depth and on the south side of the shaft. At the time of maximum rate of rise, Defect 9 appears to have lowered temperatures below the as-built depth on the east side of the shaft, but above the as-built depth on the east, south, and west sides of the shaft. (The east wire temperatures dip both above and below the as-built depth of Defect 9.) This suggests the Defect 9 sandbags floated to disperse locations.

For all three shafts, roll-off at the base of the shaft predominately occurred over the bottom 2 ft. For the Control Shaft and Test Shaft 1, the roll-off continued gradually over another 2 to 4 ft, while the roll-off in Test Shaft 2 appears to have been limited to the bottom 2 ft. For all three shafts, the roll-off effect is sharper at the time of maximum temperature rise than at the time of peak temperature.

5.2.2 Qualitative Evaluation of TIP Results: Effective Radius

Effective radius profiles were produced using PDI's TIP software. The effective radius values are based on the methodology described in Section 2.3.4, specifically a Level 2 analysis that models the temperature-radius relationship using average temperatures from TIP and the concrete volume log data from Appendix D and Figure 31. (The concrete volume log results are an input for the PDI software.) Each temperature-radius model was based on two or three points, corresponding to the number of concrete trucks used during placement. The effective radius analyses are based on the peak temperature profiles. The roll-off corrections were implemented using the default parameters from PDI's software.

The effective radius profiles lead to observations that are similar to those already offered based on the concrete yield plots in Chapter 4 and based on the qualitative evaluation of temperature records above. For the Control Shaft, effective radius values in the top half of the shaft are mostly consistent with the nominal shaft radius of 29 in., and also capture the change in diameter at the top of the shaft fairly well. Below a depth of 17 ft, effective radius is considerably greater than the nominal shaft radius of 26 in. These observations are consistent with those discussed in Section 4.3 based on the record of concrete placement volumes. The effective radius analysis of the Control Shaft also results in predictions of cage

offset toward the south (Wire 3), similar to the observation from temperatures above. Near the bottom of the Control Shaft, the effective radius decreases slightly around 29 ft and then increases at the base of the shaft (30 ft). These values are in the roll-off zone, where the PDI software effective radius interpretation is based on the hyperbolic tangent curve-fitting process described in Section 2.3.4. The decreased radius at 29 ft indicates measured temperatures were less than temperatures fitted using a hyperbolic tangent curve, whereas the increased radius at 30 ft indicates measured temperatures were greater than temperatures fitted to the same curve. The effective radius values near the base of the shaft are likely a result of the TIP data not following a clean hyperbolic tangent shape, rather than the radius of the shaft actually decreasing (necking) and then increasing (bulging) over a 2 ft span. That one point would be too great and the other too small is consistent with the mathematical nature of curve fitting (i.e. consistent with the minimization of the sum of squared errors).

For Test Shaft 1, the effective radius approach yields a similar observation regarding consistency with the concrete volume log: greater effective radius than nominal radius in the top half of the shaft, and about equal with nominal radius in the bottom half of the shaft. Notably, the effect of the defects on the effective radius values is muted compared with the effect on measured temperatures. Defect 3 (necking) produced a notable drop in temperature at peak time and especially at the time of maximum rate of temperature rise. The effect on effective radius is barely discernable. As shown in Figure 52, the effect was similarly muted even when the effective radius interpretations are based on the temperatures from the time of maximum rate of temperature rise. Defect 6 (weak concrete) would also potentially be missed from the effective radius approach, at least qualitatively. The effective radius does, in fact, decrease throughout Defect 6, but it is not clear from the effective radius approach that the decrease is due to a defect as opposed to simply roll-off. The effect of Defect 6 on the temperature results was more pronounced. The shape of the effective radius curve near the bottom of Test Shaft 1 resembles that from the Control Shaft. As for the Control Shaft, the effective radius values likely indicate limitations of hyperbolic tangent curve fitting rather than actual shaft geometry.

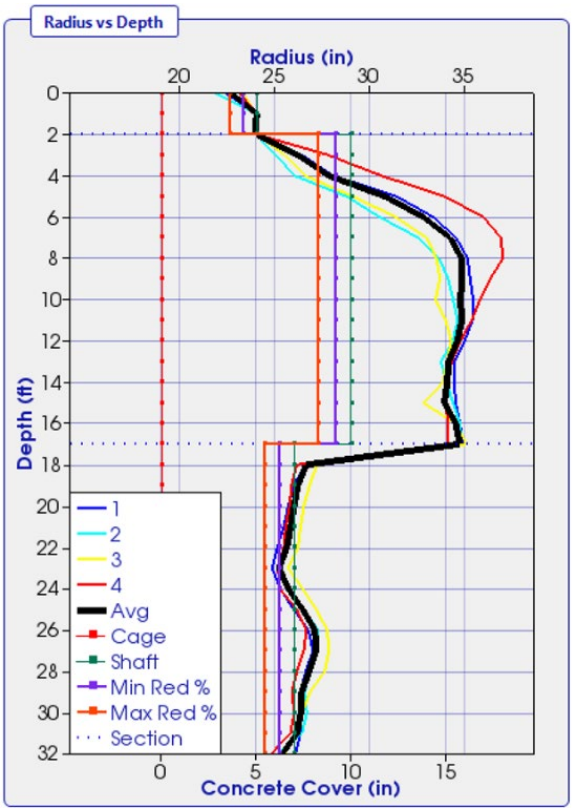

Figure 52: Effective radius interpretation for Test Shaft 1 at time of maximum rate of temperature rise. Results are very similar to the interpretation at peak temperature, as shown in Figure 47.

The effective radius approach is not terribly informative for Test Shaft 2 because of the permanent casing. The effective radius equals the casing radius except for the top 7 ft, where the effective radius decreases. Presumably this is in response to the substantial drop in temperatures attributed to the weak concrete of Defect 10. As observed for Test Shaft 1, the effect of the defect is clearer from the raw temperature data than from the effective radius interpretations.

The effective radius interpretations can also be evaluated relative to the shaft geometry, including the assumed locations of the edge of the shaft (based on the design diameter) and the reinforcing cage. In Figure 46, Figure 47, and Figure 48, the edge of shaft and reinforcing cage are shown with green and red vertical lines, respectively. For all three shafts, all below-grade effective radius values are significantly greater than the radius of the reinforcing cage, implying concrete cover along the entire length of each shaft. The amount of cover implied by the effective radius interpretation for all shafts is considerable, ranging from 5 or 6 in. to as much as 10 in. This is consistent with the large theoretical cover value of 7 to 10 in. (a result of casing availability requiring construction of shafts with diameters 6 to 12 in. greater than design, without modification to the reinforcing cage diameter). For the Control Shaft and Test Shaft 1, the effective radius values are generally equal or greater to the theoretical shaft diameter, which is consistent with the overexcavation explained previously. The effective radius interpretation of Test Shaft 2 was discussed with respect to shaft diameter previously.

The effective radius interpretation facilitates calculation of concrete cover, but concrete cover is not actually measured with TIP methods. The computed values of concrete cover are, at best, limited by the reliability of the temperature-radius models, which are typically limited by the reliability of concrete volume estimates. The cover values calculated from effective radius interpretations are better considered as another qualitative assessment of concrete integrity rather than a reliable indication of specific concrete cover distances. Finally, it is also important to consider that many drilled shaft concrete problems do not relate to cover. For instance, the weak shaft defects atop Test Shafts 1 and 2 result in reduced concrete cover values from the effective radius interpretations, but the problems associated with these defects of course have nothing to do with concrete cover. Evaluation of interpreted concrete cover is not necessarily any more logical a measure of drilled shaft concrete integrity than measured temperature differences.

5.2.3 Qualitative Evaluation of CSL Results

For the Control Shaft (Figure 49), the FAT profiles are relatively consistent with depth, with perhaps some tendency for the arrival times to decrease with depth. As described in the previous section, the interpretation threshold value affects the FAT profiles, with the 30 mV and 40 mV profiles significantly noisier than the 50 mV profile. The noise generally results in negative spikes (reductions in FAT over a short length of the shaft). Nothing in the FAT profiles would be cause for concern, although there are minor positive spikes in FAT just below Defect 1 (inside-cage inclusion). Defect 1 would be expected to produce slower arrival times if the bags were located directly in the wave paths. Defect 1 appears to have had a greater impact on relative energy than on FAT. Prominent negative spikes in relative energy records were observed for pairings between Tubes 2-3 (east-south), Tubes 1-3 (north-south), and Tubes 2-4 (east-west) at depths of approximately 13.5 ft. This suggests the sandbags were near the center of the shaft, perhaps slightly toward the southeast, and also about 1.5 ft below the intended depth.

For Test Shaft 1 (Figure 50), CSL records are relatively uniform with no obvious evidence of anomalies. The FAT profiles are quite uniform with depth, with relatively little noise, except for modest noise near the top of the shafts. As anticipated, there is no indication of Defect 2 (outside-cage soft bottom) in the CSL data. Surprisingly, there is evidence of Defect 3 (necking) in the CSL response for Tubes 1-4 (north-west), with a notable positive spike in FAT. An increase in relative energy is apparent too, although the relative energy profile for those tubes is fairly noisy. The spikes could be a coincidence, or it could be that part of a loose sandbag (Figure 24) draped into the path between Tubes 1 and 4 (north and west). Also somewhat surprising is that the wheel bearing grease of Defect 4a did not appear to produce any significant debonding. As anticipated, Defect 5 (sandbags outside one side of cage) did not result in any CSL effects. Defect 6 (weak concrete) did not result in any notable increase in arrival times (as might be expected for less stiff concrete) near the top of the shaft, but the CSL data (FAT and relative energy) are noisier in the Defect 6 zone.

The CSL records for Test Shaft 2 (Figure 51) offer greater evidence of defects than was observed for Test Shaft 1. For the FAT records, there is strong evidence of a problem near Defect 4b, which appears to have been successful in producing debonding of at least some access tubes. Some arrivals were also delayed near the bottom of the shaft in the Defect 7 soft bottom. The FAT records are otherwise fairly uniform, with little or no evidence of Defect 8 (tremie breach), Defect 9 (inside-cage inclusion), or Defect 10 (weak concrete). However, the relative energy profiles appear to reflect all of the defects except for Defect 10. The negative spikes in relative energy are particularly notable for all defects (except Defect 10) involving Tube 4 (west), which suggests the defects tended toward the west side of the cage. It is also noteworthy that the decreases in relative energy attributed to Defect 9 occurred above the as-built depth for some tube pairings and below the as-built depth for others. This is consistent with observations from TIP, which also suggested the sandbags floated to different locations.

One potential explanation for the difference in response between FAT and relative energy is that the sandbags comprised a relatively short length of the ray path, so the arrival times were not significantly delayed. However, the sand could have damped the pulse signal considerably, resulting in a significant impact on relative energy.

5.3 Quantitative Evaluation of Results

Quantitative analyses of the TIP and CSL data were performed to more precisely evaluate the trends outlined qualitatively. The quantitative analyses also facilitate a more formal evaluation of sensitivity.

5.3.1 Quantitative Evaluation of TIP Results

To quantify the effects discussed in the previous section, temperature differences and effective radius differences were calculated from the TIP data. The definitions used in the calculations are fairly intuitive albeit somewhat objective. The definitions were applied “manually”; the TIP software does not automatically compute temperature differences as defined in this section.

Temperature difference, ΔT, was defined as the difference between a baseline temperature, $T_{baseline}$, and the temperature observed at the defect, T_{defect}:

$$\Delta T = T_{baseline} - T_{defect}$$

The effective radius difference was defined similarly:

$$\Delta r_{eff} = r_{eff-baseline} - r_{eff-defect}$$

The primary challenge with these definitions is establishing the baseline temperature and radius. The baseline temperature for the analyses in this section was defined as the temperature at a nearby depth that demonstrated no clear effect from the defect. Selecting the baseline depth involved some degree of judgment; explanations are included below for the more difficult choices. The other decision to be made in selecting baseline and defect temperatures (and effective radius values) is whether to use average values or values from individual wires. For the analyses in this section, the value that produced the greatest effect was used. The selection of local versus average was always consistent with the nature of the defect, e.g. a local temperature was used for sandbags on one side of the shaft, but the average temperature was used for defects in the center of the shaft or distributed throughout the shaft.

Results of the quantitative analysis of TIP data are shown in Table 10. The table includes results for both the change in temperature and the change in effective radius. Both quantities were calculated at the time of maximum rate of temperature rise as well as at the peak time. The change in effective radius values are presented in units of inches and as a percentage of the nominal radius. Considering the temperature differences, the quantitative analysis is generally consistent with the qualitative analysis:

- All observable effects were greater at the time of maximum rate of rise than at peak time.
- The greatest effects were observed for the zones of weak concrete, with temperature differences greater than 12° F at the maximum rate of rise and equal to about 7° F at the peak time. These

differences were established using the bottom of the defect zone for T_{defect} and a depth of 6 or 7 ft for $T_{baseline}$ in order to reduce the influence of roll-off on the calculated temperature difference.
- The effect of defects outside the reinforcing cage were also significant, producing effects between 5 and 7° F at the time of maximum rate of rise. However, the effects diminished significantly by the time of peak temperature, especially for the defect on one side of the shaft (Defect 5).
- The effect of the tremie breach was limited to one wire, and to a temperature difference of less than 4° F.
- For the inside-cage inclusions, only an effect for Defect 9 was observed, with ΔT between 3 and 4° F at the time of maximum temperature rate of rise. No effect was observed for Defect 1.
- Effects of zero were listed for the soft bottom defects (Defects 2 and 7) because effects could not be discerned.

Considering effective radius differences also yields observations similar to those offered in the qualitative analysis. The defects consisting of weak concrete had the greatest effect on effective radius, producing reductions on the order of 3 or 4 in. or 13 to 14% of the nominal radius at the time of maximum rate of rise. The reductions were considerably diminished by peak time. The outside-cage defects (Defects 3 and 5) also produced reductions in effective radius. The reductions for the outside-cage defects were all between 6 to 8%, but the reduction in effective radius for Defect 5 was zero by peak time. No change in effective radius was observed for Defect 8 (tremie breach) or Defect 9 (inside-cage inclusion). Except for in the zone of weak concrete of Defect 10, the effective radius of Test Shaft 2 corresponds to the permanent casing radius.

Table 10: Results of quantitative analysis of TIP data.

Defect	Shaft	Depth, ft	Cross-section Location	% of Shaft Area	Description	Time of Max Rate of Rise		Peak Time	
						ΔT, °F	Δr_{eff}, in. (%)	ΔT, °F	Δr_{eff}, in. (%)
1	Control	15	Center of shaft	10%	Inclusion in cage interior	0	0	0	0
2	Test 1	30	Shaft perimeter	50%	Soft bottom	0	0	0	0
3	Test 1	21	Entire cage perimeter	10%	Similar to necking	*From average of all wires:* 6.7	1.9 (7.3)	5.0	1.6 (6.2)
4	Test 1	16.5	Reinforcing cage	N/A	Debonded CSL tubes	Not applicable to TIP.			
5	Test 1	12	1/3 of cage Perimeter	10%	Defect outside cage	*From south wire:* 5.2	2.3 (7.9)	0	0
6	Test 1	0-5	N/A	N/A	5-ft zone of weak concrete	*From average of all wires:* 12.3	4.1 (14)	7.4	1.7 (5.9)
7	Test 2	30	Entire shaft bottom	100%	Soft bottom	0	0	0	0
8	Test 2	21	N/A	N/A	Tremie breach	*From south wire:* 3.4	0	0	0
9	Test 2	12	Center of shaft	15%	Inclusion in cage interior	*From south wire:* 3.4	0	0	0
10	Test 2	0-5	N/A	N/A	5-ft zone of weak concrete	*From average of all wires:* 16.7	3.3 (13)	7.0	0.3 (1.2)

5.3.2 Quantitative Evaluation of CSL Results

Quantitative analysis of CSL results included calculations of increased arrival time and decreased relative energy. The increase in FAT, ΔFAT, was calculated as a percentage of the baseline, $FAT_{baseline}$:

$$\Delta FAT = \frac{FAT_{defect} - FAT_{baseline}}{FAT_{baseline}} * 100\%$$

The FAT at the defect, FAT_{defect}, was generally the greatest value of FAT at depths near the installed defect. The baseline FAT was identified from FAT values just above and just below the defect zone. The decrease in relative energy, ΔE_{rel}, was calculated in decibels (dB) from the ratio of the baseline relative energy, $E_{rel-baseline}$, to the relative energy at the defect, $E_{rel-defect}$:

$$\Delta E_{rel} = 10 \log \frac{E_{rel-baseline}}{E_{rel-defect}}$$

Decibels are a logarithmic unit of measure, which is consistent with the log scale of the relative energy plots. Values for $E_{rel-defect}$ and $E_{rel-baseline}$ were selected in a manner consistent with FAT_{defect} and $FAT_{baseline}$ (i.e. $E_{rel-defect}$ as the lowest value at depths consistent with the installed defect, $E_{rel-baseline}$ as the relative energy value just above and below the defect zone).

Results of the quantitative analysis are summarized in Table 11. For each defect, the table lists values for changes in arrival time and relative energy from one tube pairing, generally the tube pairing that produced the greatest changes in FAT and relative energy. Results in the table are compatible with the qualitative interpretation of the CSL results:

- The greatest effects were observed for the uniform soft bottom (Defect 7), which produced a 25% decrease in FAT, and for tube debonding (Defect 4), which had an effect of similar magnitude. For both defects, reductions in relative energy were observed for all tube pairings.
- Increases in arrival time between 10 and 20% were observed for both defects consisting of sandbags inside the reinforcing cage (Defects 1 and 9). An effect of similar magnitude was observed for the tremie breach defect (Defect 8). For the inside-cage defects, reductions in relative energy were observed in about half of the tube pairings, with no discernable effect in the others. For the tremie breach, reductions in relative energy were observed in all but one tube pairing.
- No response was observed for the weak concrete defects (Defects 6 and 10), the soft bottom outside the reinforcing cage (Defect 2), or the two sandbags outside one side of the reinforcing cage (Defect 5). Surprisingly, a significant effect was observed for Defect 3, which consisted of sandbags around the entire perimeter. The anomaly was only observed for one tube pairing. Such a result is not likely repeatable; CSL should not be relied on to detect defects outside the reinforcing cage.

Importantly, none of the increases in arrival time would have been designated as the most severe type of anomaly per the criteria defined in Section 2.5. Most of the criteria establish 30% and greater increases in FAT as “poor,” with increases between 10 or 20 and 30% deemed “questionable.” However, the GRL (2015) criterion that considers ΔE_{rel} in addition to ΔFAT establishes decreases in relative energy of 12 dB and greater as defective. By that standard, the center of shaft defects in Test 2 (soft bottom and sandbags in center of cage) would have been classified defects. The debonded tubes would also have been classified as defective. The difference in sensitivity between ΔE_{rel} and ΔFAT is consistent with the qualitative observation that the relative energy was more responsive to the installed defects for this research. As explained previously, this finding could be specific to the use of sandbags.

Table 11: Results of quantitative analysis of CSL data.

Defect	Shaft	Depth, ft	Cross-section Location	% of Shaft Area	Description	ΔFAT, %	ΔE_{rel}, dB
1	Control	15	Center of shaft	10%	Inclusion in cage interior	*From Tubes 2-3:* 17	7.7
2	Test 1	30	Shaft perimeter	50%	Soft bottom	0	0
3	Test 1	21	Entire cage perimeter	10%	Similar to necking	*From Tubes 1-4:* 26	5.0
4	Test 2	4.5	Reinforcing cage	N/A	Debonded CSL tubes	*From Tubes 1-4:* 13	17
5	Test 1	12	1/3 of cage Perimeter	10%	Defect outside cage	0	0
6	Test 1	0-5	N/A	N/A	5-ft zone of weak concrete	0	0
7	Test 2	30	Entire shaft bottom	100%	Soft bottom	*From Tubes 1-3:* 25	12
8	Test 2	21	N/A	N/A	Tremie breach	*From Tubes 3-4:* 14	7.2
9	Test 2	12	Center of shaft	15%	Inclusion in cage interior	*From Tubes 1-4:* 11	15
10	Test 2	0-5	N/A	N/A	5-ft zone of weak concrete	0	0

5.4 Effect of Time on TIP Temperatures and TIP Sensitivity to Defects

Various temperature versus time graphs are considered in this section to evaluate the effect of time on the interpretation of TIP records. Most of the graphs were created by plotting the average of four sensors (one per wire) for a specific depth, but for a few graphs, specific sensors from one wire were used rather than the average. All data from the sensors were considered without averaging or otherwise filtering in the time domain. The first graph, Figure 53, shows the temperature response versus time for each shaft at the depth of peak temperature. The entire time record (approximately 3 weeks) is shown. The shapes of the plotted lines are similar for each shaft, with each indicating a relatively sharp rise to peak temperatures within about one day, followed by a gradual decrease in temperatures lasting weeks. The temperature in Test Shaft 2 is notably less than that in the other two shafts. Several explanations likely contribute to the lower Test Shaft 2 temperatures: the shaft had a smaller diameter than the other two shafts because of the permanent casing, the shaft also likely had annular space around the permanent casing, and the ambient temperature on the day of placement and the day after placement was lowest for Test Shaft 2. Lastly, it is worth noting that the temperature data in Figure 53 is smooth and free of noise.

To more closely evaluate the temperature rise portion of the time records, the same data from Figure 53 are plotted for the first 48 hours only in Figure 54. For all three shafts, the temperature rose slowly for the first six hours, rose most sharply for the next six hours, began to level off around 18 to 24 hours, after which it began to decrease. As noted for Figure 53, the rate of temperature decrease was considerably slower than the rate of temperature increase from about 6 to 18 hours.

An important consideration for evaluating TIP sensitivity to defects is how the sensitivity may change with time. “When is the best time to identify defects?” is a question of considerable practical importance. To evaluate the sensitivity versus time, temperature versus time graphs were created for four types of defects: (1) concentric defect around the entire edge of the reinforcing cage (Defect 3) in Figure 55, (2) defect outside one side of the reinforcing cage (Defect 5) in Figure 56, (3) defect inside the reinforcing

cage (Defect 9) in Figure 57, and (4) weak concrete (Defect 10) in Figure 58. For each figure, four lines are included. The black dash-dot line is the temperature-time record for the peak depth (i.e. the same as was presented in Figure 53 and Figure 54). This line is included for reference. The solid blue line is the temperature-time record for the defect depth, and the solid green line is the temperature-time record for a nearby "baseline" depth that appeared to not be influenced by the defect. The purple dashed line is the temperature difference between the defect depth and the baseline depth and is plotted on the right vertical axis.

For each type of defect, the largest temperature differences attributed to the defects were observed within two hours of the time of maximum rate of temperature rise. For all defect types except the concentric outside-cage defect (Defect 3), the temperature difference attributed to the defect decreased considerably after peaking at the time of maximum rate of temperature rise. For two of the defect types, the inside-cage defect (Defect 9) and the defect outside one edge of the cage (Defect 5), the decrease in temperature difference was considerable, decreasing to zero within about 30 hours of concrete placement.

The tendency for the greatest temperature difference to occur at the time of maximum rate of temperature rise is consistent with the observation from the qualitative assessment that defects were more readily identified at the time of maximum rate of temperature rise than at the time of peak temperature. This observation has considerable practical implications. Most importantly, the observation leads to the conclusion that TIP testing by wire will enable defect identification more effectively than testing by probe. For all defect types, the temperature difference attributed to the defect decreased after the time of maximum rate of temperature rise, and for two of the three types of defects, the decrease in the temperature difference was sharp. If the probe method is used, it is unlikely to reliably occur at the time of maximum rate of temperature rise, partly because that time is quite difficult to predict and varies from shaft to shaft, and partly because of practical considerations associated with performing the test on a precise schedule.

Beyond simply lending support to using TIP wires instead of probes, the observation that TIP sensitivity changes over relatively short time intervals leads to the recommendation to explicitly evaluate temperature versus time data when interpreting TIP data. Currently, PDI's software allows users to scroll through temperature versus depth profiles, viewing the data at successive time intervals. This offers some insight as to the best time for identifying defects, but it is not as effective or straightforward as simply plotting temperature versus time as was completed for this analysis. The difference in ΔT versus time for each type of defect considered also suggests TIP interpretations could potentially be improved by identifying various temperature-time "signatures" associated with certain types of defects.

Lastly, temperature versus time records are shown for the average of the bottommost sensors in each shaft in Figure 59. Considering the similarity among the three records, Figure 59 is further evidence that the soft bottom defects (Defects 2 and 7) had no effect on the TIP records.

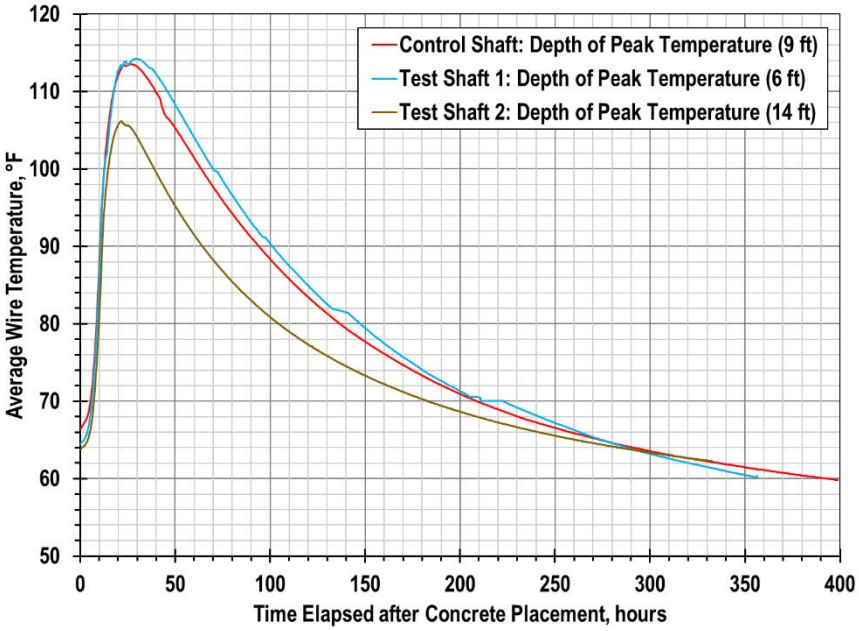

Figure 53: Temperature versus time for peak depths of each shaft.

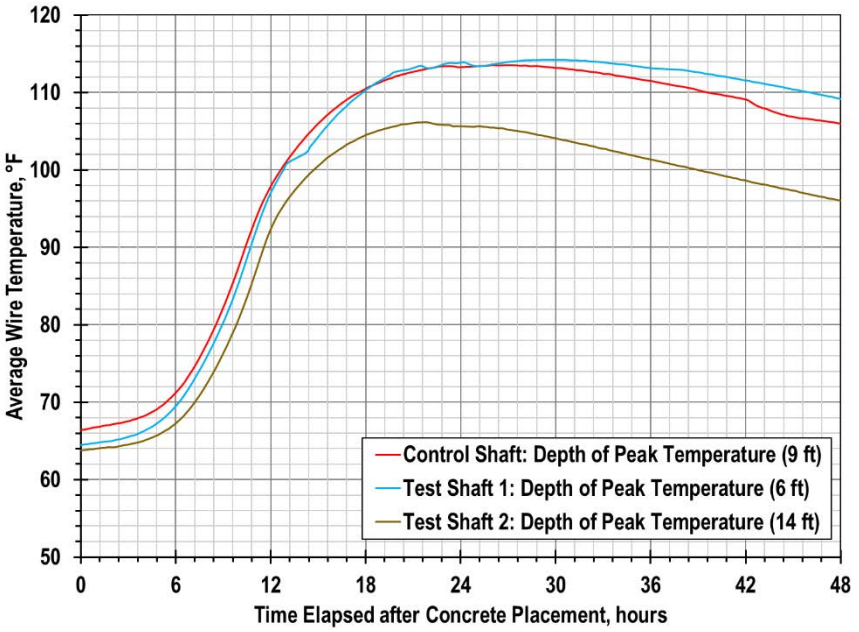

Figure 54: Temperature versus time for peak depths of each shaft during first 48 hours after concrete placement.

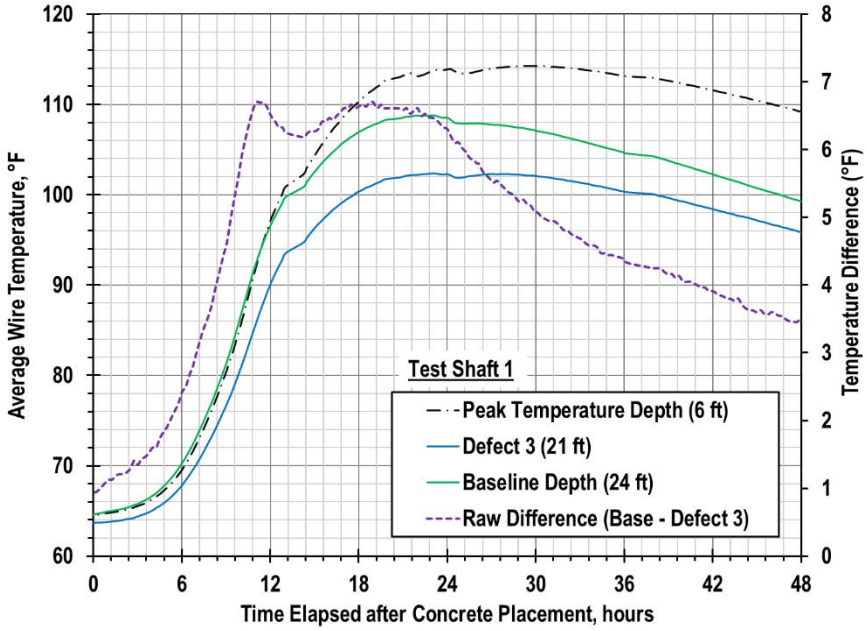

Figure 55: Temperature versus time for analysis of Defect 3, six 24 lb sandbags around entire circumference of reinforcing cage.

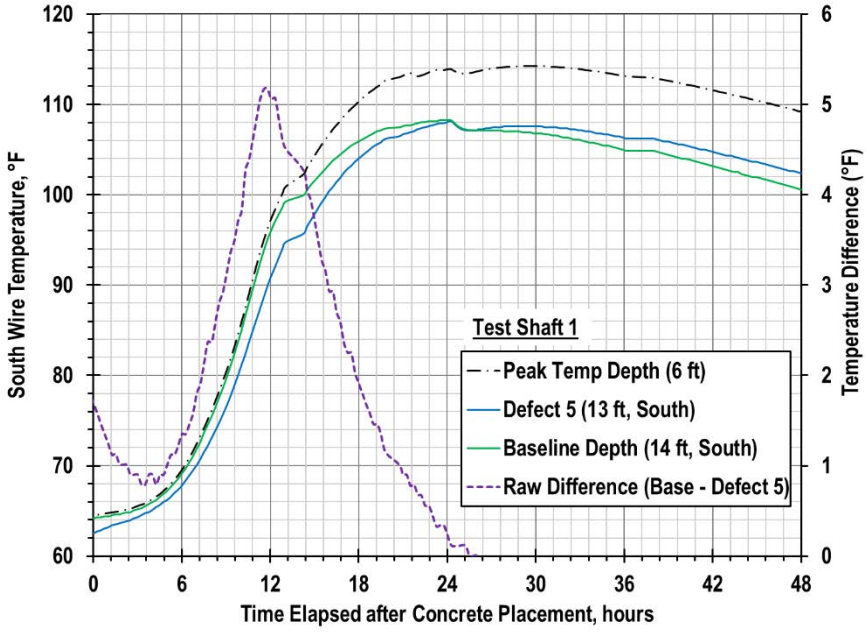

Figure 56: Temperature versus time for analysis of Defect 5, two 70 lb sandbags outside one side of reinforcing cage.

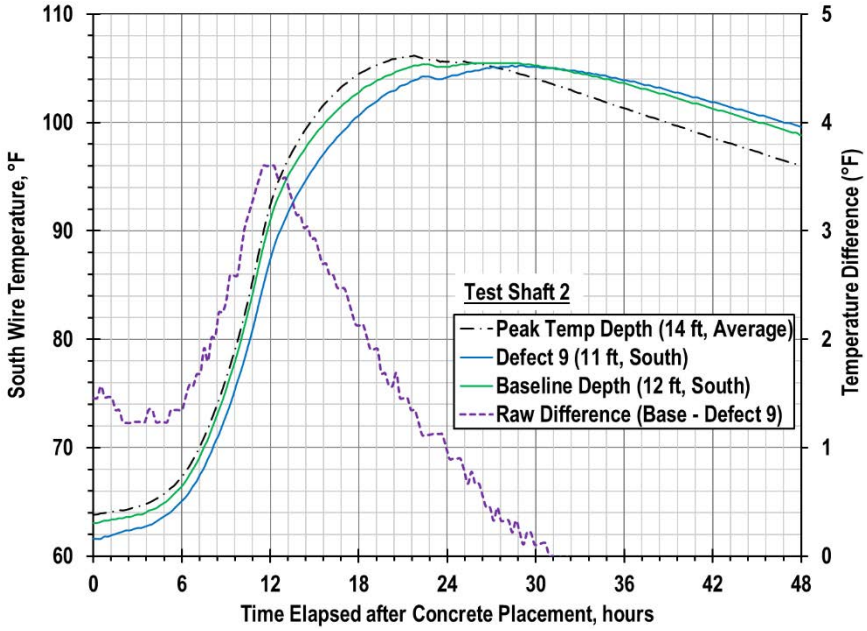

Figure 57: Temperature versus time for analysis of Defect 9, five 70 lb sandbags inside reinforcing cage.

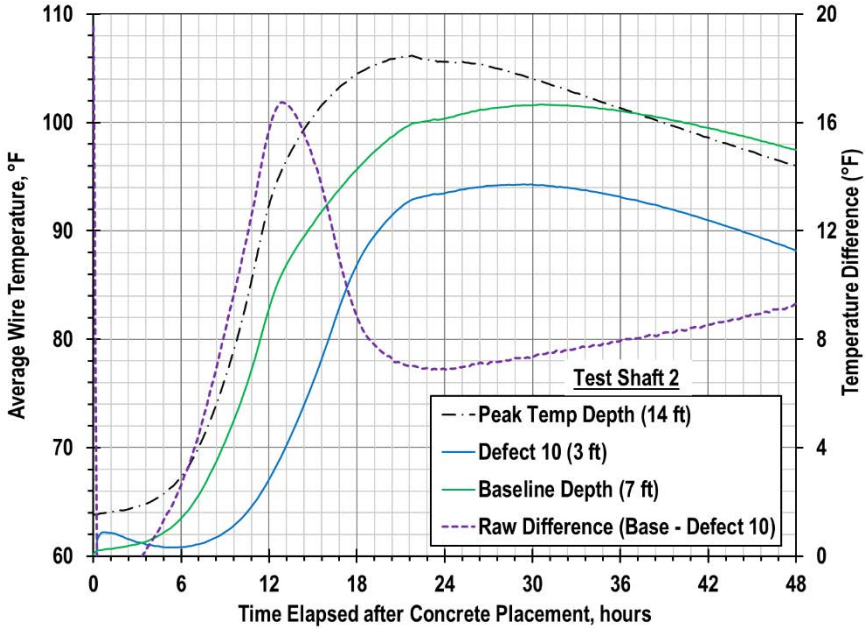

Figure 58: Temperature versus time for analysis of Defect 10, weak concrete near top of shaft.

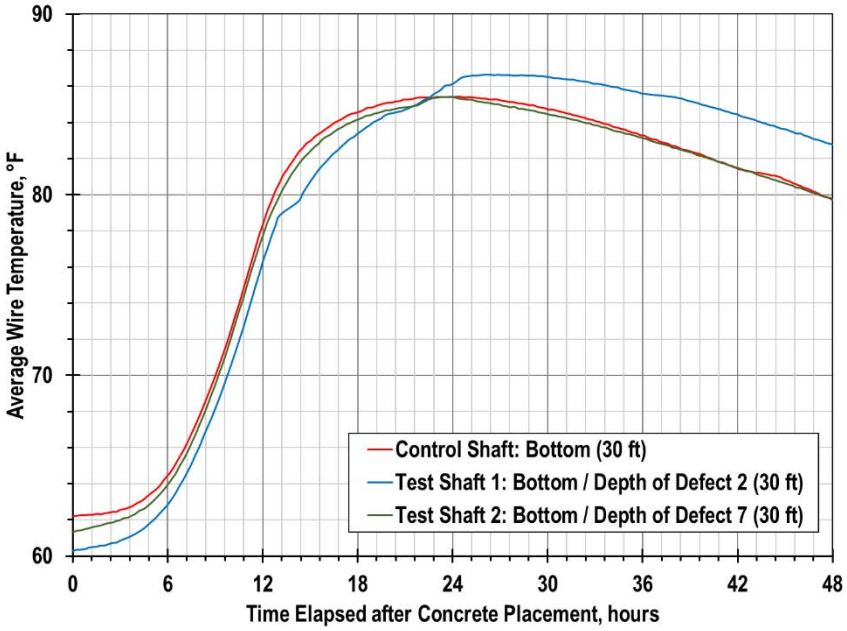

Figure 59: Temperature versus time for analysis of bottom of shaft conditions.

5.5 TIP Probe Results

TIP probe results are shown for the Control Shaft in Figure 60, for Test Shaft 1 in Figure 61, and for Test Shaft 2 in Figure 62. In each figure, the probe method TIP profile with depth is shown at left, and the wire TIP profile at approximately the same time is shown at right. The wire method results show significantly greater temperatures, and significantly greater temperature variation with depth. The greater variation is associated with greater sensitivity to defects for the wire measurements. The probe temperatures are too low, could not be used to identify any defects, and are almost certainly erroneous. The most likely cause for the error is inadequate time for the probe to acclimate to tube temperatures, which was likely exacerbated by the cold temperatures during the week of concrete placement. It is also important to note that measuring time-domain variations in temperature with the probe method presents practical challenges associated with collecting multiple sets of data and potential changes in temperature during the time required for data collection.

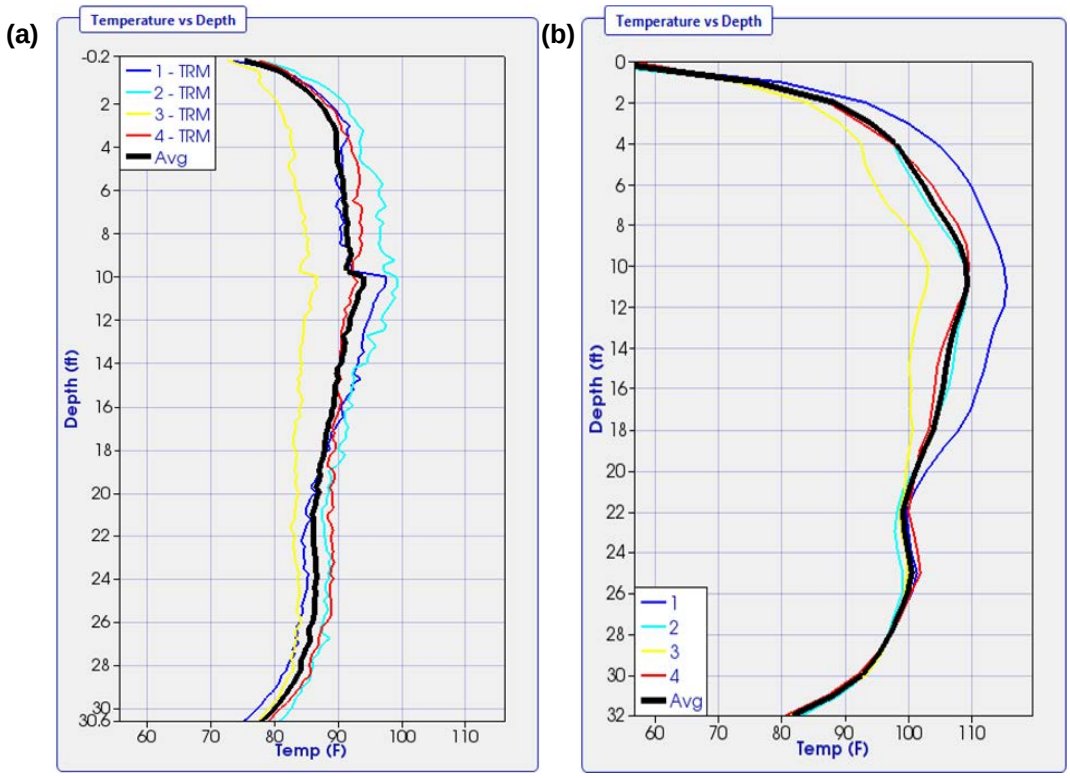

Figure 60: TIP results for Control Shaft 42 hours after concrete placement: (a) probe and (b) wire.

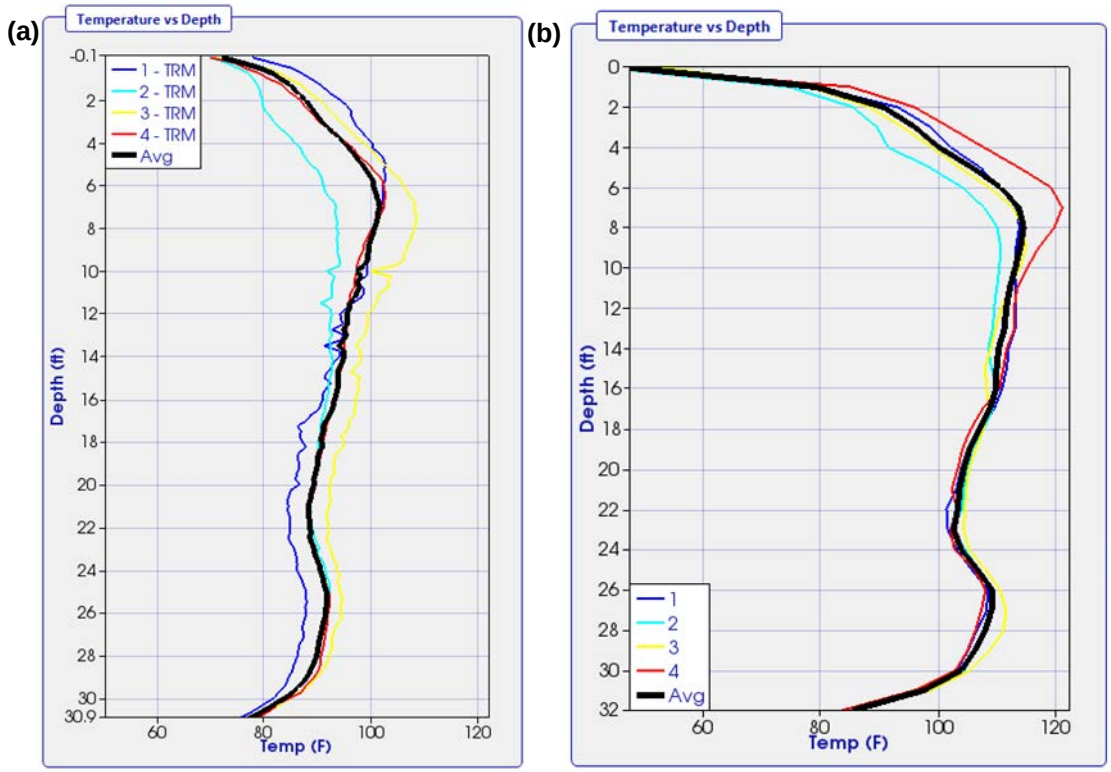

Figure 61: TIP results for Test Shaft 1 24 hours after concrete placement: (a) probe and (b) wire.

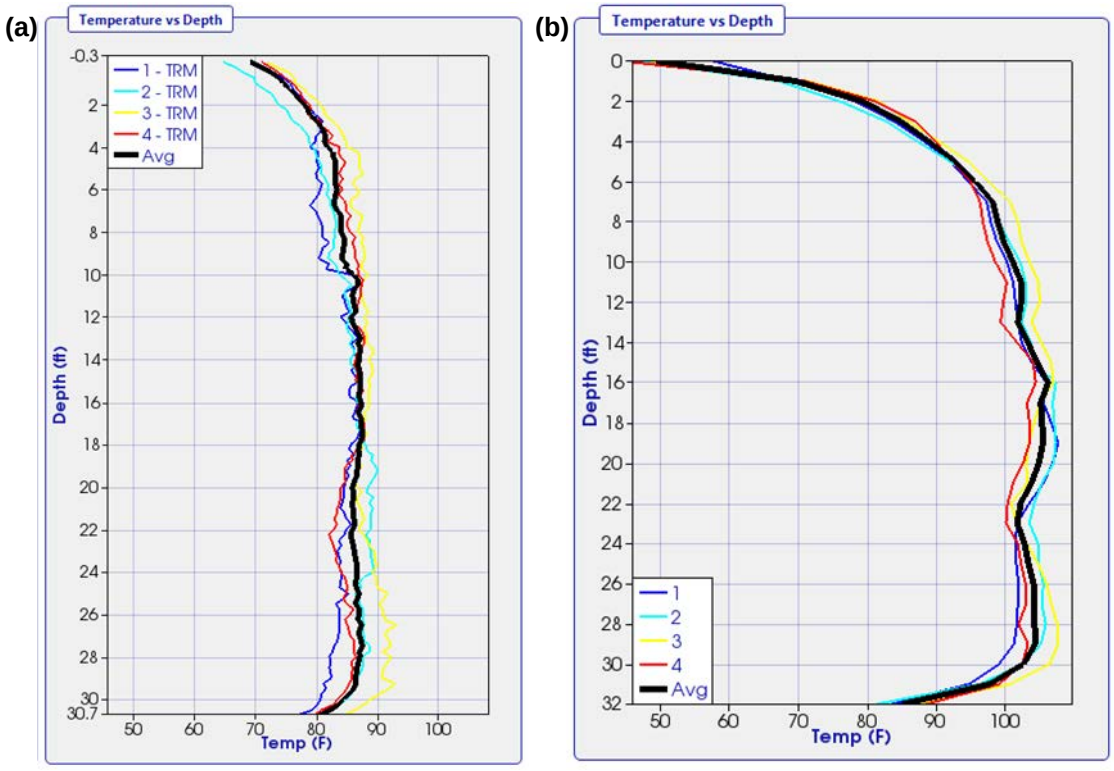

Figure 62: TIP results for Test Shaft 2 22 hours after concrete placement: (a) probe and (b) wire.

6. Summary and Discussion

This chapter begins with a list of findings that captures the most relevant information from previous chapters. The findings are then synthesized, first with a general assessment of the ability to detect defects for CSL and TIP and then with a summary of advantages and limitations of each method.

6.1 Summary of Results from Previous Work and Field Tests

This report has documented many significant results regarding TIP capabilities, limitations, and interpretation methods. The findings are summarized in the list below, which is organized by topic.

Effect of Defects on Structural Resistance

- Sarhan et al. (2000) investigated the effect of various drilled shaft concrete defects on structural resistance with an experimental study involving full-scale drilled shafts, physical model tests, and analytical models. The defects investigated included necking voids representing 15% of the cross-section, 4 in. cage offsets, corrosion representing a loss of 15% of reinforcement, and concrete with compressive strength reduced by 15%. Both axial and flexural resistance were evaluated. The defect with the largest effect was a necking void, which reduced axial resistance by 18% and flexural resistance by 27%. Combinations of multiple defects at critical locations had more significant impacts but were also noted as highly unlikely.

TIP and CSL Sensitivity to Defects based on Previous Research

- Schoen et al. (2018) performed TIP and CSL testing on a 5 ft diameter drilled shaft with two defects consisting of gravel bags attached to the inside of the reinforcing cage. For both defects, the bags represented 15% of the shaft cross section. TIP measurements 14 hours after concrete placement indicated temperature drops of 12 and 14° F due to the bags. TIP measurements at time of peak temperature of 34 hours indicated the effect of the gravel bags had diminished to between 3 and 8° F.

- Mullins et al. (2007) performed TIP testing on a 4 ft diameter drilled shaft with intentional defects consisting of sandbags outside the reinforcing cage. The defects represented about 10% of the shaft diameter. For one defect, the bags were on opposite sides of the reinforcing cage; for the other, the bags were all on one side of the cage. The effect of the sandbags was evident from temperature drops of perhaps 3 or 4° F, but difficult to interpret because of significant temperature variation among the access tubes. The timing of the TIP probe measurements is believed to have been close to the time of peak concrete temperatures.

- Ashlock and Fotouhi (2014) performed TIP and CSL testing on two 5 ft diameter drilled shafts with intentional defects. The TIP tests were completed by probe method. For the first shaft, cylinders of hardened but weak concrete were tied to the reinforcing cage. The cylinders represented only 3 to 4% of the shaft cross-section and did not produce any significant anomalies in TIP or CSL tests. For the second shaft, cylinders of aggregate and water representing 8% of the shaft cross-section were included. The TIP response was unclear because cage misalignment led to significant variations in temperature across the shaft, but it is possible to attribute an effect less than 5° F to the defects. CSL testing found a 25% increase in arrival times for the second shaft.

TIP and CSL Sensitivity to Defects based on WisDOT Projects

- Drilled shaft concrete placement issues, primarily soft bottom conditions and tremie breaches, were experienced for the Zoo Interchange project. CSL detected defects at two tremie breaches and three soft bottoms; all five defects were confirmed by coring. TIP reports for the project did not recommend further action (e.g. coring) for any of the Zoo Interchange defects. Most of the defects were not identified from TIP results because of wire breakage, but a drop in temperature was observed for one of the tremie breaches. The TIP report for that shaft recommended “provisionally accepting” the shaft,

contingent on the CSL report for the same shaft and noting adequate concrete cover based on the effective radius analysis.

TIP and CSL Sensitivity to Defects based on this Research

- Of the nine intentional defects (neglecting Defect 4, tube debonding), TIP measurements produced temperature decreases greater than 5° F for four defects, decreases between 3 and 5° F for two defects, and no discernable temperature decrease for the other three defects. The greatest temperature decreases were observed for weak concrete defects and defects outside the reinforcing cage, while limited temperature decreases were observed for inclusions within the reinforcing cage and the tremie breach defect. No temperature decrease was observed for the soft bottom defects or the smaller inside-cage inclusion.

- CSL measurements indicated at least 10% increases in arrival times and at least 5 dB decreases in relative energy for five of the intentional defects, with no discernable increase in arrival time or decrease in relative energy for the other four defects. However, results for one of the five "successful" defects, Defect 3, are suspect as the anomaly was only apparent in one of the tube pairings. The remaining successfully identified defects were defects within the reinforcing cage, including a soft bottom defect, and the tremie breach defect. CSL measurements did not produce significant indications for defects outside the reinforcing cage (except the suspect result) or for weak concrete. The tendency for false positive CSL results due to tube debonding was demonstrated with significantly delayed arrival times and decreased relative energy for CSL measurements at Defect 4.

- Based on the results of this study, the ability to detect defects with TIP is greatest at about the time temperatures are rising most quickly. This generally occurs at roughly half the peak time. For three of four types of defects evaluated, temperature differences attributed to the defects diminished significantly after peaking at the time of maximum rate of temperature increase. For two defect types, the temperature differences had decreased to zero within 30 hours of concrete placement.

TIP Procedures

- TIP wire breakages were problematic for the Zoo Interchange project, but improved wire design has significantly reduced the incidence of wire failures, according to users who routinely use TIP wires. None of the 12 wires installed for this project experienced any malfunctions.

- The effectiveness of probe measurements depends on the timing of the measurements with respect to the development of temperature differences due to defects (as described in the preceding list). Such timing is very difficult to control. The wire method, in contrast, results in a full time record of TIP measurements.

TIP Interpretation

- Mullins et al. (2007) outlined four levels of TIP analysis. Level 1 is the simplest type of analysis that involves a primarily qualitative review of the TIP temperature measurements. The other levels involve inferring the "effective radius" of the shaft from the TIP results using models relating temperature and radius. For Level 2, the model is based on concrete volume measurements during construction. Analytical thermal models are used to develop the temperature-radius models for Level 3, and the same thermal models are calibrated using the TIP measurements in Level 4. Currently, TIP reports that present effective radius interpretations are generally derived from the Level 2 approach.

- Results of this research indicate defects are more difficult to detect from effective radius interpretations than from simply evaluating the measured temperatures. Effective radius profiles combine observations from concrete placement with temperature observations from TIP. This can have the effect of obscuring effects that might be evident from separate consideration of concrete volume and temperature measurements. For Test Shaft 1 of this research, the temperature effect of weak concrete at the top of the shaft was offset by the volume effect of over excavation, resulting in

effective radius values that were generally greater than the nominal radius despite the presence of significantly "watered down" concrete.

- Findings from both Mullins et al. (2007) and Ashlock and Fotouhi (2014) indicate the presence of cage misalignment makes identification of defects more challenging. Cage misalignment causes temperatures to vary among the TIP wires (or access tubes) and can also cause temperatures to vary with depth. Both of these sources of variation may mask variation due to defects.

6.2 Sensitivity of TIP and CSL to Concrete Defects

Assessments of the sensitivity of TIP and CSL test methods to drilled shaft concrete defects are presented in Table 12. The assessments are based on the results summarized above from previous studies, this study, and project applications. Comparison of the evaluations in the table reveals TIP and CSL are generally complementary in terms of the types of defects they can detect. Each test is particularly well suited for some types of defects and rather poorly suited for other types of defects, but together the tests can identify virtually any type of defect.

The assessments of Table 12 are based on experimental studies, including this one, that attempt to identify a lower bound for the severity of defect that can be detected. Accordingly, the defects evaluated represent relatively small portions of the drilled shaft cross-section, typically 10 to 15%. As described in Section 2.6, defects of similar size were studied by Sarhan et al. (2000) and were shown to have a relatively modest effect on structural resistance, although the effects of defects depend on the specific details of a given project and shaft. It is also important to consider that the use of small defects in the experimental studies generally means the assessments of Table 12 can be considered lower bound assessments. For instance, tremie pipe breach defects that are relatively insignificant are potentially detectible with TIP, while more significant tremie pipe breach defects could be readily detectible.

Table 12: Summary of the ability to detect various types of defects for TIP and CSL.

Defect Type	Ability to Detect Relatively Modest Defects[1]	
	TIP	CSL
Inclusions in cage interior	Difficult to detect	Readily detectible
Defects outside reinforcing cage	Readily detectible	Not detectible
Soft bottom	Not detectible	Readily detectible
Weak concrete	Readily detectible	Difficult to detect
Breach of tremie pipe	Potentially detectible	Readily detectible

[1]Detection ability assessments are generally based on relatively small defects. Detection ability assessments would likely be greater for more significant defects.

6.3 Summary of Advantages and Limitations of TIP and CSL

The advantages and limitations of CSL and TIP testing are summarized in Table 13. One of the most significant differences between the two test methods is the zone of concrete within the shaft that is tested. CSL results are unaffected by defects outside the reinforcing cage since the ultrasonic wave is measured between access tubes affixed to the cage. TIP results should be influenced by defects anywhere within the shaft cross-section, and especially defects outside the reinforcing cage since such defects disproportionately affect one or two wires or access tubes. That TIP can detect defects outside the reinforcing cage is significant since concrete outside the reinforcing cage is critical for shaft side resistance, structural integrity, and durability. Results of this research indicate TIP results are not very sensitive to localized defects within the center of the reinforcing cage, at least for the size and character of defects considered.

Table 13: Significant advantages and limitations of TIP and CSL for evaluation of drilled shaft concrete integrity.

	Advantages	Limitations
TIP	• Can identify defects outside the reinforcing cage. • In addition to identifying defects, data can be used to indicate misalignment of reinforcing cage. • Tests can generally be performed within a day after concrete placement, resulting in potential construction schedule advantages. • Temperature information may provide additional value for large-diameter shafts subject to mass concrete considerations.	• No information about soft bottom conditions. • Ability to detect defects in the center of the shaft may be limited. • Challenges interpreting test data: o Distinguishing defects from nuisance effects. o Acceptance criteria are not well established. • Test window closes within days of concrete placement; optimal test time varies with diameter and shaft boundary conditions. This limitation is mostly insignificant for the wire method.
CSL	• Relatively long history of experience. • Reliably identifies concrete defects within central core of shafts. • Relatively simple interpretation.	• No information outside reinforcing cage: o Cannot identify defects outside of cage. o No indication of cage misalignment. • Relatively frequent “false positives,” particularly due to debonding of concrete from access tubes. • Must wait at least three days to perform test, potentially impacting overall construction schedule.

7. Conclusions & Recommendations

The most pertinent conclusions regarding the effectiveness of TIP and CSL test methods are presented in this chapter before recommendations for implementing TIP methods are discussed. Additional recommendations regarding CSL and future research are also provided.

7.1 Conclusions

This report has presented evaluations of the effectiveness of TIP and CSL concrete integrity test methods using documented TIP project experience, previous research, and original research involving testing of three full-scale drilled shafts with intentional defects. Significant findings included:

- TIP is a viable concrete integrity test method. TIP methods have been shown to effectively respond to many types of defects. The test has limitations, but so does every concrete integrity test method.

- TIP and CSL are complementary test methods. Neither test provides a perfectly reliable assessment of drilled shaft integrity, but combined, they can be used to detect most conceivable defects. Based on integrity test results of the drilled shafts for this study:

    - TIP measurements were clearly responsive to defects associated with weak concrete. TIP methods were also reasonably effective for identifying defects outside the reinforcing cage. TIP methods were less effective for identification of defects near the center of the shaft cross-section, and not useful for identifying soft bottom conditions.

    - CSL methods were effective for identifying a variety of defects within the reinforcing cage, including inclusions, effects of tremie breach, and inside-cage soft bottom defects. CSL measurements were ineffective for identifying defects outside the reinforcing cage, including outside-cage soft bottom defects as well as defects associated with zones of weak concrete.

- Defects are significantly more detectable with TIP methods when temperatures are evaluated prior to the development of peak temperatures. For this research, the largest temperature differences attributed to defects were observed around the time of maximum rate of rise in temperatures, which occurred at roughly half the time of peak temperature.

- Effective radius interpretations based on correlation of temperatures with concrete volume logs can have the effect of obscuring observations that could otherwise be made by separate evaluations of (1) TIP temperature profiles and (2) concrete yield plots. Accordingly, interpretation of TIP results using the effective radius method can make identification of defects more difficult.

- Reinforcing cage misalignment makes identification of concrete defects via TIP methods significantly more difficult.

- Evaluation of relative energy for CSL test results can be used to identify defects that are not apparent in CSL arrival time results for the same shaft.

- The field tests for this project included ten intentional defects of varying type, size, and location. With the exception of the weak concrete defects, the defects were generally relatively small, typically representing 15% or less of the drilled shaft cross section.

    - Small defects were specified in order to more effectively evaluate the detectability of TIP and CSL. In this respect, the experiment was successful in that some defects were detected and others were not; such an alignment of results helps clarify detection limits.

  - Defects of similar size were found by Sarhan et. al (2000) to produce modest reductions in structural resistance: at most an 18% reduction in axial resistance and a 27% reduction in flexural resistance for a single defect.

  - For more significant defects, the detection abilities of each test would generally be greater, although some fundamental limitations would likely remain (e.g. CSL's ability to detect defects outside the reinforcing cage, TIP's ability to detect soft bottom conditions).

- Improvements to current methods for interpreting TIP measurements may improve the ability to detect drilled shaft defects with TIP methods. Two potential improvements involve closer examination of how TIP measurements for a shaft change with time and processing TIP data within the context of analytical or numerical thermal models that account for effects from concrete mix, ground conditions, and other significant factors.

7.2 Recommendations: Implementation of TIP

It follows from the conclusions that TIP methods should be an allowable concrete integrity test method that could be used as a replacement for CSL, an allowable alternative to CSL, or in conjunction with CSL. Practical implementation of TIP for routine use requires important, agency-wide decisions regarding appropriate implementation approaches for TIP, procedures for TIP testing and interpretation, and acceptance criteria for TIP measurements. Recommendations for each topic are included in the following sections.

The recommendations in this section form the basis for the proposed TIP specification included as Appendix E. The proposed TIP specification begins with language referencing the ASTM standard, which provides a basis for most of the procedural aspects of TIP test methods. The rest of the proposed TIP specification addresses specific test procedures and interpretation and reporting requirements that follow from the recommendations presented below. The specification is focused on a project-level application of TIP methods. The specification does not address use of TIP versus use of CSL, although recommendations regarding this issue are included in Section 7.2.1. The specification also does not address how many shafts should be subjected to TIP testing for a given project. Both the approach to TIP (versus CSL) and the frequency of TIP testing are general issues of drilled shaft concrete integrity testing, and both issues are better addressed in a specification or special provision more generally focused on drilled shafts. Similarly, the proposed TIP specification language of Appendix E is likely best implemented as a sub-section of a general drilled shaft specification or special provision. The general drilled shaft specification should also include language regarding CSL testing, coring, potential repair methods, and payment for integrity testing.

It is important to recognize and appreciate that drilled shaft integrity testing is not the sole quality assurance measure for drilled shafts. Quality assurance for drilled shafts is also derived from agency requirements and evaluations related to design (e.g. reinforcement restrictions, concrete mix characteristics), shaft construction methods (e.g. methods for maintaining hole stability, slurry control requirements, concrete placement requirements), and controls on characteristics of fresh concrete (e.g. trial batching procedures, workability constraints and measurements). It is important and appropriate to explicitly consider these requirements collectively to avoid requiring excessive quality assurance that can unnecessarily increase costs and risks associated with drilled shaft construction. In this context, drilled shaft integrity testing is one of several measures for assuring quality for drilled shafts.

7.2.1 Potential Approaches to Implementing TIP

There are numerous potential approaches for implementing TIP methods agency-wide. Three specific recommendations below are appropriate considering the conclusions of this research:

1. Both TIP and CSL should be considered allowable concrete integrity test methods.
2. TIP testing should be preferred over CSL for drilled shafts with designs controlled by lateral loading. CSL testing should be preferred over TIP for drilled shafts with designs controlled by axial loading and relying on substantial tip resistance.

3. Both TIP and CSL should be used for method/technique shafts to help identify systematic issues with construction and concrete placement so that techniques for production shafts can be adapted to project-specific conditions and challenges.

These recommendations are consistent with the conclusion that TIP and CSL are generally complementary in terms of their detection abilities. It is worth noting that TIP specifications could also be developed without specifying when the test is to be used. If the TIP specifications are silent with respect to when the test is required, integrity test method decisions could be made on a project-by-project basis. Such specifications would likely require implementation through special provisions.

7.2.2 TIP Test Procedures and Use of Probe

TIP testing should be performed using sacrificial wires, with data collection beginning at the time of concrete placement and continuing until at least 24 hours after the peak temperature has been observed. The continuous record of concrete temperatures facilitates the most effective detection of concrete defects because the maximum temperature deviation can be computed by evaluating results throughout the test period. In addition, evaluation of trends in the time record may clarify interpretation of TIP results. These abilities are lost with the probe method. In addition, TIP procedures using the wires are simpler to specify and execute.

7.2.3 TIP Test Interpretation

Interpretation is perhaps the most challenging component of TIP testing. Several recommendations regarding interpretation techniques follow from the results of this report:

- TIP interpretation should include evaluation of temperature versus time plots for suspected defects. The plots should include records for the depth of the suspected defect as well as a nearby depth that appears to be uninfluenced by the potential defect (i.e. the baseline measurement).
- Evaluation of TIP data should be based on raw temperature measurements rather than interpreted values of effective radius. If effective radius profiles are included in TIP reports, they should be presented as for visualization only, rather than as a means for evaluating the data or inferring specific values of concrete cover.
- Evaluation of TIP data should be accompanied by evaluation of available records of drilled shaft installation, including concrete yield plots. Conclusions regarding the interpretation of TIP results should be encouraged to consider observations from drilled shaft construction records.

7.2.4 Acceptance Criteria

The final component of a TIP specification is acceptance criteria, which assign standards for evaluating the interpreted test results. Two approaches for acceptance criteria are presented below, along with discussion of the advantages and limitations of the approaches.

<u>Preferred Approach: Evaluations based on Engineering Judgment</u>

The preferred approach for acceptance criteria within the TIP specifications is to include open-ended language that relies on the professional judgement of the TIP engineer. As noted in Table 2, this approach was adopted by Florida DOT (2018) and is included in the PDI sample specifications (2017). Both the FDOT and PDI specifications require TIP reports to indicate the presence of any significant temperature deviations, but no definition is provided for what qualifies as a significant deviation. If the engineering judgment approach is adopted, any significant temperature deviations would be identified in a TIP report, and the significant deviations would trigger evaluation by the design engineer for the shaft. The design engineer would deem the deviations as either permissible or requiring further investigation (e.g. by coring or other means). If the engineering judgment approach is adopted, TIP reports potentially could be required to be sealed by a licensed professional engineer. This presents some practical complications, because typically the engineer(s) responsible for designing the shaft are not also responsible for testing.

The downside of the engineering judgment approach is a potential lack of consistency from one project to the next, with acceptance or rejection subject to the judgment of the TIP engineer. However, a substantial volume of TIP project records and TIP literature were reviewed for this project, and a virtually indisputable conclusion of the review is that temperature development in drilled shaft concrete is complicated. The degree of complication is perhaps so great that any quantitative approach to TIP acceptance criteria would result in a significant number of inappropriate red flags for some projects and missed defects for others. Moreover, there would be benefits to the judgement approach: avoiding rigid criteria would place the responsibility for interpretation and evaluation of TIP data squarely on TIP professionals, which would promote a greater degree of thoughtfulness in TIP analyses. Such thoughtfulness is frequently missing in concrete integrity reports. In fact, concrete integrity reports are frequently generated by algorithm, a disconcerting practice that is at least compatible with rigid acceptance criteria, if not a direct result of such criteria.

Alternative Approach: Specific Criteria

The other approach for TIP acceptance criteria is to include rigid, quantitative criteria that flag anomalous results as potential defects requiring further action. Further action typically involves either engineering analysis of the potential defect or further investigation by coring or other means. The specific criteria approach is consistent with the way most agencies evaluate CSL records (Table 2). Several of the specifications listed in Table 2 include specific criteria for TIP acceptance as well. For example, WSDOT defines a 6% increase in effective radius as “questionable”; Piscalko et al. (2016) and Likins and Mullins (2011) also included specific criteria based on effective radius interpretations. However, as explained in the previous section, effective radius interpretations are not recommended. In draft specifications for Florida DOT, Mullins et al. (2009) identified a 5° F deviation as its specific criteria for further analysis. If the specific criteria approach is to be adopted, 5° F or similar is likely a reasonable criterion based on the results of this research (e.g. Table 10). However, additional guidance regarding the definition of temperature deviation would be required, e.g. to clarify over what distance the deviation would be allowed and to define the baseline temperature. The specific criteria approach should also adopt familiar recommendations for further engineering analysis of the specific defect, accompanied by further investigation as warranted by the analysis.

The primary advantage of the specific criteria approach is consistency among TIP interpretations. In addition, if the criteria are set at a relatively conservative level such as 5° F, the possibility of missing a significant defect is likely relatively small. However, the specific criteria approach will likely produce a significant number of false positives since there are several other factors that could produce a 5° F deviation (e.g. changes in geometry, geology, groundwater, etc.). Moreover, the specific criteria approach encourages a concrete integrity test report “culture” that often does not include critical evaluation of test results. In the absence of critical evaluation, it is feasible that potential defects could go unrecognized, especially if the potential defect is not flagged by the specific criterion. For these reasons, the approach emphasizing engineering judgment is preferred.

7.3 Recommendations: CSL

CSL test reports should include interpretations based on relative energy, not just arrival time. Interpretations that consider both measures will likely result in better defect identification.

7.4 Recommendations: Future Research

Based on the findings and recommendations of this project, two additional research topics are worthy of study:

1. Current practices for interpretation of TIP measurements focus on trends with depth, but this research demonstrated trends with time can also be used to identify defects. TIP interpretation methods based on the time-domain response should be developed. Based on the results of this research, at least two potential approaches for time-based interpretation are possible. The first method would involve investigating the possibility that different types of defects are associated with different “signatures” in the time domain like those shown in Section 5.4. The other potential

approach for time interpretation would consider TIP results in the context of analytical or numerical thermal models that account for effects of concrete mix design, boundary conditions, and time. Calibration of such models using TIP measurements (i.e. the Level 4 analysis proposed by Mullins et al. (2007)) would likely result in significant improvements in defect detection. Results from the proposed research may reveal changes to TIP test procedures that could further improve defect detection, e.g. through placement of additional temperature sensors near the bottom of the shaft.

2. Research should be performed to collect additional data regarding the effect of defects on TIP measurements. Such data would be particularly useful if specific temperature deviation criteria are to be established for acceptance criteria. In addition, the work described in this report and others, notably work by Mullins et al. (2007), Ashlock and Fotouhi (2014), and Schoen et al. (2018), have more or less established a reasonable lower bound for the magnitude of various types of defects that can be detected with TIP methods. Evaluation of TIP responses to larger defects would be beneficial. TIP data for larger defects would improve calibrations of thermal models and likely lead to improvements in TIP interpretation, especially if combined with the first proposed research topic. The response to larger, known defects would serve as a valuable reference response for evaluation purposes when TIP measurements indicate potential defects.

References

Ashlock, J.C. and M.K. Fotouhi (2014), "Thermal Integrity Profiling and Crosshole Sonic Logging of Drilled Shafts with Artificial Defects," Geo-Congress 2014 Technical Papers, GSP 234, American Society of Civil Engineers, pp. 1795-1805.

ASTM Standard C39 (2018), "Standard Test Method for Compressive Strength of Cylindrical Concrete Specimens," ASTM International, West Conshohocken, PA, 2018, DOI: 10.1520/C0039_C0039M-18, www.astm.org.

ASTM Standard C143 (2015), "Standard Test Method for Slump of Hydraulic-Cement Concrete," ASTM International, West Conshohocken, PA, 2015, DOI: 10.1520/C0143_C0143M-15A, www.astm.org.

ASTM Standard D6760 (2016), "Standard Test Method for Integrity Testing of Concrete Deep Foundations by Ultrasonic Crosshole Testing," ASTM International, West Conshohocken, PA, 2014, DOI: 10.1520/ D6760M-16, www.astm.org.

ASTM Standard D7949 (2014), "Standard Test Methods for Thermal Integrity Profiling of Concrete Deep Foundations," ASTM International, West Conshohocken, PA, 2014, DOI: 10.1520/D7949-14, www.astm.org.

Boeckmann, A.Z. and J.E. Loehr (2015), *Concrete Mass Pours for Deep Foundations – Synthesis Report*, Final Phase I Report to Federal Highway Administration, 81 p.

Brown, D.A., J.P. Turner, and R.J. Castelli (2010), Drilled Shafts: Construction Procedures and LRFD *Design Methods*, Publication FHWA-NHI-10-016, NHI Course 132014 and GEC 010, 972 pp.

Deep Foundations Institute, "Terminology and Evaluation Criteria of Crosshole Sonic Logging (CSL) as applied to Deep Foundations," In preparation.

Florida Department of Transportation (2018), Standard Specifications for Road and Bridge Construction, July 2018 eBook.

Google Earth (2018), 43º 02' 19.39" N and 88º 13' 16.46" W. Google Earth. Accessed 21 July 2018.

GRL Engineers (2015), "Sample Specification for Crosshole Sonic Logging (CSL)," September 2015, accessible via http://www.grlengineers.com/specifications/

Likins, G. and G. Mullins (2011), "Structural integrity of drilled shaft foundations by thermal measurements," Structural Engineering, p. 46-48.

Johnson, K.R. (2014), "Temperature Prediction Modeling and Thermal Integrity Profiling of Drilled Shafts," Geo-Congress 2014 Technical Papers, GSP 234, American Society of Civil Engineers, pp. 1781-1794.

Johnson, K.R. (2016), "Analyzing thermal integrity profiling data for drilled shaft evaluation," DFI Journal – The Journal of the Deep Foundations Institute, Vol. 10, No. 1, pp. 25-33, DOI: 10.1080/19375247.2016.1169361

Mullins, G. (2010), "Thermal integrity profiling of drilled shafts," DFI Journal – The Journal of the Deep Foundations Institute, Vol. 4, No. 2, pp. 54-64, DOI: 10.1179/dfi.2010.010

Mullins, G. (2013) "Advancements in drilled shaft construction, design, and quality assurance: the value of research" International Journal of Pavement Research and Technology, Vol. 6, No. 2, pp. 93–99, doi:106136/ijprt.org.tw/2013.6(2).93

Mullins, G., K. Johnson, and D. Winters (2007), *Thermal Integrity Testing of Drilled Shafts*, Final Report Prepared for Florida Department of Transportation, 214 p.

Mullins, G. and D. Winters (2011), *Infrared Thermal Integrity Testing Quality Assurance Test Method to Detect Drilled Shaft Defects*, Final Report Washington State DOT, WA-RD 770.1, 176 p.

Mullins, G., D. Winters, and K. Johnson (2009), Attenuating Mass Concrete Effects in Drilled Shafts, Final Report to Florida DOT, Report No. BD-544-39.

Pile Dynamics, Inc. (2017), “Sample Specification for Testing Foundations with the Thermal Integrity Profiler (TIP),” October 2017, accessible via http://www.grlengineers.com/specifications/

Piscalko, G., G. Likins, and G. Mullins (2016), “Drilled Shaft Acceptance Criteria Based Upon Thermal Integrity Profiling,” Proceedings of the 41st Annual Conference on Deep Foundations: New York, NY, Deep Foundations Institute, 10 p.

Sarhan, H.A., M.W. O’Neill, and S.W. Tabsh (2000), *Structural Resistance Factors for Drilled Shafts with Minor Anomalies—Deterministic Study*. Final Report to ADSC.

Schoen, D.L., G.J. Canivan, and W.M. Camp III (2018), “Evaluation of Thermal Integrity Profiling (TIP) Methods—Probe, Embedded Wire, and Wire Suspended in CSL Tubes,” Proceedings of IFCEE 2018, ASCE GSP 294, pp. 550-560.

Washington State Department of Transportation (2018), Standard Specifications for Road, Bridge, and Municipal Construction 2018, M 41-10.

Appendix A – Final Construction Plans for Field Research Drilled Shafts

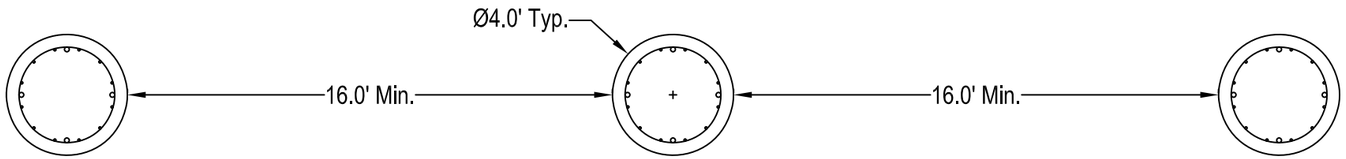

Preferred Shaft Plan

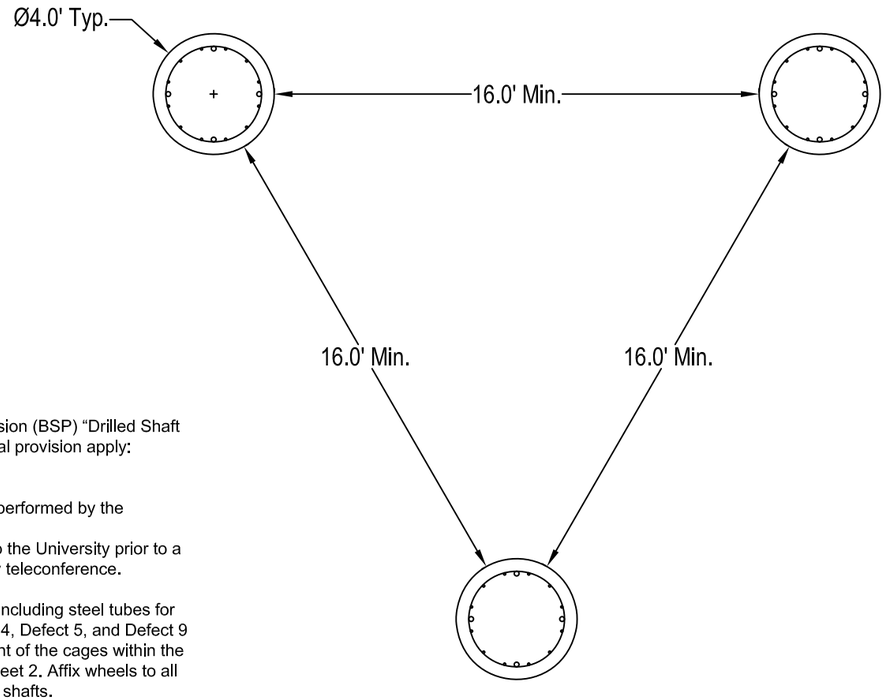

Alternative Shaft Plan

General Notes

1. Construct shafts according to WisDOT Bridge Special Provision (BSP) "Drilled Shaft Foundation." The following exceptions to the WisDOT special provision apply:
   a. Remove Section A.1.
   b. Remove Section C.2.8.9.
   c. Remove Section C.2.12. Non-destructive testing to be performed by the University.

   Contractor's Drilled Shaft Installation Plan to be submitted to the University prior to a preconstruction meeting. The meeting may be conducted by teleconference.

2. Reinforcing cage: Contractor to assemble reinforcing cage, including steel tubes for CSL testing, as shown. Defect 1, Defect 2, Defect 3, Defect 4, Defect 5, and Defect 9 are to be installed on the reinforcing cages prior to placement of the cages within the excavated shafts. Details for the defects are provided on Sheet 2. Affix wheels to all reinforcing cages to maintain centrality within the excavated shafts.

3. Concrete: Concrete mix shall be in accordance with the table below. The mix has a water-to-cement ratio of 0.45. The slump shall be between 7 and 9.5 in.

Normal Mix Design For use in all shafts except in weak zones associated with Defect 6 and Defect 10.		
Material	Quantity per Cubic Yard of Concrete Mix	Specification
Cement	460 lb	ASTM C150, Type I
Fly Ash	200 lb	ASTM C618, Class C
Fine Aggregate	1,777 lb	WisDOT 501.2.5.3
Coarse Aggregate	1,185 lb	WisDOT 501.2.5.4 but with AASHTO No. 89 stone (ASTM D448) gradation. Use rounded stone (e.g. pea gravel).
Water (potable)	35.5 gal	
Air Entrainment Admixture	1.6 oz	ASTM C260
Retarder Admixture	40 oz	ASTM C494, Type B
Water Reducing Admixture	40 oz	ASTM C494, Type D
High-Range Water Reducing Admixture	26 oz	ASTM C494, Type F

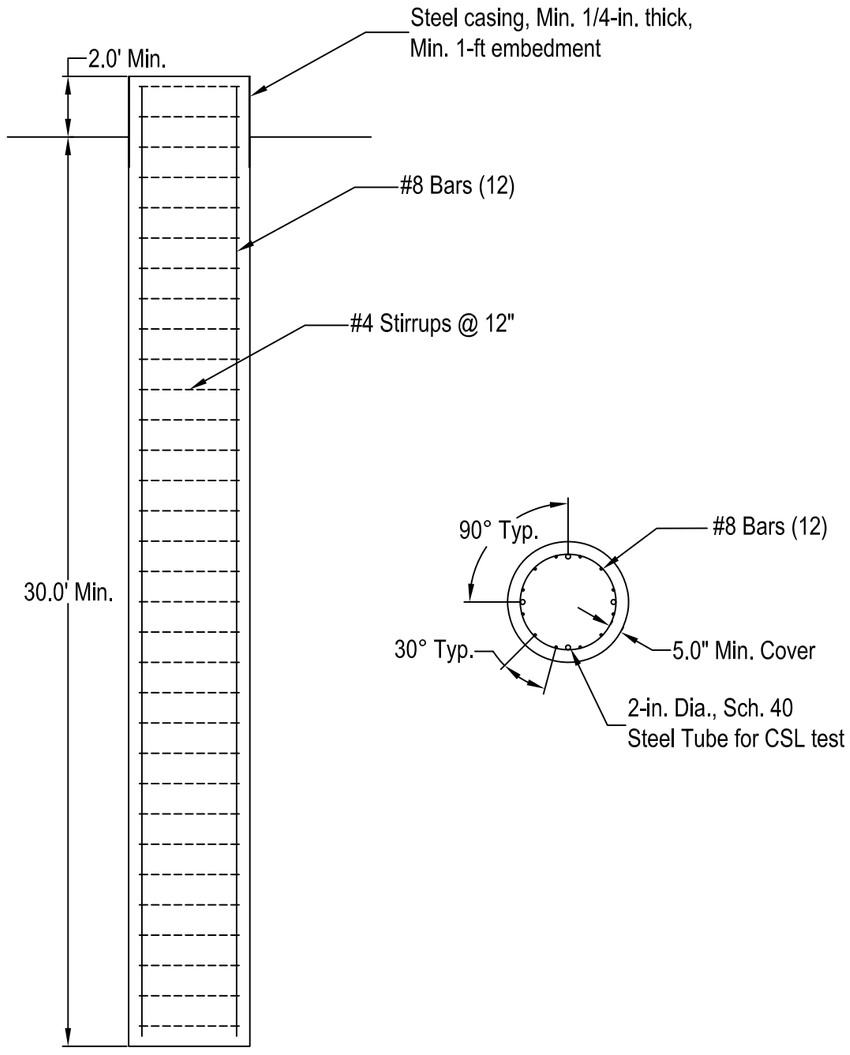

Shaft Elevation and Reinforcement (All Shafts)

5 4 3 2 1 0 5
1" = 5'

Drilled Shaft Details
WisDOT Thermal Integrity Profiling Research
Date: May 17, 2017 Sheet 1 of 2

University of Missouri
Civil and Environmental Engineering

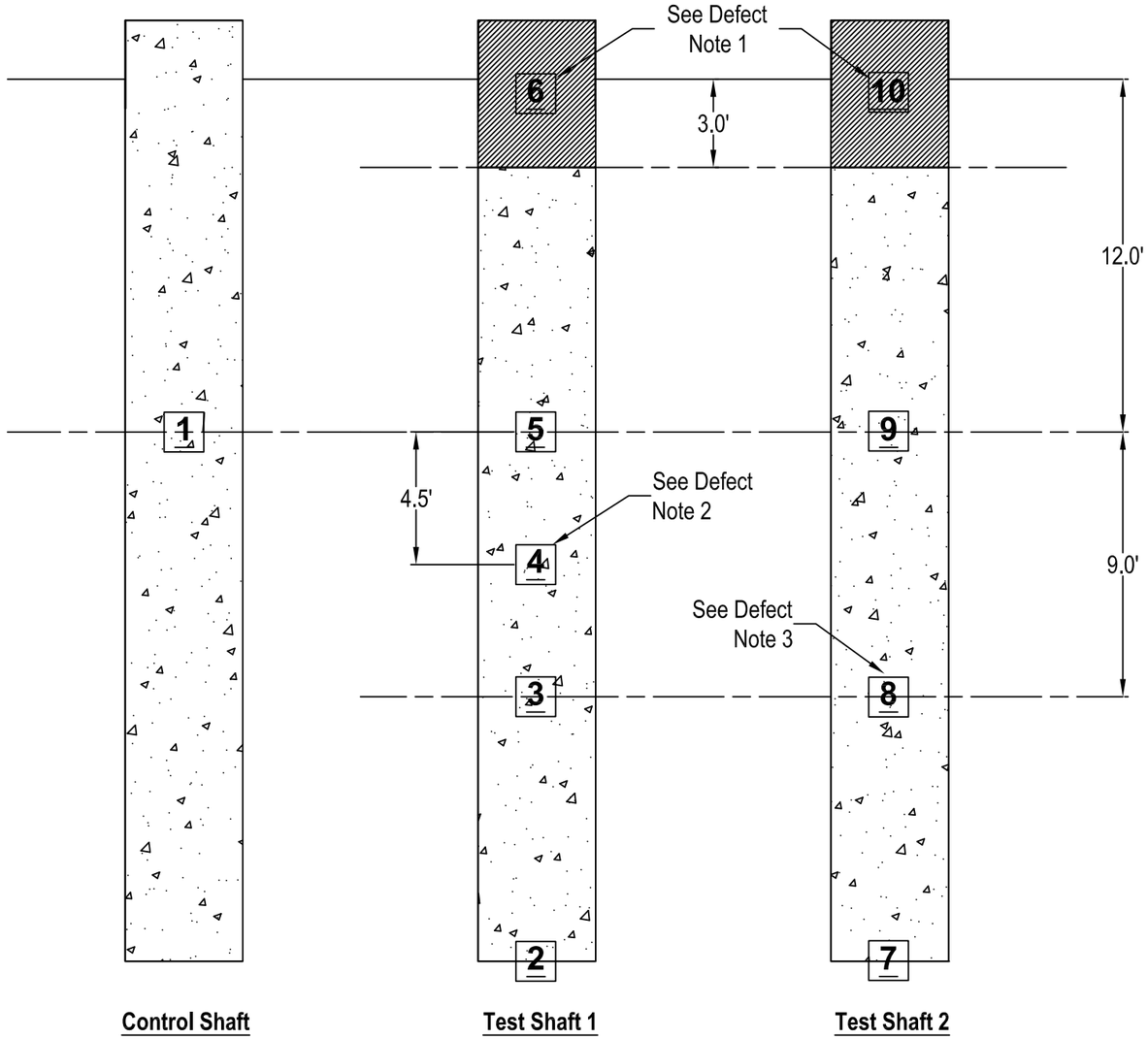

Shaft Profiles with Defect Locations

Legend

- 1 — Defect number at square location
- Normal mix concrete
- Soil defect
- Zone of weak concrete

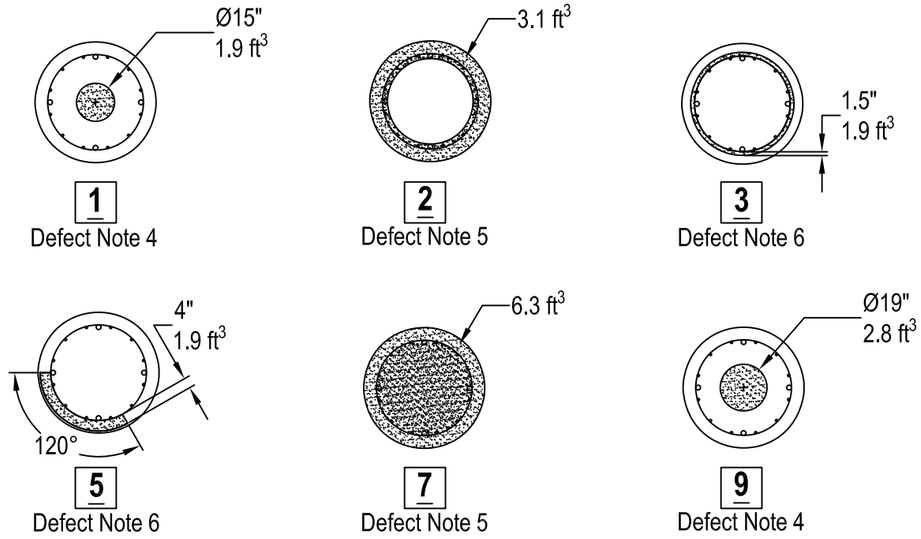

Defect Details

Defect Notes

1. Zones of weak concrete (Defect 6 and Defect 10): In Test Shaft 1 and Test Shaft 2, terminate concrete placement and remove the tremie pipe when the concrete level reaches the bottom of zones indicated by hatching for Defects 6 and 10. Complete concrete placement for Test Shaft 1 using concrete equivalent to the Normal Mix Design shown on Sheet 1 but with additional water to achieve a water-to-cement (w/c) ratio equal to 0.60. Complete concrete placement for Test Shaft 2 using concrete equivalent to the Normal Mix Design shown on Sheet 1 but with additional water to achieve a water-to-cement (w/c) ratio equal to 0.75. Concrete for Defect 6 and Defect 10 to be placed by the free-fall method. Suggested concrete placement procedure: Place all Normal Mix Design concrete prior to placing concrete for Defect 6 and Defect 10. Add 12 gallons of water for each remaining cubic yard of Normal Mix Design concrete and then complete concrete placement for Test Shaft 1. Add another 12 gallons of water for each remaining cubic yard of concrete and then complete concrete placement for Test Shaft 2.

2. CSL tube debonding (Defect 4): Apply wheel bearing grease along 1-ft of each CSL tube at the location corresponding to the Defect 4 depth shown for Test Shaft 1. Grease to be applied liberally around the entire circumference of each CSL tube after assembling reinforcing cage but prior to installing the cage in the excavated shaft.

3. Tremie breach (Defect 8): When the top of concrete in Test Shaft 2 reaches the level shown for Defect 8, pause concrete placement and lift tremie pipe such that the bottom of the tremie is above the top of concrete. University to place slurry or water in shaft to create Defect 8. After creation of Defect 8, concrete placement to resume with the discharge end of the tremie positioned approximately 1 ft above Defect 8. Establish a new head of concrete above the tremie discharge end and proceed according to SPV.0900 Section C.2.10.4.

4. Inclusion near center of shaft (Defect 1 and Defect 9): Defect 1 and Defect 9 are to consist of sandbags containing native soil or imported sand tied to the inside of the reinforcing cage in order to ultimately achieve the dimensions and volumes shown in the defect details. Prior to placement of the reinforcing cages in the excavated shafts, the University to suspend sandbags at points distributed evenly around the inside of the cage perimeter using wire free lengths approximately equal to the cage radius. Contractor to slow concrete placement when the level of the top of concrete is approximately 5 ft below the locations shown for Defect 1 (Control Shaft) and Defect 8 (Test Shaft 2) to allow University to inspect and document ultimate sandbag locations as the sandbags rise with the top of concrete.

5. Soft bottom (Defect 2 and Defect 7): Defect 2 is to consist of sandbags containing native soil or imported sand tied along the outside of the reinforcing cage at the bottom of the cage. Sandbags for Defect 2 to be affixed to the reinforcing cage for Test Shaft 1 by the University prior to placement of the cage in the excavated shaft. Defect 7 is to be installed by pouring the volume of sand noted on the defect details into the bottom of Test Shaft 2 after placement of the reinforcing cage, prior to concrete placement.

6. Defects outside reinforcing cage (Defect 3 and Defect 5): Defect 3 and Defect 5 are to be installed on the reinforcing cage for Test Shaft 1 by the University prior to placement of the cage in the excavated shaft. Both defects to consist of native soil or imported sand in sandbags tied to the outside of the reinforcing cage to achieve the dimensions and volumes shown in the defect details.

5 4 3 2 1 0 5
1" = 5'

Shaft Profiles and Defect Details
WisDOT Thermal Integrity Profiling Research
Date: May 17, 2017 | Sheet 2 of 2

University of Missouri
Civil and Environmental Engineering

Appendix B – As-Built Construction Plans for Field Research Drilled Shafts

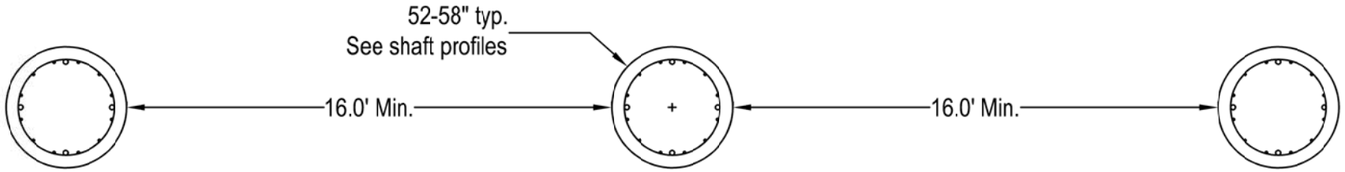

Plan

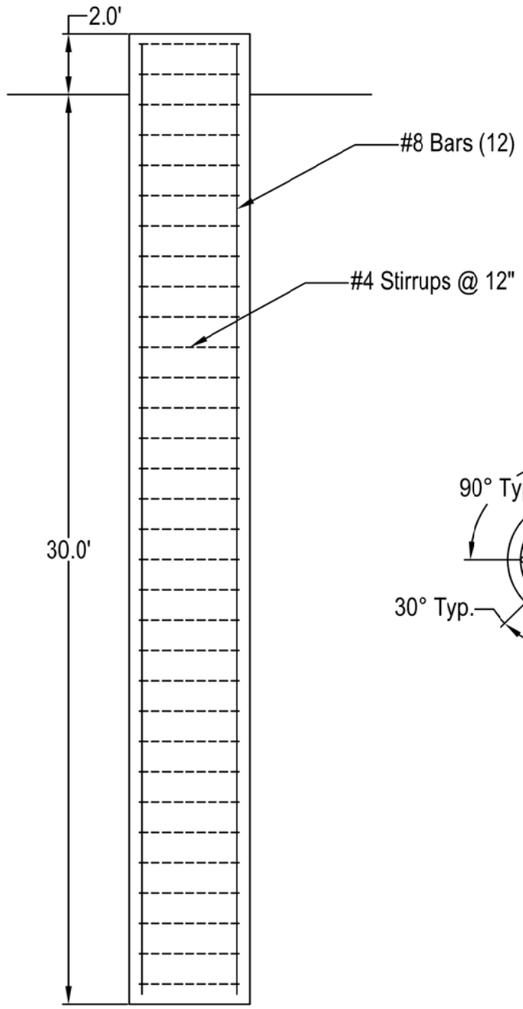

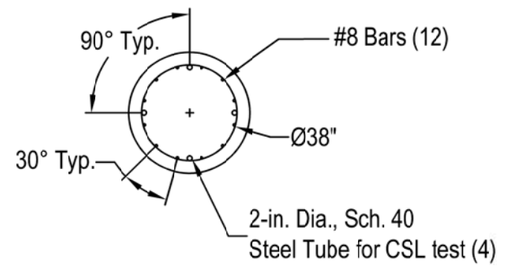

Shaft Reinforcement (All Shafts)

General Notes

1. Construct shafts according to WisDOT Bridge Special Provision (BSP) "Drilled Shaft Foundation." The following exceptions to the WisDOT special provision apply:
   a. Remove Section A.1.
   b. Remove Section C.2.8.9.
   c. Remove Section C.2.12. Non-destructive testing to be performed by the University.

   Contractor's Drilled Shaft Installation Plan to be submitted to the University prior to a preconstruction meeting. The meeting may be conducted by teleconference.

2. Reinforcing cage: Contractor to assemble reinforcing cage, including steel tubes for CSL testing, as shown. Defect 1, Defect 2, Defect 3, Defect 4, Defect 5, and Defect 9 are to be installed on the reinforcing cages prior to placement of the cages within the excavated shafts. Details for the defects are provided on Sheet 2. Affix wheels to all reinforcing cages to maintain centrality within the excavated shafts.

3. Concrete: Concrete mix shall be in accordance with the table below. The mix has a water-to-cement ratio of 0.45. The slump shall be between 7 and 9.5 in.

Normal Mix Design
For use in all shafts except in weak zones associated with Defect 6 and Defect 10.

Material	Quantity per Cubic Yard of Concrete Mix	Specification
Cement	460 lb	ASTM C150, Type I
Fly Ash	200 lb	ASTM C618, Class C
Fine Aggregate	1,777 lb	WisDOT 501.2.5.3
Coarse Aggregate	1,185 lb	WisDOT 501.2.5.4 but with AASHTO No. 89 stone (ASTM D448) gradation. Use rounded stone (e.g. pea gravel).
Water (potable)	35.5 gal	
Air Entrainment Admixture	1.6 oz	ASTM C260
Retarder Admixture	40 oz	ASTM C494, Type B
Water Reducing Admixture	40 oz	ASTM C494, Type D
High-Range Water Reducing Admixture	26 oz	ASTM C494, Type F

5 4 3 2 1 0 5
1" = 5'

As-built Drilled Shaft Details
WisDOT Thermal Integrity Profiling Research
Installation Dates: November 13-17, 2017 | Sheet 1 of 2

University of Missouri
Civil and Environmental Engineering

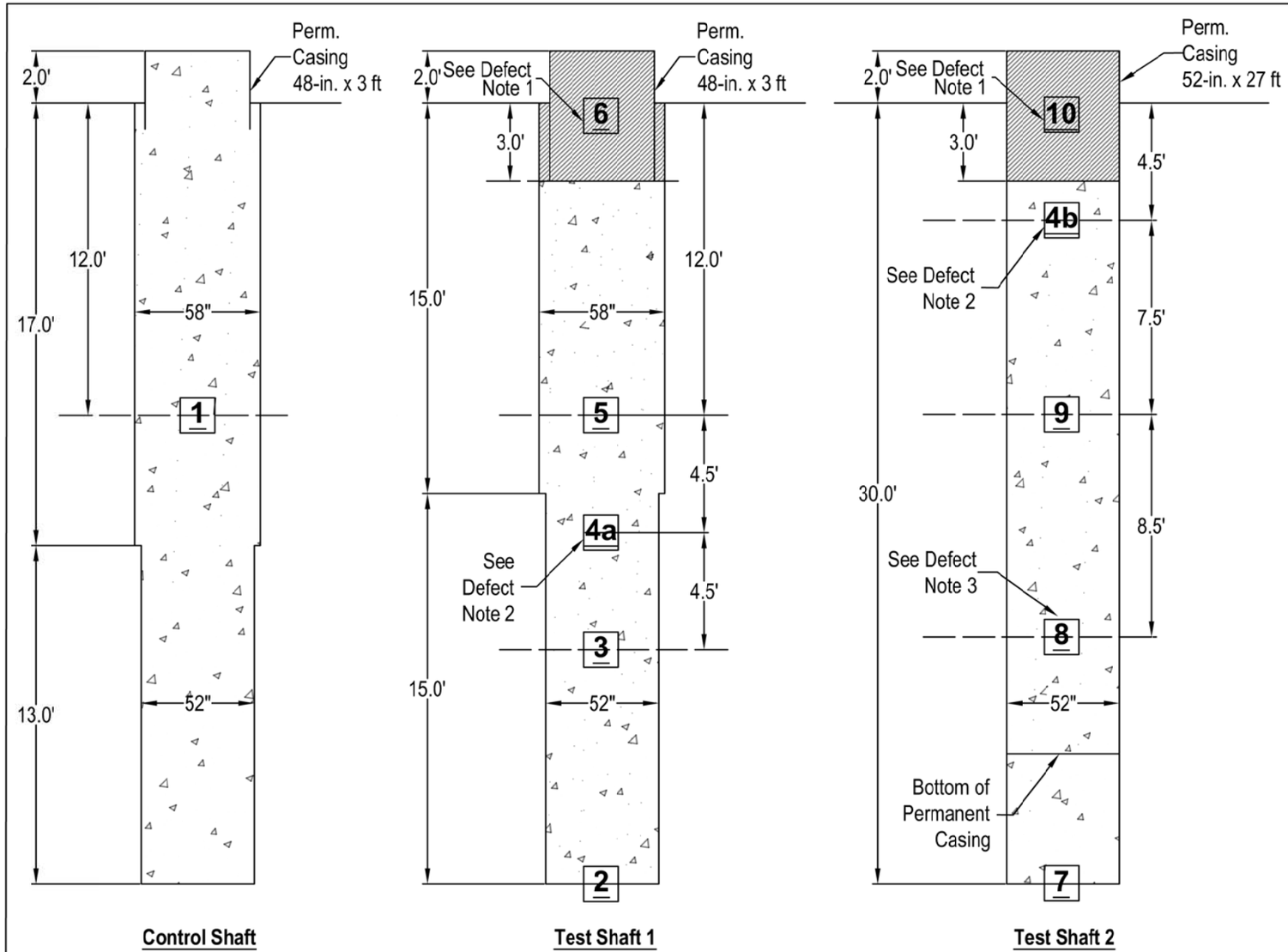

Shaft Profiles with Defect Locations

Legend

- 1 — Defect number at square location
- Normal mix concrete
- Soil defect
- Zone of weak concrete

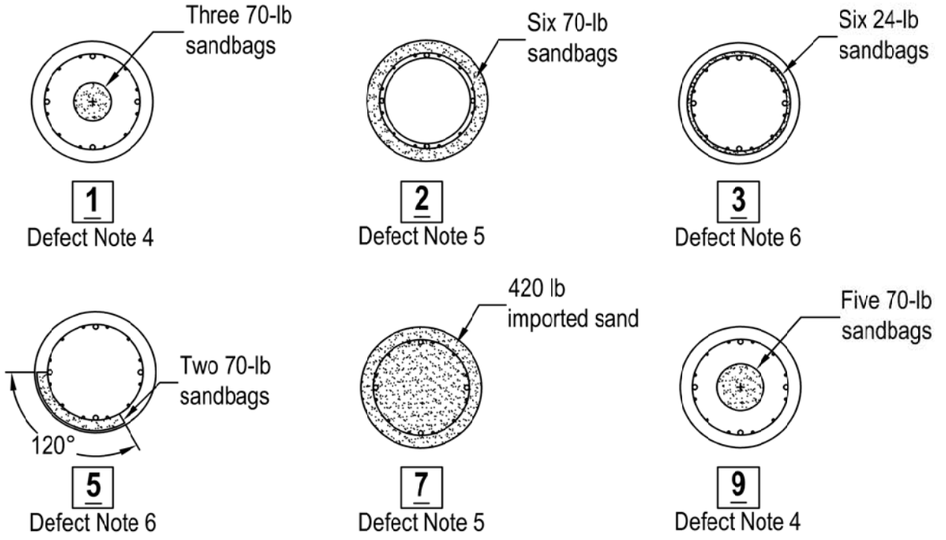

Defect Details

Defect Notes

1. Zones of weak concrete (Defect 6 and Defect 10): In Test Shaft 1 and Test Shaft 2, terminate concrete placement and remove the tremie pipe when the concrete level reaches the bottom of zones indicated by hatching for Defects 6 and 10. Complete concrete placement for Test Shaft 1 using concrete equivalent to the Normal Mix Design shown on Sheet 1 but with additional water to achieve a water-to-cement (w/c) ratio equal to 0.60. Complete concrete placement for Test Shaft 2 using concrete equivalent to the Normal Mix Design shown on Sheet 1 but with additional water to achieve a water-to-cement (w/c) ratio equal to 0.52. Concrete for Defect 6 and Defect 10 to be placed by the free-fall method.
   Concrete placement procedure: Place all Normal Mix Design concrete prior to placing concrete for Defect 6 and Defect 10. For Test Shaft 1, add 12 gallons of water for each remaining cubic yard of Normal Mix Design concrete and then complete concrete placement. For Test Shaft 2, add another 5 gallons of water for each remaining cubic yard of concrete and then complete concrete placement.

2. CSL tube debonding (Defect 4): Apply wheel bearing grease along 1-ft of each CSL tube at the location corresponding to the Defect 4 depth shown for Test Shaft 1 and Test Shaft 2. Grease to be applied liberally around the entire circumference of each CSL tube after assembling reinforcing cage but prior to installing the cage in the excavated shaft.

3. Tremie breach (Defect 8): When the top of concrete in Test Shaft 2 reaches the level shown for Defect 8, pause concrete placement and lift tremie pipe such that the bottom of the tremie is above the top of concrete. University to place 30 gallons of water and 70 lbs of sand in shaft to create Defect 8. After creation of Defect 8, concrete placement to resume with the discharge end of the tremie positioned approximately 1 ft above Defect 8. Establish a new head of concrete above the tremie discharge end and proceed according to SPV.0900 Section C.2.10.4.

4. Inclusion near center of shaft (Defect 1 and Defect 9): Defect 1 and Defect 9 are to consist of sandbags containing imported sand tied to the inside of the reinforcing cage. Prior to placement of the reinforcing cages in the excavated shafts, the University to suspend sandbags at points distributed evenly around the inside of the cage perimeter using wire free lengths approximately equal to the cage radius. Contractor to slow concrete placement when the level of the top of concrete is approximately 5 ft below the locations shown for Defect 1 (Control Shaft) and Defect 8 (Test Shaft 2) to allow University to inspect and document ultimate sandbag locations as the sandbags rise with the top of concrete.

5. Soft bottom (Defect 2 and Defect 7): Defect 2 is to consist of sandbags containing imported sand tied along the outside of the reinforcing cage at the bottom of the cage. Sandbags for Defect 2 to be affixed to the reinforcing cage for Test Shaft 1 by the University prior to placement of the cage in the excavated shaft. Defect 7 is to be installed by pouring the weight of sand noted on the defect details into the bottom of Test Shaft 2 after placement of the reinforcing cage, prior to concrete placement.

6. Defects outside reinforcing cage (Defect 3 and Defect 5): Defect 3 and Defect 5 are to be installed on the reinforcing cage for Test Shaft 1 by the University prior to placement of the cage in the excavated shaft. Both defects to consist of imported sand in sandbags tied to the outside of the reinforcing cage as shown in the defect details.

5 4 3 2 1 0 5
1" = 5'

As-built Shaft Profiles and Defect Details
WisDOT Thermal Integrity Profiling Research
Installation Dates: November 13-17, 2017 | Sheet 2 of 2

University of Missouri
Civil and Environmental Engineering

Appendix C – Boring Logs

November 9, 2017

Midwest Drilled Foundations and Engineering, Inc.
200 S. Prairie Ave.
Waukesha, WI 53186

Attn: Mr. Riley Padron
Assistant Project Manager

Re: Subcontract Drilling and Boring Log Preparation
WisDOT Drilled Pier Research Project
2105 Pewaukee Road
Waukesha, Wisconsin
PSI Project No.: 00522038

Dear Mr. Padron:

In accordance with your request and executed PSI Proposal 226522, dated October 27, 2017, PSI has completed the soil test borings for the proposed project. Copies of the Soil Boring Logs are enclosed. As requested, no engineering analysis or recommendations have been provided. It is understood that the boring logs are being supplied to Midwest Dilled Foundations and Engineering, Inc. for its own evaluation and use.

Field Exploration

Two soil test borings (B-1 and B-2) were drilled for this project as requested to a depth of 40 feet below the existing ground surface. The borings were performed at the locations chosen by the client. Ground surface elevations for the soil test borings were not provided by the client.

The soil test borings were performed with a truck-mounted rotary drilling rig utilizing continuous flight hollow stem augers to advance the holes. It should be noted that at boring B-2, mud rotary drilling was employed beginning at a depth of 20 feet below the ground surface due to difficulty experienced with advancement of hollow stem augers in the very dense materials. Representative samples were obtained by split spoon sampling

at 2.5 foot intervals to a depth of 10 feet and every 5 feet thereafter in accordance with ASTM D-1587 procedures. N-values were obtained during sampling and provide a means of estimating the relative density of granular soils and comparative consistency of cohesive soils, thereby providing a method of evaluating the relative strength and compressibility characteristics of the subsoil.

The soil samples were transferred to clean glass jars immediately after retrieval, and returned to the laboratory upon completion of the field operations. Samples will be stored for a period of 60 days at which time they will be discarded unless other instructions are received. All soil samples were visually classified by a PSI soils engineer in general accordance with the Unified Soil Classification System (ASTM D-2488-75).

Copies of the Soil Boring Logs are enclosed. The soil stratification shown on the logs represents the soil conditions in the actual boring locations at the time of the exploration. The terms and symbols used on the logs are described in the General Notes enclosed. After completion of the boring, the auger holes were backfilled to the ground surface with bentonite chips.

Laboratory Physical Testing

Soil samples obtained from the exploration were visually classified by a soils engineer in the laboratory, and subjected to laboratory testing, which included moisture content determination. The values of strength tests performed on soil samples obtained by the Standard Penetration Test Method (SPT) during sampling are considered approximate, recognizing that the SPT method provides a representative but somewhat disturbed soil sample. The laboratory testing was performed in general accordance with the respective ASTM methods, as applicable, and the results are shown on the boring logs.

General

A description of the subsurface conditions encountered at the test boring locations is shown on the enclosed Soil Boring Logs. The lines of demarcation shown on the logs represent approximate boundaries between the various soil classifications. It must be recognized that the soil descriptions are considered representative of the specific test location, and that variations may occur between the sampling intervals. Soil depths, topsoil and layer thicknesses, and demarcation lines utilized for preliminary construction calculations should not be expected to yield exact and final quantities.

We appreciate the opportunity to have been of service on this project. If there are any questions, please contact us at any time.

Respectfully Submitted,

PROFESSIONAL SERVICE INDUSTRIES, INC.

Benjamin J. Kroeger, E.I.T.
Staff Engineer
Geotechnical Services

Ted A. Cera, P.E.
Department Manager
Geotechnical Services

Enclosures: Boring Location Plan
Soil Boring Logs (2)
General Notes

Intertek psi

Boring Location Plan
WisDOT Drilled Pier Research Project
2105 Pewaukee Road
Waukesha, Wisconsin
PSI Project No: 00522038

Professional Service Industries, Inc.
821 Corporate Court, Suite 100
Waukesha, WI 53189
Telephone: (262) 521-2125
Fax: (262) 521-2471

LOG OF BORING B-1

PSI Job No.: 00522038
Project: WisDOT Drilled Pier Research
Location: 2105 Pewaukee Road
Waukesha, WI

Drilling Method: Hollow Stem Auger
Sampling Method: 2-in SS
Hammer Type: Automatic
Boring Location:

WATER LEVELS
While Drilling: Not Obsvd.
Upon Completion: Not Obsvd.
Delay: N/A

Station: N/A
Offset: N/A

Elevation (feet)	Depth, (feet)	Graphic Log	Sample Type	Sample No.	Recovery (inches)	MATERIAL DESCRIPTION	USCS Classification	SPT Blows per 6-inch (SS)	Moisture, %	STANDARD PENETRATION TEST DATA N in blows/ft ◎ / STRENGTH, tsf	Additional Remarks
	0					Topsoil (6"± Thick)	OL				
				1	14	Brown Lean Clay with Gravel, Trace Sand, Moist, Very Stiff	CL	4-11-14 N=25	13		Q_r = 1.7 tsf
				2	13	Brown Silty Sand with Gravel, Moist, Dense	SM	10-17-18 N=35	4		
	5			3	16	Brown Sandy Silt with Gravel, Possible Cobble, Moist, Dense to Very Dense		10-19-23 N=42	7		
				4	18			19-30-38 N=68	6		
	10			5	18			11-32-46 N=78	6		
	15			6	10			27-50/4"	5		
	20			7	10		ML	23-50/5"	6		
	25			8	11			21-47-50/3"	7		
	30			9	9			32-50/5"	8		
	35			10	10			30-50/4"	7		
	40					End of Boring at 40'					
						Cave-In at 25'					

STANDARD PENETRATION TEST DATA
N in blows/ft ◎
× Moisture ◪ PL ✚ LL
0 25 50
STRENGTH, tsf
▲ Qu ✳ Qp
0 2.0 4.0

Completion Depth: 40.0 ft
Date Boring Started: 11/6/17
Date Boring Completed: 11/6/17
Logged By: DH
Drilling Contractor: PSI, Inc.

Sample Types:
Auger Cutting
Split-Spoon
Rock Core
Shelby Tube
Hand Auger
Calif. Sampler
Texas Cone

Latitude:
Longitude:
Drill Rig: 2016 F-750 Ford (Truck Mount)
Remarks:

The stratification lines represent approximate boundaries. The transition may be gradual.

Professional Service Industries, Inc.
821 Corporate Court, Suite 100
Waukesha, WI 53189
Telephone: (262) 521-2125
Fax: (262) 521-2471

LOG OF BORING B-2

PSI Job No.: 00522038
Project: WisDOT Drilled Pier Research
Location: 2105 Pewaukee Road
Waukesha, WI

Drilling Method: Hollow Stem Auger
Sampling Method: 2-in SS
Hammer Type: Automatic
Boring Location:

WATER LEVELS
While Drilling: Not Obsvd.
Upon Completion: Not Obsvd.
Delay: N/A

Station: N/A
Offset: N/A

Elevation (feet)	Depth, (feet)	Graphic Log	Sample Type	Sample No.	Recovery (inches)	MATERIAL DESCRIPTION	USCS Classification	SPT Blows per 6-inch (SS)	Moisture, %	Additional Remarks
	0					Topsoil (6"± Thick)	OL			
				1	15	Brown Silty Clay, Trace Root Matter, Very Moist, Very Stiff	CL-ML	6-5-6 N=11	22	
				2	5	Brown Silty Fine Sand with Gravel, Moist, Dense	SM	19-20-17 N=37	7	
	5			3	14			6-11-19 N=30	6	
				4	3	Brown Silty Sand with Silt Lenses and Gravel, Moist, Medium Dense to Very Dense		11-13-12 N=25		Poor Recovery
	10						SM			
				5	16			8-15-19 N=34	12	
	15									
				6	12	Brown Sandy Silt with Gravel, Possible Cobble, Moist, Very Dense		11-35-50/3"	7	
	20									
				7	10			20-50/5"	7	
	25						ML			
				8	10			27-48-50/2"	7	
	30									
				9	8			34-50/4"	7	
	35									
				10	9			39-50/4"	8	
	40					End of Boring at 40'				
						Cave-In at 28'				
						Switched to Mud Rotary Drilling at 20'				

STANDARD PENETRATION TEST DATA
N in blows/ft ◎
× Moisture ◪ PL ✚ LL
0 25 50
STRENGTH, tsf
▲ Qu ✳ Qp
0 2.0 4.0

Completion Depth: 40.0 ft
Date Boring Started: 11/6/17
Date Boring Completed: 11/6/17
Logged By: DH
Drilling Contractor: PSI, Inc.

Sample Types:
Auger Cutting
Split-Spoon
Rock Core
Shelby Tube
Hand Auger
Calif. Sampler
Texas Cone

Latitude:
Longitude:
Drill Rig: 2016 F-750 Ford (Truck Mount)
Remarks:

The stratification lines represent approximate boundaries. The transition may be gradual.

GENERAL NOTES

SAMPLE IDENTIFICATION

The Unified Soil Classification System (USCS), AASHTO 1988 and ASTM designations D2487 and D-2488 are used to identify the encountered materials unless otherwise noted. Coarse-grained soils are defined as having more than 50% of their dry weight retained on a #200 sieve (0.075mm); they are described as: boulders, cobbles, gravel or sand. Fine-grained soils have less than 50% of their dry weight retained on a #200 sieve; they are defined as silts or clay depending on their Atterberg Limit attributes. Major constituents may be added as modifiers and minor constituents may be added according to the relative proportions based on grain size.

DRILLING AND SAMPLING SYMBOLS

SFA: Solid Flight Auger - typically 4" diameter flights, except where noted.
HSA: Hollow Stem Auger - typically 3¼" or 4¼ I.D. openings, except where noted.
M.R.: Mud Rotary - Uses a rotary head with Bentonite or Polymer Slurry
R.C.: Diamond Bit Core Sampler
H.A.: Hand Auger
P.A.: Power Auger - Handheld motorized auger

SS: Split-Spoon - 1 3/8" I.D., 2" O.D., except where noted.
ST: Shelby Tube - 3" O.D., except where noted.
RC: Rock Core
TC: Texas Cone
BS: Bulk Sample
PM: Pressuremeter
CPT-U: Cone Penetrometer Testing with Pore-Pressure Readings

SOIL PROPERTY SYMBOLS

N: Standard "N" penetration: Blows per foot of a 140 pound hammer falling 30 inches on a 2-inch O.D. Split-Spoon.
N_{60}: A "N" penetration value corrected to an equivalent 60% hammer energy transfer efficiency (ETR)
Q_u: Unconfined compressive strength, TSF
Q_p: Pocket penetrometer value, unconfined compressive strength, TSF
w%: Moisture/water content, %
LL: Liquid Limit, %
PL: Plastic Limit, %
PI: Plasticity Index = (LL-PL),%
DD: Dry unit weight, pcf
▼,▽,⧩ Apparent groundwater level at time noted

RELATIVE DENSITY OF COARSE-GRAINED SOILS

Relative Density	N - Blows/foot
Very Loose	0 - 4
Loose	4 - 10
Medium Dense	10 - 30
Dense	30 - 50
Very Dense	50 - 80
Extremely Dense	80+

ANGULARITY OF COARSE-GRAINED PARTICLES

Description	Criteria
Angular:	Particles have sharp edges and relatively plane sides with unpolished surfaces
Subangular:	Particles are similar to angular description, but have rounded edges
Subrounded:	Particles have nearly plane sides, but have well-rounded corners and edges
Rounded:	Particles have smoothly curved sides and no edges

GRAIN-SIZE TERMINOLOGY

Component	Size Range
Boulders:	Over 300 mm (>12 in.)
Cobbles:	75 mm to 300 mm (3 in. to 12 in.)
Coarse-Grained Gravel:	19 mm to 75 mm (¾ in. to 3 in.)
Fine-Grained Gravel:	4.75 mm to 19 mm (No.4 to ¾ in.)
Coarse-Grained Sand:	2 mm to 4.75 mm (No.10 to No.4)
Medium-Grained Sand:	0.42 mm to 2 mm (No.40 to No.10)
Fine-Grained Sand:	0.075 mm to 0.42 mm (No. 200 to No.40)
Silt:	0.005 mm to 0.075 mm
Clay:	<0.005 mm

PARTICLE SHAPE

Description	Criteria
Flat:	Particles with width/thickness ratio > 3
Elongated:	Particles with length/width ratio > 3
Flat & Elongated:	Particles meet criteria for both flat and elongated

RELATIVE PROPORTIONS OF FINES

Descriptive Term	% Dry Weight
Trace:	< 5%
With:	5% to 12%
Modifier:	>12%

GENERAL NOTES

(Continued)

CONSISTENCY OF FINE-GRAINED SOILS

Q_U - TSF	N - Blows/foot	Consistency
0 - 0.25	0 - 2	Very Soft
0.25 - 0.50	2 - 4	Soft
0.50 - 1.00	4 - 8	Firm (Medium Stiff)
1.00 - 2.00	8 - 15	Stiff
2.00 - 4.00	15 - 30	Very Stiff
4.00 - 8.00	30 - 50	Hard
8.00+	50+	Very Hard

MOISTURE CONDITION DESCRIPTION

Description	Criteria
Dry:	Absence of moisture, dusty, dry to the touch
Moist:	Damp but no visible water
Wet:	Visible free water, usually soil is below water table

RELATIVE PROPORTIONS OF SAND AND GRAVEL

Descriptive Term	% Dry Weight
Trace:	< 15%
With:	15% to 30%
Modifier:	>30%

STRUCTURE DESCRIPTION

Description	Criteria
Stratified:	Alternating layers of varying material or color with layers at least ¼-inch (6 mm) thick
Laminated:	Alternating layers of varying material or color with layers less than ¼-inch (6 mm) thick
Fissured:	Breaks along definite planes of fracture with little resistance to fracturing
Slickensided:	Fracture planes appear polished or glossy, sometimes striated
Blocky:	Cohesive soil that can be broken down into small angular lumps which resist further breakdown
Lensed:	Inclusion of small pockets of different soils
Layer:	Inclusion greater than 3 inches thick (75 mm)
Seam:	Inclusion 1/8-inch to 3 inches (3 to 75 mm) thick extending through the sample
Parting:	Inclusion less than 1/8-inch (3 mm) thick

SCALE OF RELATIVE ROCK HARDNESS

Q_U - TSF	Consistency
2.5 - 10	Extremely Soft
10 - 50	Very Soft
50 - 250	Soft
250 - 525	Medium Hard
525 - 1,050	Moderately Hard
1,050 - 2,600	Hard
>2,600	Very Hard

ROCK BEDDING THICKNESSES

Description	Criteria
Very Thick Bedded	Greater than 3-foot (>1.0 m)
Thick Bedded	1-foot to 3-foot (0.3 m to 1.0 m)
Medium Bedded	4-inch to 1-foot (0.1 m to 0.3 m)
Thin Bedded	1¼-inch to 4-inch (30 mm to 100 mm)
Very Thin Bedded	½-inch to 1¼-inch (10 mm to 30 mm)
Thickly Laminated	1/8-inch to ½-inch (3 mm to 10 mm)
Thinly Laminated	1/8-inch or less "paper thin" (<3 mm)

ROCK VOIDS

Voids	Void Diameter
Pit	<6 mm (<0.25 in)
Vug	6 mm to 50 mm (0.25 in to 2 in)
Cavity	50 mm to 600 mm (2 in to 24 in)
Cave	>600 mm (>24 in)

GRAIN-SIZED TERMINOLOGY

(Typically Sedimentary Rock)

Component	Size Range
Very Coarse Grained	>4.76 mm
Coarse Grained	2.0 mm - 4.76 mm
Medium Grained	0.42 mm - 2.0 mm
Fine Grained	0.075 mm - 0.42 mm
Very Fine Grained	<0.075 mm

ROCK QUALITY DESCRIPTION

Rock Mass Description	RQD Value
Excellent	90 -100
Good	75 - 90
Fair	50 - 75
Poor	25 -50
Very Poor	Less than 25

DEGREE OF WEATHERING

Slightly Weathered: Rock generally fresh, joints stained and discoloration extends into rock up to 25 mm (1 in), open joints may contain clay, core rings under hammer impact.

Weathered: Rock mass is decomposed 50% or less, significant portions of the rock show discoloration and weathering effects, cores cannot be broken by hand or scraped by knife.

Highly Weathered: Rock mass is more than 50% decomposed, complete discoloration of rock fabric, core may be extremely broken and gives clunk sound when struck by hammer, may be shaved with a knife.

SOIL CLASSIFICATION CHART

NOTE: DUAL SYMBOLS ARE USED TO INDICATE BORDERLINE SOIL CLASSIFICATIONS

MAJOR DIVISIONS			SYMBOLS GRAPH	SYMBOLS LETTER	TYPICAL DESCRIPTIONS
COARSE GRAINED SOILS MORE THAN 50% OF MATERIAL IS LARGER THAN NO. 200 SIEVE SIZE	GRAVEL AND GRAVELLY SOILS MORE THAN 50% OF COARSE FRACTION RETAINED ON NO. 4 SIEVE	CLEAN GRAVELS (LITTLE OR NO FINES)		GW	WELL-GRADED GRAVELS, GRAVEL - SAND MIXTURES, LITTLE OR NO FINES
				GP	POORLY-GRADED GRAVELS, GRAVEL - SAND MIXTURES, LITTLE OR NO FINES
		GRAVELS WITH FINES (APPRECIABLE AMOUNT OF FINES)	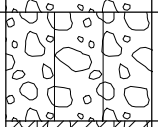	GM	SILTY GRAVELS, GRAVEL - SAND - SILT MIXTURES
			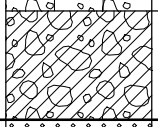	GC	CLAYEY GRAVELS, GRAVEL - SAND - CLAY MIXTURES
	SAND AND SANDY SOILS MORE THAN 50% OF COARSE FRACTION PASSING ON NO. 4 SIEVE	CLEAN SANDS (LITTLE OR NO FINES)	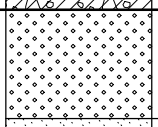	SW	WELL-GRADED SANDS, GRAVELLY SANDS, LITTLE OR NO FINES
			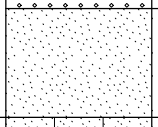	SP	POORLY-GRADED SANDS, GRAVELLY SAND, LITTLE OR NO FINES
		SANDS WITH FINES (APPRECIABLE AMOUNT OF FINES)	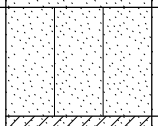	SM	SILTY SANDS, SAND - SILT MIXTURES
			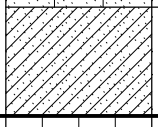	SC	CLAYEY SANDS, SAND - CLAY MIXTURES
FINE GRAINED SOILS MORE THAN 50% OF MATERIAL IS SMALLER THAN NO. 200 SIEVE SIZE	SILTS AND CLAYS	LIQUID LIMIT LESS THAN 50	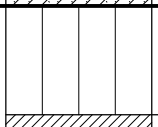	ML	INORGANIC SILTS AND VERY FINE SANDS, ROCK FLOUR, SILTY OR CLAYEY FINE SANDS OR CLAYEY SILTS WITH SLIGHT PLASTICITY
			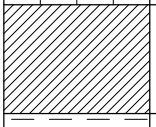	CL	INORGANIC CLAYS OF LOW TO MEDIUM PLASTICITY, GRAVELLY CLAYS, SANDY CLAYS, SILTY CLAYS, LEAN CLAYS
			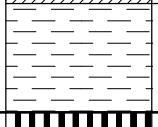	OL	ORGANIC SILTS AND ORGANIC SILTY CLAYS OF LOW PLASTICITY
	SILTS AND CLAYS	LIQUID LIMIT GREATER THAN 50	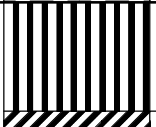	MH	INORGANIC SILTS, MICACEOUS OR DIATOMACEOUS FINE SAND OR SILTY SOILS
			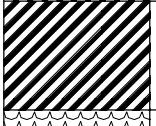	CH	INORGANIC CLAYS OF HIGH PLASTICITY
			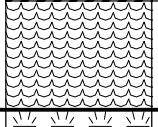	OH	ORGANIC CLAYS OF MEDIUM TO HIGH PLASTICITY, ORGANIC SILTS
HIGHLY ORGANIC SOILS			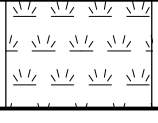	PT	PEAT, HUMUS, SWAMP SOILS WITH HIGH ORGANIC CONTENTS

Appendix D – Concrete Placement Logs

WisDOT Thermal Integrity Profiling Research Project

Summary of Tremie Concrete Placement

Date: 11/14/2017 Shaft: Control Depth: 32 (2' Stickup)
Weather: Cloudy, mid-40s By: AZB

Truck Number	Time Arrival	Initial Volume, cy	Time Placement Started	Time Placement Finished	Depth of Top of Concrete (from Top of Shaft) upon Finish, ft	Slump, in.	Temp-erature, ^{0}F	Cylinder Number	Notes, including defects
									Truck volumes are paid quantities. Paid for 7 but could have been carrying up to 7.5? Concrete slump values high but samples appeared cohesive and showed no signs of segregation or bleed.
1	14:30	7	14:35 15:15	14:53 15:20	23	10		CS-1-1 CS-1-2	
						10	65	- -	14:53 - 15:15: Pull on inner casing to ~break it loose, but do not remove it. Getting the casing to budge required force of crane, rig, and dozer.
2	14:55	7	15:25 15:48	15:32 15:55	9.5	10.5	60	CS-2-1 CS-2-2	15:32 - 15:48: Remove inner casing. Concrete is visible on bottom 7 ft of outside of casing, above clean.
3	16:00	7	16:15 17:00	16:22 17:10	0.5	11	68	CS-3-1	16:22 -- Remove tremie with 5 ft shaft left to be poured. Pour by free fall to just below ground surface. Pull outer temporary casing and set 3-ft long permanent casing, which is also 58-in. diameter, prior to completing pour.
								CS-3-2	17:00: Final pour. Permanent casing not set deep enough -- concete seeps under and out at surface. Soil from surface used to stop seepage, but top ~1 ft BGS has diameter of 64" +/-, with some soil mixed in outer concrete. Top of concrete is ~6 in. below top of permanent casing, but above top of rebar.

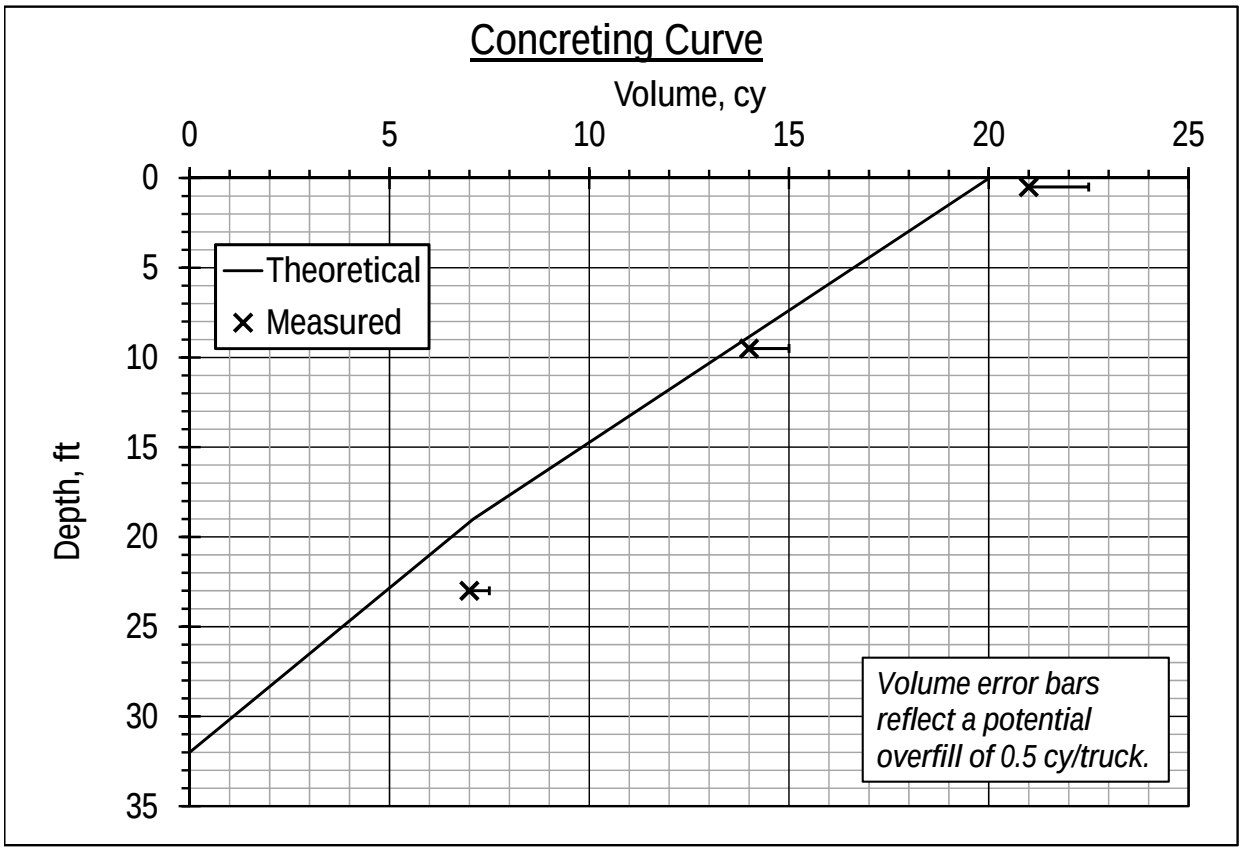

WisDOT Thermal Integrity Profiling Research Project

Summary of Tremie Concrete Placement

Date: 11/16/2017 Shaft: Test Shaft 1 Depth: 32 (2' Stickup)
Weather: Cloudy, mid-40s By: AZB

Truck Number	Time Arrival	Initial Volume, cy	Time Placement Started	Time Placement Finished	Depth of Top of Concrete (from Top of Shaft) upon Finish, ft	Slump, in.	Temp-erature, °F	Cylinder Number	Notes, including defects
									CSL tubes not filled with water until 11/17 morning (appx. 24 hours after pour). Truck volumes are paid quantities. Paid for 7 cy/truck, but could get 7.5. Except Truck 4 -- just 3 cy. Concrete slump values high but samples appeared cohesive and showed no signs of segregation or bleed.
1	8:25	7	8:39	08:55 09:00	20 19	10	60	TS1-1-1 TS1-1-2	Looks like more cover on the north side of cage.
2	8:59	7	09:13 09:37	09:18 09:40	11	10	60	TS1-2-1 TS1-2-2	09:18-09:37: Pull inner casing.
3a	9:23	4 (?)	9:45	9:50	5	10.5	58	TS1-3-1 TS1-3-2	Truck 3 had 7 cy. Upon reaching 5 ft below cage, estimated 3 cy left based on the previous depth of 11 ft and the estimated total truck volume of 7 cy. Added 36 gallons (12 per cy) after placing the 4 cy. Also pulled tremie between 3a and 3b (when water was added).
3b		3 (?)	10:16	10:30	2.75			TS1-4-1 TS1-4-2 TS1-4-3	
4	11:25	3	11:31	11:42	0	Very high -- watery	52	TS1-5-1 TS1-5-2	Pulled outer casing after placing 3b. Concrete level dropped about 1 ft, presumably because of a gap outside the permanent casing resulting from material caving in (cobbles, sand). Placed 3-ft long, 58-in. dia. permanent casing.

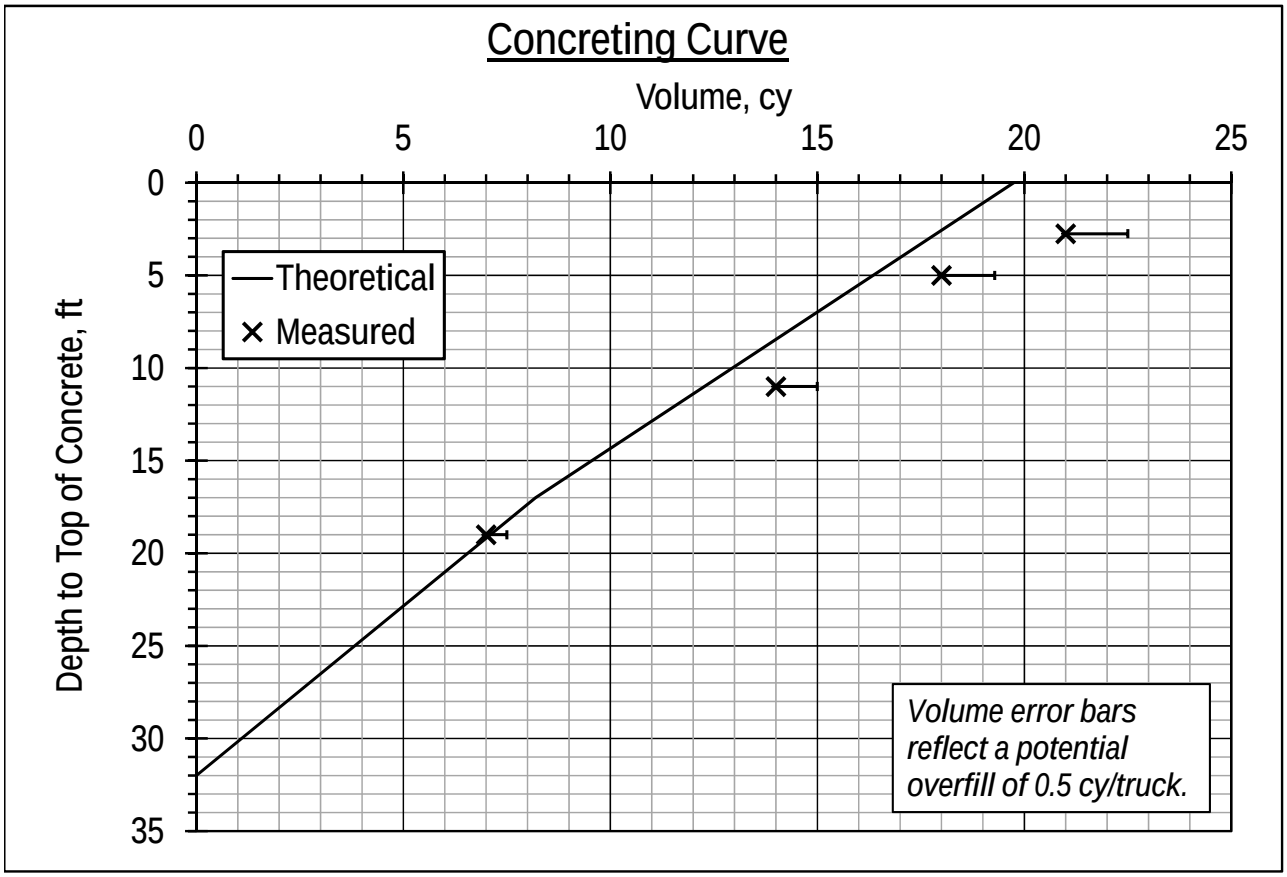

WisDOT Thermal Integrity Profiling Research Project

Summary of Tremie Concrete Placement

Date: 11/17/2017 Shaft: Test Shaft 2 Depth: 32 (2' Concrete Stickup)
Weather: Cloudy, mid-40s By: AZB

Truck Number	Time Arrival	Initial Volume, cy	Time Placement Started	Time Placement Finished	Depth of Top of Concrete (from Top of Shaft) upon Finish, ft	Slump, in.	Temp-erature, °F	Cylinder Number	Notes, including defects
									Before starting, realize CSL tubes for TS-1 were not filled with water yesterday. Add a replicate of Defect 4 (grease to promote debonding along CSL tubes) at a depth of appx. 6.5 ft below top of shaft to TS-2. Truck volumes are paid quantities. Paid for 7 cy/truck, but could get 7.5. Concrete slump values high but samples appeared cohesive and showed no signs of segregation or bleed.
1	8:25	7	09:25 10:05	09:40 10:10	22.5 18.5	11		TS2-1-1 TS2-1-2	Slump is high, as for previous trucks. Called plant. QC rep comes for Truck 2, which had lower slump. At 9:40, pull tremie and add 7 mostly full 5-gal. buckets (appx. 30 gal.) of water to create Defect 8 at a depth of 22.5 ft below cage (9.5 ft above bottom). Also dump in 70 lbs of sand midway through bucket of water placement. 9:55: Break seal of inner casing and remove another segment of tremie. Resume placement with tremie suspended above Defect 8.
2	8:59	7	10:14 11:44	10:20 11:50	7.5	7.5		TS2-2-1 TS2-2-2	Looks like water from Defect 8 has been pushed to sides and up along inside of casing. 10:20-11:44: Remove tremie. Rest to be placed by free fall. Attempt to pull inner casing, which is 52-in. diameter by 30-ft long. Had previously been pulled up 5 ft, so has 25-ft embedment, but will not budge now. After 1.5 hours, decide to abandon casing, so temporary is now permanent. Bottom 5 ft of shaft is uncased, likely with bulbing of extra concrete. Top 27 ft is cased.
3a	10:39	1.4	11:54	11:56	5	11		TS2-3-1 TS2-3-2	Truck 3 had 7 cy. Upon reaching 5 ft below cage, estimated 5.6 cy left based on the previous depth of 7.5 ft and the estimated total truck volume of 7 cy. Added 30 gallons (5 per cy) after placing the 1.4 cy. After finishing placement, pull outer casing, which is 58-in. dia. and 14-ft embedment. Subsequently finish shaft construction by backfilling gap between inner/permanent casing and hole created by outer temporary casing with gravel.
3b		5.6	12:08	12:12	0	Very high -- watery (but not as watery as TS-1)		TS2-4-1 TS2-4-2	

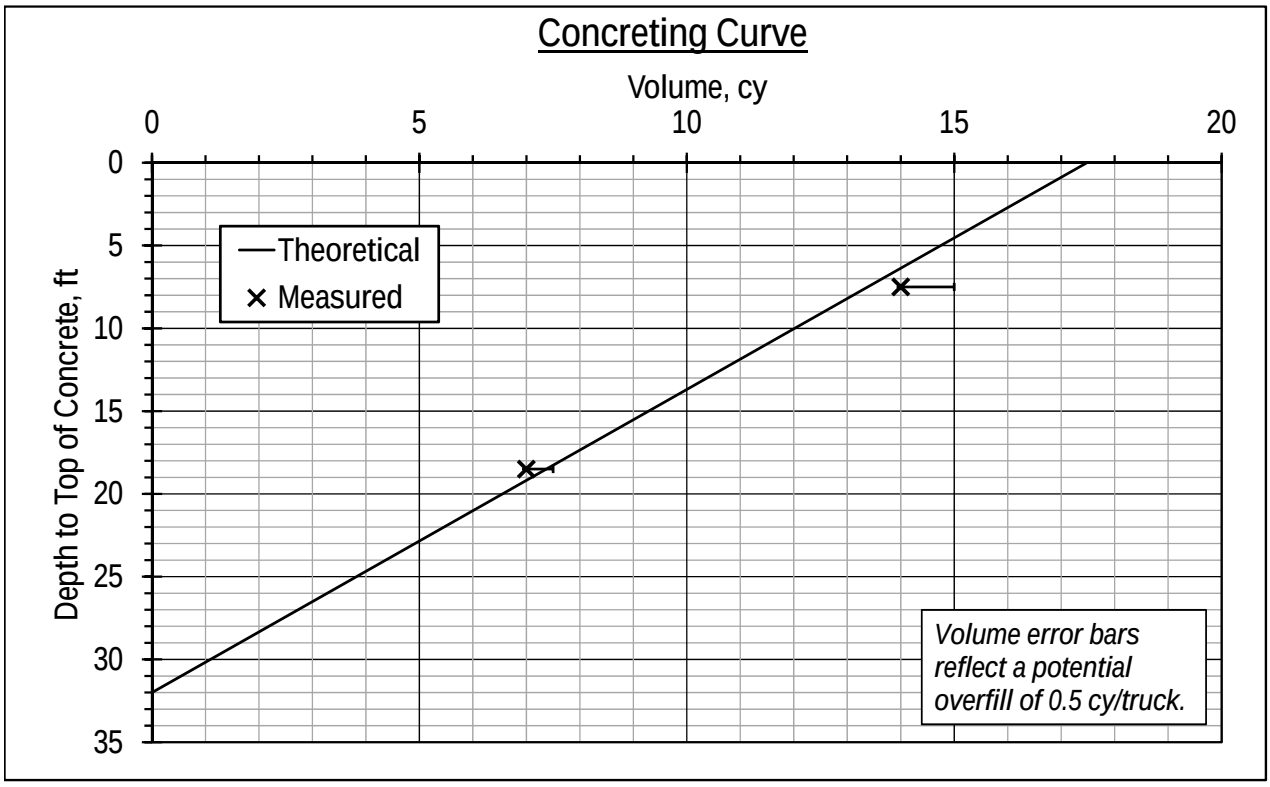

Appendix E – Proposed TIP Specification

The proposed TIP specification language below is based on the recommendations presented in Chapter 7. The proposed specification is likely best implemented as a sub-section of a general drilled shaft specification or special provision. The general drilled shaft specification should also include language regarding CSL testing, frequency of integrity testing, coring, repair methods, and payment for integrity testing.

1. General

   Performance of Thermal Integrity Profiling (TIP) test methods shall conform to ASTM D7949, Method B. In the event of any conflict between this specification and ASTM D7949, this specification shall control over ASTM D7949.

   The TIP probe method (Method A of ASTM D7949) shall not be used, except as a supplemental test when crosshole sonic logging (CSL) is the primary concrete integrity test method. When the probe method is used as a supplemental test to CSL test methods, the probe method test shall be performed according to ASTM D7949, Method A.

   The TIP testing organization is the party responsible for overseeing performance of the TIP test methods and for preparing the final TIP report. The testing organization shall have documented prior experience with TIP testing on deep foundations projects. Final TIP reports produced by the TIP testing organization shall be prepared and sealed by a professional engineer licensed in the state of Wisconsin.

   Peak temperature is defined as the maximum temperature at any depth for the average temperature profile (i.e. the profile defined by averaging results from each of the wires).

2. TIP Wires and Wire Placement

   Each TIP wire shall consist of a cable with one temperature sensor per foot of cable length. TIP wires shall be connected to data acquisition equipment capable of recording and storing temperature data from each sensor every 15 minutes for a recording period of at least one week.

   The number of TIP wires per shaft shall be one per each foot of shaft diameter or four, whichever is greater. For the purposes of determining the number of TIP wires, shaft diameters shall be rounded up to the next greatest whole number. The TIP wires shall extend from the bottom of the reinforcing cage to at least the top of concrete, with an additional 10 ft of slack wire above the top of concrete. TIP wires shall be evenly spaced around the circumference of the reinforcing cage. The TIP wires shall be installed parallel to the longitudinal axis of the reinforcing cage. TIP wires shall be affixed to the shaft reinforcing cage using plastic cable ties, with at least one tie per temperature sensor. Cable ties shall not be placed directly on the temperature sensors. The TIP wires shall be affixed to the cage tautly but with sufficient slack to prevent damage during lifting of the reinforcing cage.

   After the reinforcing cage has been placed in the shaft but prior to the placement of concrete, each TIP wire shall be checked to ensure temperature data can be read and recorded for each sensor. Any defective TIP wires shall be replaced prior to placement of concrete.

3. Recording Period

   Recording of temperature data from all TIP wires in a shaft shall start within one hour of the completion of concrete placement for the shaft, or earlier. Recording of temperature data shall continue until at least 24 hours after the peak temperature has been observed. Temperature measurements shall be recorded for each sensor every 15 minutes during the recording period.

4. Results and Reporting

   TIP reports shall be submitted within three working days of the end of the recording period.

TIP reports shall include for each shaft at least two temperature profile plots. Each temperature profile plot shall present temperatures on the horizontal axis versus depth or elevation on the vertical axis. On each temperature profile plot, one line shall be included for each TIP wire, and an additional line shall be included for the average of all TIP wires. One temperature profile plot shall present temperatures at the time of peak temperature development, and another temperature profile plot shall present temperatures at approximately half of the time to peak temperature development. Depths corresponding to the top of shaft, bottom of shaft, and any of the following features shall be indicated on the temperature profile plots: top of temporary casing, bottom of temporary casing, top of permanent casing, bottom of permanent casing, shaft diameter change, and any other installation details deemed relevant to the TIP analysis (e.g. depth of tremie breach). The date and time of analysis and the time elapsed since the completion of concrete pouring shall be noted on each temperature profile plot. Each temperature profile plot shall also include a legend noting the location of each TIP wire with respect to North.

TIP reports shall also include plots of temperature versus time for depths of any suspected defects. Suspected defect depths shall be identified from shaft installation records (e.g. depth of tremie breach) or from the temperature profile plots (e.g. depth of low observed temperatures). The temperature versus time plots shall include at least three lines: (1) a line representing temperatures for the depth of the suspected defect, (2) a line representing temperatures for a nearby depth that appears to be uninfluenced by the potential defect, and (3) a line representing the temperature difference between (1) and (2). The line for (3) shall be plotted on a secondary axis. Alternatively, the line for (3) may be plotted on a separate plot.

Effective radius profiles may be included in TIP reports. If included, effective radius profiles shall be presented as for visualization purposes only. Effective radius profiles shall not be used as a means for evaluating the data or for inferring specific values of concrete cover.

5. Evaluation and Recommendation

   Evaluation of TIP data shall consider any available records of drilled shaft installation, including concrete yield plots. TIP report conclusions regarding the interpretation of TIP results shall consider observations from drilled shaft construction records.

   TIP reports shall include a conclusion stating either that no integrity defects were indicated in the TIP records, or listing specific locations and characteristics of potential defects. If integrity defects are suspected, the depth of each suspected defect shall be indicated in the report. The cross-sectional location of each suspected defect shall also be indicated in the report in terms of cardinal direction (e.g. northwest quadrant of the shaft).

   TIP reports shall include a recommendation to accept the shaft as-is, a recommendation for further review by the shaft design engineer or their designee, a recommendation for further investigation, or a recommendation for repair.

6. Acceptance

   The shaft design engineer or their designee shall make the final determination of shaft acceptance based on review of the TIP report and any subsequent analysis, investigation, and repair of the shaft.